

**TECHNICAL REPORT
NATICK/TR-11/016**



AD _____

DEVELOPMENT OF A QUADCON REFRIGERATED CONTAINER WITH FIRST GENERATION PROTOTYPE SOLAR ADSORPTION REFRIGERATION SYSTEM

**by
J. Donald Carruthers**

**Advanced Technology Materials Inc.
Danbury, CT 06810-4131**

June 2011

**Final Report
October 2007 - April 2010**

Approved for public release; distribution is unlimited.

**Prepared for
U.S. Army Natick Soldier Research, Development and Engineering Center
Natick, Massachusetts 01760-5018**

UNCLASSIFIED

DISCLAIMERS

The findings contained in this report are not to be construed as an official Department of the Army position unless so designated by other authorized documents.

Citation of trade names in this report does not constitute an official endorsement or approval of the use of such items.

DESTRUCTION NOTICE

For Classified Documents:

Follow the procedures in DoD 5200.22-M, Industrial Security Manual, Section II-19 or DoD 5200.1-R, Information Security Program Regulation, Chapter IX.

For Unclassified/Limited Distribution Documents:

Destroy by any method that prevents disclosure of contents or reconstruction of the document.

UNCLASSIFIED

REPORT DOCUMENTATION PAGE				Form Approved OMB No. 0704-0188	
Public reporting burden for this collection of information is estimated to average 1 hour per response, including the time for reviewing instructions, searching existing data sources, gathering and maintaining the data needed, and completing and reviewing this collection of information. Send comments regarding this burden estimate or any other aspect of this collection of information, including suggestions for reducing this burden to Department of Defense, Washington Headquarters Services, Directorate for Information Operations and Reports (0704-0188), 1215 Jefferson Davis Highway, Suite 1204, Arlington, VA 22202-4302. Respondents should be aware that notwithstanding any other provision of law, no person shall be subject to any penalty for failing to comply with a collection of information if it does not display a currently valid OMB control number.					
PLEASE DO NOT RETURN YOUR FORM TO THE ABOVE ADDRESS.					
1. REPORT DATE (DD-MM-YYYY) 30-06-21011		2. REPORT TYPE Final		3. DATES COVERED (From - To) October 2007 - April 2010	
4. TITLE AND SUBTITLE DEVELOPMENT OF A QUADCON REFRIGERATED CONTAINER WITH FIRST GENERATION PROTOTYPE SOLAR ADSORPTION REFRIGERATION SYSTEM				5a. CONTRACT NUMBER W911QY-07-C-0073	
				5b. GRANT NUMBER	
				5c. PROGRAM ELEMENT NUMBER 622786	
6. AUTHOR(S) J. Donald Carruthers				5d. PROJECT NUMBER W91A2K70939050	
				5e. TASK NUMBER	
				5f. WORK UNIT NUMBER	
7. PERFORMING ORGANIZATION NAME(S) AND ADDRESS(ES) Advanced Technology Materials Inc. (ATMI) 7 Commerce Drive Danbury, CT 06810-4131				8. PERFORMING ORGANIZATION REPORT NUMBER	
				ATMI-AGT#28	
9. SPONSORING / MONITORING AGENCY NAME(S) AND ADDRESS(ES) US Army Natick Soldier Research, Development and Engineering Center ATTN: RDNS-CFE (A. Schmidt) Kansas Street, Natick, MA 01760-5018				10. SPONSOR/MONITOR'S ACRONYM(S) NSRDEC	
				11. SPONSOR/MONITOR'S REPORT NUMBER(S) NATICK/TR-11/016	
12. DISTRIBUTION / AVAILABILITY STATEMENT Approved for public release; distribution is unlimited.					
13. SUPPLEMENTARY NOTES					
14. ABSTRACT <i>Report for Broad Agency Announcement (BAA) Congressional Plus-up.</i> The Army recognizes the merits of using renewable energy to power refrigeration systems aboard mobile cold-storage systems used for perishable rations in operational theaters. This report documents efforts to develop a solar-powered adsorption refrigerator for food refrigeration in a QuadCon container. The work was performed between October 2007 and April 2010 under a Broad Agency Announcement project funded as a Congressional Plus-Up by the Natick Soldier Research, Development and Engineering Center (NSRDEC). Plate-style heat-exchanger generators for the device were developed, the equipment was assembled and tested at laboratory scale, and it was shipped to the high insolation region of Tucson, AZ for on-site testing. The plan was to operate the unit for a month to develop ideal operational conditions and then compare performance alongside an electrically-powered QuadCool. Although the system operated safely without any external electric power for 6 weeks at the test location in March and April 2010 and many aspects of the system functioned well, performance did not meet expectations, and final testing was foreshortened. Improvements in the design of the generators, the carbon, and the evaporator are necessary for future developments.					
15. SUBJECT TERMS					
MOBILE RATIONS COOLING QUADCON PROTOTYPES ADSORPTION	GENERATORS BATTLEFIELDS SOLAR ENERGY COLD STORAGE POWER SUPPLIES FORWARD AREAS	FIELD EQUIPMENT PERISHABLE CARGO RENEWABLE ENERGY PORTABLE EQUIPMENT SHIPPING CONTAINERS BAA(BROAD AGENCY ANNOUNCEMENT)	TEST AND EVALUATION REFRIGERATION SYSTEMS THEATER LEVEL OPERATIONS OPERATIONAL EFFECTIVENESS QUADCON(QUADRUPLE CONTAINER)		
16. SECURITY CLASSIFICATION OF:			17. LIMITATION OF ABSTRACT	18. NUMBER OF PAGES	19a. NAME OF RESPONSIBLE PERSON
a. REPORT	b. ABSTRACT	c. THIS PAGE			Alex Schmidt
U	U	U	SAR	92	19b. TELEPHONE NUMBER (include area code) 508-233-6042

UNCLASSIFIED

This page intentionally left blank

UNCLASSIFIED

Table of Contents

List of Figures.....	v
List of Tables	vi
Preface.....	vii
Acknowledgements	viii
1. Introduction.....	1
1.1 Background.....	2
1.2 Adsorption Refrigeration Process and Operation Principles	2
2. Methods, Assumptions and Procedures.....	5
2.1 Adsorbent Development	5
2.1.1 Improving Heat and Mass Transfer	5
2.1.2 Increasing the Gas Storage.....	6
2.2 Design of Adsorption Generators	7
2.2.1 Heat Transfer Fluid.....	7
2.2.2 Heat-Exchanger Design	7
2.2.3 Load Calculations	8
2.2.4 Collector Modeling and Selection	8
2.2.5 Evaporator Specification and Design.....	11
2.2.6 Modeling of System Level Performance	12
2.2.7 Check Valves	14
2.2.8 Water Three-Way Valve.....	15
2.3 Carbon Plate Sets	16
2.3.1 Scale-up Production	18
2.3.2 Generator Construction.....	21
2.3.3 Plate Installation.....	24
2.3.4 Leak Testing.....	26
2.3.5 Carbon Drying	26
2.4 Generator Testing in the Laboratory.....	27
2.4.1 Ammonia Charging.....	27
2.4.2 Laboratory Testing.....	28
2.5 Frame Fabrication	30
2.5.1 Frame and Ancillary Equipment.....	30
2.5.2 Testing the Equipment in the Assembled Frame	32
3. Field Testing	35
3.1 Commissioning and Bake-Out of the Carbon.....	36
3.2 Solar-Powered Adsorption Refrigerator Operation	37
3.3 Daily Operations: Changing Process Conditions and Monitoring Ammonia.....	38
3.4 Evaluation of Changes in Process Conditions	38
4. Results	40
4.1 Conditions for Maximum Ammonia Generation.....	40
4.2 Conditions Which Produced the Coldest Temperatures in the QuadCon.....	42
4.3 Best Operations	44
4.4 Discussion Regarding Ultimate Performance	44
4.4.1 Temperature Limitations.....	44

4.4.2 Condition of Carbon	45
4.4.3 Evaporator Sizing Issue	46
4.4.4 Overall Coefficient of Performance.....	46
5. Conclusions.....	48
6. Recommendations	49
7. References.....	50
Appendix A - Results of Testing Carbon Samples	51
Appendix B - Permeability Test Results	53
Appendix C - Safety Review	55
Appendix D - Wiring Diagrams for Photovoltaic Parasitic Electric Power.....	71
Appendix E - Images of Video Monitor Screens	75
Appendix F - Solar-Powered Adsorption Refrigerator Commissioning.....	81
Appendix G - Summary Tables for Solar-Powered Adsorption Refrigerator Site Test.....	89

List of Figures

Figure 1. Adsorption Refrigerator Process Schematic.....	3
Figure 2. Thermal Behavior of 12-mm Carbon-Containing Aluminum Fins.....	6
Figure 3. Solar Collector Modeling.....	10
Figure 4. Solar Collector Output, Refrigerator Heat Demand & Cooling Output.....	11
Figure 5. Evaporator Design.....	12
Figure 6. System Modeling – Cooling Power at 30°C Ambient	13
Figure 7. System Modeling – Cooling Power 40°C Ambient	14
Figure 8. High-Pressure Ammonia Isotherms	18
Figure 9. One of the Generators Machined to Receive Manifolds with O-ring Seals	22
Figure 10. Water Manifold Plate	22
Figure 11. Generator showing Bracing Rods & Clamping Bolts	23
Figure 12. Generator Undergoing Preliminary Pressurization to 3 Bar	24
Figure 13. Carbon Plates ready for Loading into Generator.....	25
Figure 14. Laboratory Test Rig.....	26
Figure 15. Bake-out of the Carbon Plates.....	27
Figure 16. Generator Water Temperatures	28
Figure 17. Measured Carbon Temperatures	29
Figure 18. Condenser Heat Output	29
Figure 19. Generator Pressures	30
Figure 20. The Frame Connected to the QuadCon	31
Figure 21. Other Views of the Frame	31
Figure 22. Emergency Water Tank in the QuadCon	32
Figure 23. Evaporator in Place	33
Figure 24. Testing of the System -- Temperatures Inside the QuadCon	34
Figure 25. Photovoltaic Panels on Roof of SunDanzer	35
Figure 26. Solar Thermal Panels at QuadCon Adsorption Refrigeration System	35
Figure 27. QuadCon with Refrigeration Unit.....	36
Figure 28. Water Temperatures on 3/20/2010.....	40
Figure 29. Pressures in Generators 1 & 2 During Operation 3/20/2010.....	41
Figure 30. Temperatures in the QuadCon on 3/20/2010	41
Figure 31. Best Conditions HP = 180 s, MR = 10 s, and HR = 20 s	43
Figure 32. Results for Conditions HP= 180 s, MR = 10 s, and HR = 20 s.....	43
Figure 33. Best Conditions HP = 180 s, MR = 10 s, HR = 20 s	44
Figure 34. Coefficient of Performance vs. Heat Cycle Period (in seconds).....	46

List of Tables

Table 1.	Load Calculation Results.....	9
Table 2.	Check Calve Evaluation (RS-237-2470) with Compressed Air.....	15
Table 3.	Properties of Carbon Plates Submitted for Evaluation.....	17
Table 4.	Properties of First Batch of 15 mm Thick Plates	19
Table 5.	Thermal Data for Test Pieces of Finished Plates	21
Table 6.	Selected Characterization for Plate Test Pieces	21
Table 7.	Baseline, Target, and Achieved Properties	25
Table 8.	Loading Data for Generators.....	26
Table 9.	Ammonia Charging	27
Table 10.	Test Conditions.....	28
Table 11.	Changes in Operational Settings During March 13 – 28.....	39
Table 12.	Changes in Operational Settings During 3/12 – 3/28.....	47

Preface

This report documents efforts to develop a solar-powered adsorption refrigerator for food refrigeration in a QuadCon container. The work was performed between October 2007 and April 2010 under a Broad Agency Announcement (BAA) Contract (W911QY-07-C-0073) awarded by the Natick Soldier Research, Development and Engineering Center (NSRDEC) to Advanced Technology Materials Inc. (ATMI). The BAA contract was funded as a Congressional Plus-Up (under Program Element 622786 and Project W91A2K70939050) because of great emphasis by the Army on minimizing the use of JP-8, the standard battlefield fuel, for soldier support operations. The BAA solicitation addressed the Combat Feeding Equipment and Systems category "Combat Food Service Equipment for Individual and Group Feeding".

ATMI's proposal was to develop a stand-alone refrigeration system requiring no external power source. It was to be based on an entirely different refrigeration cycle and energy supply than provided by current technology options -- heat-driven absorption vs. electrically driven vapor compression. The key deliverable of this contract was to be an alpha-prototype refrigeration system using adsorption refrigeration integrated with a standard Army QuadCon insulated container with energy requirement based primarily on solar thermal and solar photovoltaic power.

ATMI engaged the University of Warwick as a subcontractor to develop plate-style heat-exchanger generators for the device. ATMI developed monolithic carbon plates for the generators

Acknowledgements

The following individuals are recognized for their contribution to specific parts of the project:

Project Management:

Dr. Joshua Sweeney, Dr. Don Carruthers, Professor. Robert Critoph

Modeling, generator design, construction and hardware and software implementation:

Professor Robert Critoph, Dr. Stan Shire, Dr. Steven Metcalf, Dr. Zak Tamainot-Telto

Carbon development:

Dr. Don Carruthers, Dr Melissa Petruska, Mr. Ed Sturm, Mr. Eric Condo, Mr. Jeremiah Brown,

Solar Photovoltaic Power Panels and Solar Thermal Collectors:

Dr. Shaun Wilson, Mr. Steve Lurcott, Mr. Shkelqim Letaj

Programming:

Mr. Shkelqim Letaj

Test-Site Monitoring and Supervision:

Dr. Shaun Wilson, Mr. Shkeqim Letaj, Mr. Ed Jones, Mr. Joseph Sweeney, Mr. John Blanchard, Mr. Joseph Dupres, Mr. Ed Sturm, Mr. Michael Wodjenski, Dr. Don Carruthers, Dr. Steven Metcalf and the staff at Sundanzer, Tucson, Arizona

DEVELOPMENT OF A QUADCON REFRIGERATED CONTAINER WITH FIRST GENERATION PROTOTYPE SOLAR ADSORPTION REFRIGERATION SYSTEM

1. Introduction

This report documents efforts to develop a solar-powered adsorption refrigerator for food refrigeration in a QuadCon container. The work was performed under a Broad Agency Announcement (BAA) contract awarded by the Natick Soldier Research, Development and Engineering Center (NSRDEC) to Advanced Technology Materials Inc. (ATMI) in October 2007. Through a partnership with research staff at the University of Warwick School of Engineering, Coventry, U.K., ATMI undertook materials development, product design, fabrication, and site testing of a solar-powered adsorption refrigeration system with the goal of providing refrigeration to a QuadCon insulated container. The work continued until April 2010.

The contract, which was funded as a Congressional Plus-Up, was awarded because of great emphasis by the Army on minimizing the use of JP-8, the standard battlefield fuel, for soldier support operations. It was reported that in WWII the average fuel requirement per soldier was 1 gallon per day -- today it is 17 gallons per day. Further exacerbating the supply problem is the difficulty of transporting fuel into forward operating regions -- contemporarily Afghanistan and Iraq. "Pentagon officials have told the House Appropriations Defense Subcommittee a gallon of fuel costs the military about \$400 by the time it arrives in the remote locations in Afghanistan where U.S. troops operate." [1].

Following award of the BAA contract in 2007, ATMI negotiated a sub-contractual arrangement with the University of Warwick to perform the following work:

- Design and fabricate two compact generators for this application based upon designs previously developed for an EU-TOPMACS¹ program.
- Engineer a frame to accommodate the generators which would mate with the QuadCon;
- Design and engineer the pumping and valve systems.
- Design and engineer the condenser and water coolant systems with electric-powered fans;
- Design and engineer the evaporator.
- Provide all plumbing connections between the various components.
- Design into the system regenerative heat transfer between the adsorbent beds.
- Maintain close contact with the materials development team at ATMI to ensure a smooth consolidation.

During the project, ATMI had to modify its original monolithic carbon blocks (developed before the contract award) for this project, as follows:

- Modify the properties of the carbon adsorbent blocks to increase their heat and mass transfer capabilities.
- Enhance the refrigerant gas adsorption capacity of the carbon.
- Maintain/ensure high thermal contact conduction between the carbon and the heat-exchange surfaces of the generators;.

¹ European Union - Thermally Operated Mobile Air Conditioning Systems

- Acquire an insulated Quadcon from Charleston Marine Containers, Inc. (sans standard refrigeration unit).
- Integrate solar thermal collectors to provide the necessary heat to operate the generators.
- Design and fabricate a solar photovoltaic electric power supply system charging batteries with an inverter to supply parasitic power to the switches, pumps and fans.
- Develop software to control and operate the system automatically without operator involvement.
- Identify a suitable, high insolation region for site testing.

1.1 Background

Several technical accomplishments pointed the way toward developing a solar-powered adsorption refrigeration device. The first achievement was that in 2005 ATMI commercialized the production of a high adsorbent capacity carbon in the form of smooth-sided monolith blocks or "pucks". The second was that this high-density carbon material could lend itself very well to new, compact, plate heat-exchanger reactor designs for adsorption refrigeration devices being developed by a research team at the University of Warwick (U.K.) under the guidance of Professor Bob Critoph. These along with improvements in solar thermal collector designs lent weight to the concept of a truly grid-free/fuel-free refrigeration system. While it was understood that the final unit should incur minimum weight and space requirements, it was felt that such refinements could be included in a beta-version rather than this proof-of-principle prototype.

The decision regarding refrigerant was easily made. An ideal refrigerant should have the highest latent heat per unit volume and be liquid at reasonable pressures. Water has high performance, but suffers from a low vapor pressure near 0°C, and the possibility of freezing makes it difficult to use at evaporating temperatures below about 10°C [2]. Hence, it could never be used in refrigeration systems requiring temperatures of 5°C. Ammonia comes in a close second, and because it is considered to be more environmentally friendly than fluorocarbon refrigerants and is not a greenhouse gas, its use was recommended. Critoph has completed extensive studies with various refrigerants over the years, coming to this conclusion [3, 4].

In 2005, R. Z. Wang at the Institute of Refrigeration and Cryogenics in Shanghai Jiao Tong University reviewed all of the published literature describing adsorption refrigeration systems and, of the systems for ice-making, identified the carbon–ammonia working pair as superior to both carbon–methanol and silica-gel–water [5]. Then, in 2007, Wang reviewed recently patented novel technologies [6].

Early conversations with the Warwick team coupled with a detailed search of the technical literature indicated that the most effective refrigerant gas for a compact adsorption refrigeration unit was ammonia. The QuadCon would be cooled by a carbon–ammonia adsorption refrigeration system.

1.2 Adsorption Refrigeration Process and Operation Principles

The principle behind adsorption refrigeration systems (referring to the schematic in Figure 1) is that the adsorbent bed acts as a thermal compressor to drive the refrigerant off the carbon bed during the heating period. The gas, under pressure is then conveyed to a cooled condenser where

it liquefies. The condensed liquid under pressure is then expanded through an expansion valve, and low pressure condensate passes to the evaporator. Heat from the space to be conditioned is transferred to the evaporator, and this heat vaporizes the gas in the evaporator. The gas is then drawn by the adsorbing power of the carbon back to the second generator. After about one minute the optimum amount of ammonia has been desorbed by one generator and adsorbed by the other. The heating and cooling circuits to each generator are then switched so that the flow continues to flow through the condenser, expansion valve and evaporator. Cooling is continuous as the generators switch function every minute.

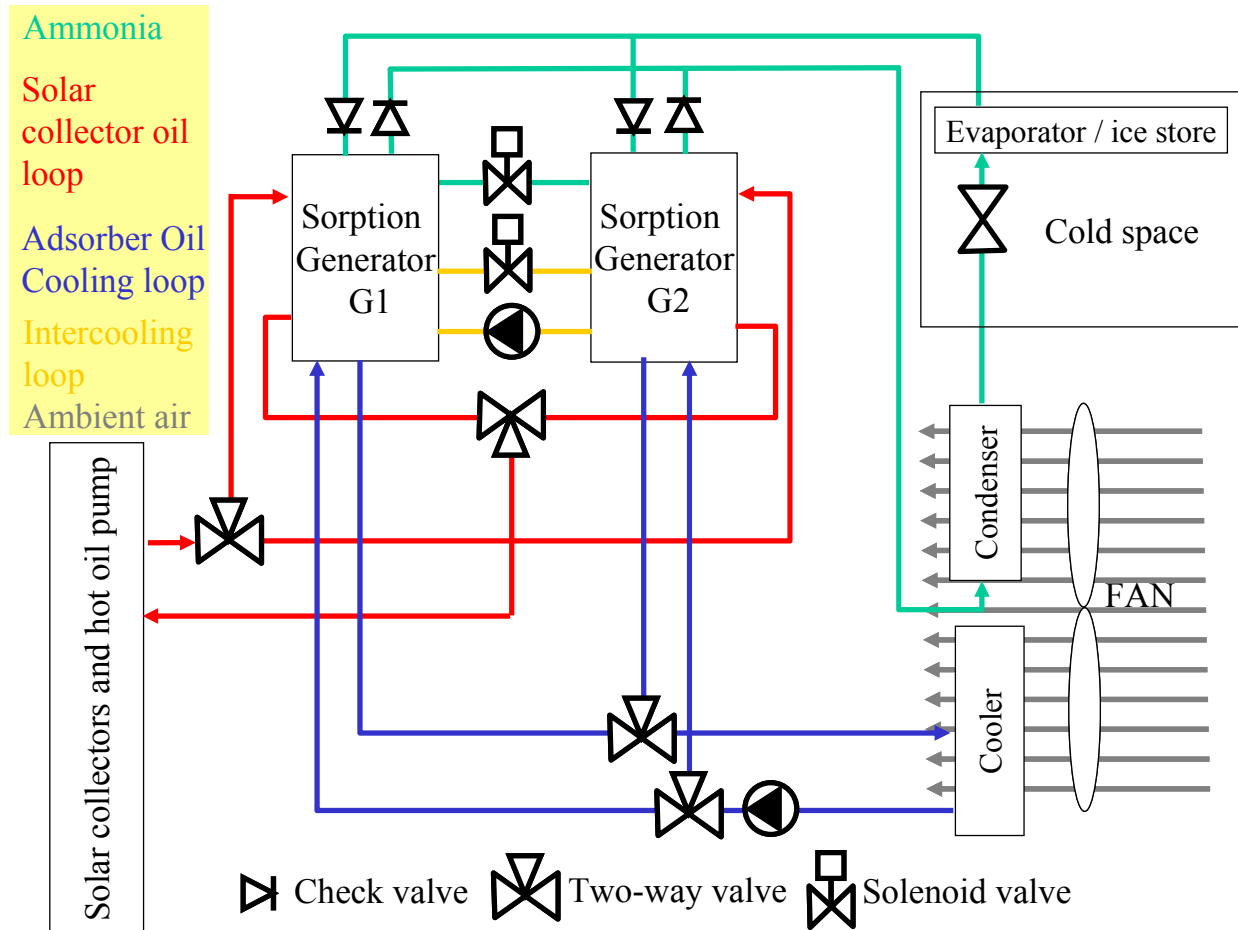


Figure 1. Adsorption Refrigerator Process Schematic

The efficiency of adsorption refrigeration systems depends markedly on the properties of the adsorbent, namely the adsorbent thermal conductivity and its permeability. The adsorbent must be heated (desorption phase) and then cooled (adsorption phase) back to ambient temperature in order to complete a thermodynamic cycle. High efficiencies require that the rates of heat transfer into and out of the adsorbent must be high, and the time per cycle must be short (on the order of minutes) [7].

To obtain continuous and stable cooling in the operation of a solar-powered adsorption refrigeration system, at least two adsorbent beds are necessary; one bed is heated during the

desorption period while the other is cooled during the adsorption period. The time required to complete a full cycle of adsorption and desorption is known as the cycle time. The heating and cooling steps are reversed when the beds reach the desired upper and lower temperature limits of the adsorption period. In addition, because the solar operation will cease as solar intensity declines later in the day, the evaporator must be designed to produce sufficient ice during the day to maintain a 5°C environment even during night-time hours. This design is referred to as a basic cycle, and although there are drawbacks to the concept, it can be improved by circuits that recover heat between generators and enable refrigerant to pass between them at one point in the cycle.

The efficiency of cooling is called the coefficient of performance (COP) and is the ratio of the cooling effect to the energy input. The cooling power per unit of adsorbent weight is known as the specific cooling power (SCP).

2. Methods, Assumptions and Procedures

2.1 Adsorbent Development

2.1.1 Improving Heat and Mass Transfer

Mixtures of the high-density carbon with additives were prepared according to a specific Design of Experiment (DOE) protocol at ATMI. The first pass series incorporated additives to enhance permeability and thermal conductivity. Beaded, granular or finely-ground carbon was added to the precursor polymer prior to pyrolysis to improve the gas permeability. The inclusion of high thermal-conductivity carbons -- such as graphitic carbon fibers or graphite -- to the polymer addressed the need to enhance heat transfer. Equilibrium properties of these additive-containing carbons were characterized using existing analytical instruments, while transport properties were characterized by two instruments: a PMI Permeameter and a Netzsch Nano-Flash thermal conductivity analyzer.

The challenge in carbon development was to achieve a high permeability while attempting to increase thermal conductivity and yet maintain a high overall density. The compromise among these properties while maintaining piece integrity required the preparation of more than 150 test coupons, each of which was subjected to comprehensive property analysis.

To define the most favorable thermal properties of the carbon, system-level simulations were performed. Results were generated by modeling the effective conductivity of carbon mixed with aluminum fins, as well as the results from fabrication trials and the production techniques likely to be employed in construction of the generators. The generator used for simulations employed the same design as the one used for testing of the brazed construction. The carbon used in this generator was modeled on the results from the geometry where aluminum fins were packaged in the carbon with a pitch of 4 mm. Figure 2 shows results from the model. The figure displays the average temperature of the carbon bed over time, assuming a constant wall temperature. This result is a fair representation because the plate-type generators were designed to operate isothermally, and the flow rate of the heating water was sufficiently high to give a steady heating temperature (low temperature drop in water).

The performance of the expected design is shown by the blue line in Figure 2. This behavior corresponds to the use of granular carbon (conductivity 0.4 W/mK) pressed between 0.1 mm thick aluminum fins with a pitch of 4 mm. The yellow and green lines represent alternate fin pitches. Each of the orange lines represents the behavior of a model carbon with higher conductivity. It can be seen that the carbon with the desired fin design responded in a very similar way to the model carbon with a conductivity of 2.5 W/mK. This value was used to model the behavior of the carbon in the system simulations. The mass of the aluminum fins was also considered.

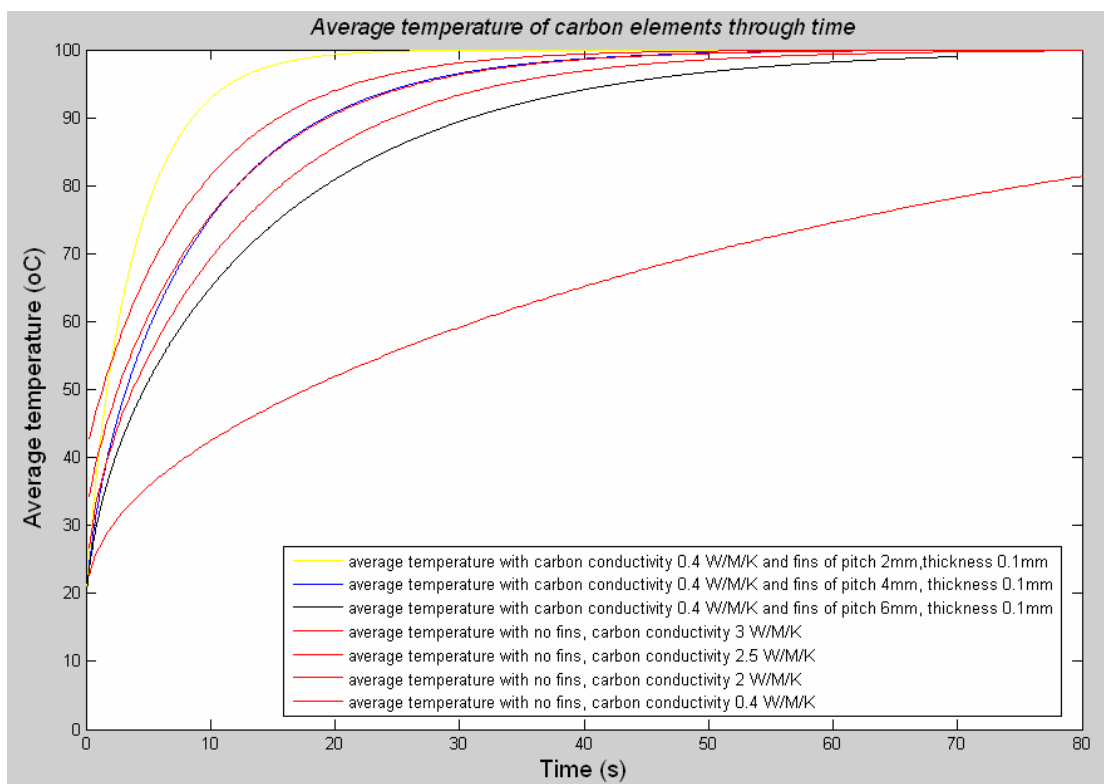


Figure 2. Thermal Behavior of 12-mm Carbon-Containing Aluminum Fins

2.1.2 Increasing the Gas Storage

Because the monolith carbon was to be modified with low-porosity (or zero-porosity) additives to enhance thermal conductivity and permeability, to reach the required high gas adsorption capacity it became necessary to increase the carbon porosity to compensate for the loss. The first R&D thrust concentrated on third-party technology that ATMI was evaluating for this and other applications. It focused on ways of removing amorphous carbon deposits to increase the micropore volume of the monolith available for gas storage. These deposits are formed during the PVDC pyrolysis process that generates the carbon, and they block access to porosity that is known to exist deeper in the carbon monolith.

The second thrust was based on established ATMI carbon materials technology previously developed and protected with filed patents. It involved developing methods to cause a permanent restructuring of the carbon. Evidence had been generated showing that when gases adsorb on the carbon (in particular, water vapor), some restructuring occurs. X-ray diffraction studies revealed the development of some long-range order where previously none existed. When such ordering occurs, gas storage capacities increase significantly; however, the effect is not permanent; the carbon undergoes a relaxation with time.

A third thrust was to enhance the gas capacity by high-temperature activation of the carbon in a mildly oxidizing atmosphere (CO_2). This approach required ATMI to set-up a laboratory furnace and gas handling equipment to achieve the desired level of burn-off of the carbon on a small scale and then transfer this technology to the larger scale furnaces. This strategy was eventually selected as the preferred method for enhancing storage capacities for this project.

2.2 Design of Adsorption Generators

The overall design of the adsorption refrigerator was modeled on the design used for the TOPMACS project as shown schematically by Figure 1. The plate heat exchangers used for the TOPMACS project were re-designed for improved efficiency and performance under the expected conditions. The design of both carbon and liquid sides of the exchanger were modified to increase the relative volume of carbon and improve the heat transfer on the liquid side.

2.2.1 Heat Transfer Fluid

The heat transfer on the liquid side had been modeled in isolation to provide a heat transfer coefficient for use in the refrigeration system simulation and to allow different heat transfer liquids to be easily assessed. This approach allowed ruling out the use of oil, as the viscosity and conductivity gave very low heat transfer coefficients. The modeling result led to the decision to use a pressurized water system to transfer heat to and from the beds.

2.2.2 Heat-Exchanger Design

Several designs had been developed, some of which required different manufacturing techniques. The intention was to develop a plate exchanger that was more easily and inexpensively manufactured. Trials in welding new plate designs met with a certain degree of success: a single plate had been welded to a new design (as opposed to the previously brazed exchangers) and pressure tested to 30 bar. Concurrent to the design of a welded exchanger, new designs of brazed exchangers were investigated. Pressure testing of the welded generator demonstrated that very thin walls could be used around each plate. New shims could be produced that were not excessively massive, ensuring that a viable and tested manufacturing process could be used.

Re-design of the exchangers was essential to optimizing the performance of the refrigerator. System level simulations of the exchanger designs were required to determine the best exchanger design and to select and match the components of the system. Test pieces were brazed up in order to establish a production methodology for the generators. A new fabrication technique was developed for the deep carbon plates required for this particular application. The technique involved fabrication of new spacers for the construction of the plates that hold the carbon. Early trials involving the welding of the generator plates were encouraging yet could not offer the assurance of successful integration into the complete generator module. The tried and trusted method of brazing was believed to offer a more reliable approach to the construction of the final units. Pressure testing of single welded plates indicated that initial concerns over the wall thickness of the U-bars were unfounded.

Any adsorption-refrigeration system performs best when the ambient temperature is low, when the heating water temperature is high, and when the evaporator temperature is high. However, it was necessary for the evaporating temperature of the ammonia to be fairly constant near -10°C in order to chill the container and make ice. Only during the initial cooling of the container would the ammonia boil at much higher temperatures, which allowed a higher cooling power and COP to be achieved.

The cold approach temperature of the carbon bed towards ambient -- ΔT_{cold} -- is a variable that can be actively controlled. The choice of ΔT_{cold} allows the system to be optimized for cooling

power or COP and also determines the cycle time. As ΔT_{cold} is increased (or cycle time reduced) the cooling power increases but the COP decreases. In the last row of Table 1 it can be seen that a COP of 0.32 can be achieved if the carbon bed is cooled to 42.5°C ($T_{\text{amb}}=40^\circ\text{C}$), but the system delivers less than 1 kW of cooling. Fifty-percent more cooling power could be delivered if the carbon were cooled to only 55°C (fourth row from bottom), but the COP would drop to 0.26. This result may look promising but a significant amount of heat must be collected and dumped (almost 5.7 kW in this case), requiring large collector areas and large fan coils. These factors must be assessed in specifying the system components in order to deliver as much cooling as possible in an efficient manner, over the course of each day.

The results of these simulations determined the final collector specification in terms of the required operating temperature and collector area. Once the system performance had been determined, the outsourced parts (such as condenser and fan coils) could be specified and ordered.

2.2.3 Load Calculations

Additional load calculations were carried out (using software developed to model cold rooms) to estimate the likely cooling required by the refrigeration system over the course of a day. The results of this simulation were slightly more encouraging than the "back of the envelope" calculations performed previously; this is to say that a slightly lower cooling load was predicted. The model highlighted the high power required to maintain the container temperature after door opening events, and hence the requirement for good heat transfer and/or a large heat transfer surface area on the evaporator. The information provided by the U.S. Army on likely door openings and thermal loads allowed a more realistic simulation of the anticipated cooling load.

2.2.4 Collector Modeling and Selection

Six different solar collectors were modeled. The collectors represented the entire range of evacuated (vacuum) panels offered by Thermomax[®], a company who manufactures some of the best collectors on the market.

Initial work was carried out to determine the likely environment under realistic operating conditions. Some meteorological data for the likely test sites were obtained to optimize the entire refrigeration system performance.

Flat panel evacuated tube collectors from Thermomax[®] were assessed for their performance characteristics. Thermomax[®] manufactures two different types of evacuated tube collectors, and each of these comes in either 2m² or 3m² packages. The two collector types offered by Thermomax[®] are a direct-flow type, whereby the operating fluid flows down and back up the evacuated tube, and a heat-pipe type, which uses a heat-pipe within the evacuated tube to collect heat and transfer it to the operating fluid in a manifold above the tubes. The plots in Figure 3 suggest that the 2m² direct-flow collector would perform better under all conditions.

Assessment continued by matching the solar collector characteristics with more accurate and realistic modeling of the refrigeration unit. Figure 4 contains a plot of the system performance under steady-state conditions (i.e., the evaporating temperature is set low for making ice).

Table 1. Load Calculation Results

T _{amb} , °C	T _{HW} , °C	T _{evap} , °C	ΔT _{co} , °C	CP _{avg} , kW	CP _{avg} /COP _r	COP _r	t _{cycle} , s
30	120	10	15.0	1756.1	3669.0	0.4786	257.1
30	120	10	10.0	1662.4	3202.4	0.5191	326.8
30	120	10	5.0	1475.2	2688.6	0.5487	424.4
30	120	10	2.5	1293.9	2311.7	0.5597	511.6
30	120	0	15.0	1791.9	4845.7	0.3698	178.4
30	120	0	10.0	1628.2	3998.2	0.4072	254.2
30	120	0	5.0	1340.3	2998.8	0.4469	376.0
30	120	0	2.5	1137.5	2456.5	0.4630	478.6
30	120	-10	15.0	1298.8	4562.8	0.2847	144.9
30	120	-10	10.0	1349.6	4045.7	0.3336	205.3
30	120	-10	5.0	1199.3	3274.2	0.3663	305.2
30	120	-10	2.5	1010.8	2673.4	0.3781	402.9
30	140	10	15.0	1942.9	3811.7	0.5097	303.5
30	140	10	10.0	1832.4	3436.2	0.5333	363.8
30	140	10	5.0	1610.5	2923.9	0.5508	455.4
30	140	10	2.5	1409.9	2528.7	0.5576	540.6
30	140	0	15.0	1852.6	4539.0	0.4082	244.6
30	140	0	10.0	1693.6	3846.7	0.4403	316.0
30	140	0	5.0	1448.3	3113.5	0.4651	420.6
30	140	0	2.5	1241.3	2611.1	0.4754	517.7
30	140	-10	15.0	1777.2	5470.9	0.3249	177.4
30	140	-10	10.0	1634.9	4630.2	0.3531	240.8
30	140	-10	5.0	1343.3	3544.7	0.3789	348.6
30	140	-10	2.5	1114.1	2850.1	0.3909	451.4
30	160	10	15.0	2053.1	4056.8	0.5061	325.1
30	160	10	10.0	1914.1	3664.2	0.5224	382.1
30	160	10	5.0	1672.3	3121.4	0.5358	471.9
30	160	10	2.5	1465.5	2706.1	0.5415	556.8
30	160	0	15.0	1905.9	4535.5	0.4202	278.6
30	160	0	10.0	1754.2	3974.3	0.4414	341.3
30	160	0	5.0	1502.9	3268.9	0.4598	441.2
30	160	0	2.5	1293.2	2761.6	0.4683	537.1
30	160	-10	15.0	1833.8	5452.7	0.3363	213.2
30	160	-10	10.0	1641.4	4550.3	0.3607	278.3
30	160	-10	5.0	1363.7	3567.0	0.3823	382.1
30	160	-10	2.5	1147.6	2923.7	0.3925	482.3
T _{amb} , °C	T _{HW} , °C	T _{evap} , °C	ΔT _{co} , °C	CP _{avg} , kW	CP _{avg} /COP _r	COP _r	t _{cycle} , s
40	120	10	15.0	1461.5	4354.7	0.3356	156.9
40	120	10	10.0	1473.5	3912.8	0.3766	217.9
40	120	10	5.0	1239.0	3001.7	0.4128	331.1
40	120	10	2.5	1037.4	2400.5	0.4322	435.5
40	120	0	15.0	929.1	4140.3	0.2244	121.1
40	120	0	10.0	1077.0	3629.5	0.2967	182.4
40	120	0	5.0	1009.8	2939.0	0.3436	262.8
40	120	0	2.5	865.3	2404.8	0.3598	379.2
40	120	-10	15.0	264.9	4303.6	0.0616	81.5
40	120	-10	10.0	583.0	3507.4	0.1662	133.2
40	120	-10	5.0	677.7	2697.7	0.2512	231.0
40	120	-10	2.5	607.3	2162.6	0.2808	325.7
40	140	10	15.0	1794.5	4735.0	0.3790	212.1
40	140	10	10.0	1600.1	3828.9	0.4179	290.9
40	140	10	5.0	1366.4	3048.8	0.4482	397.4
40	140	10	2.5	1172.1	2547.7	0.4601	492.5
40	140	0	15.0	1543.7	5029.6	0.3069	165.6
40	140	0	10.0	1511.8	4467.7	0.3384	222.6
40	140	0	5.0	1273.8	3496.4	0.3643	325.2
40	140	0	2.5	1062.0	2825.8	0.3758	423.7
40	140	-10	15.0	1055.3	4806.8	0.2196	132.4
40	140	-10	10.0	1134.6	4224.7	0.2686	185.9
40	140	-10	5.0	1026.3	3384.2	0.3033	277.1
40	140	-10	2.5	867.3	2742.4	0.3163	368.1
40	160	10	15.0	1834.5	4481.8	0.4093	266.0
40	160	10	10.0	1695.6	3910.4	0.4336	329.4
40	160	10	5.0	1458.3	3217.0	0.4533	427.2
40	160	10	2.5	1256.1	2719.6	0.4619	519.7
40	160	0	15.0	1818.6	5585.9	0.3256	196.5
40	160	0	10.0	1612.9	4573.0	0.3527	264.8
40	160	0	5.0	1333.9	3545.5	0.3762	369.6
40	160	0	2.5	1120.7	2898.3	0.3867	467.8
40	160	-10	15.0	1486.1	5663.5	0.2624	159.8
40	160	-10	10.0	1429.5	4965.5	0.2879	210.0
40	160	-10	5.0	1192.8	3840.7	0.3106	303.3
40	160	-10	2.5	992.3	3100.5	0.3201	394.3

Where:

- T_{amb} - ambient temperature (temperature of the outside air)
- T_{HW} - temperature attained by the water in the solar panels
- T_{evap} - evaporating temperature of the ammonia in the container
- DT_C - temperature differential between carbon and ambient
- CP_{avg} - average cooling power delivered by the system
- COP_r - refrigeration coefficient of performance (cooling capacity/power input)
- CP_{avg}/COP_r - ratio of average cooling power and the COP
- Cycle Time - time necessary for the carbon bed to complete one cycle

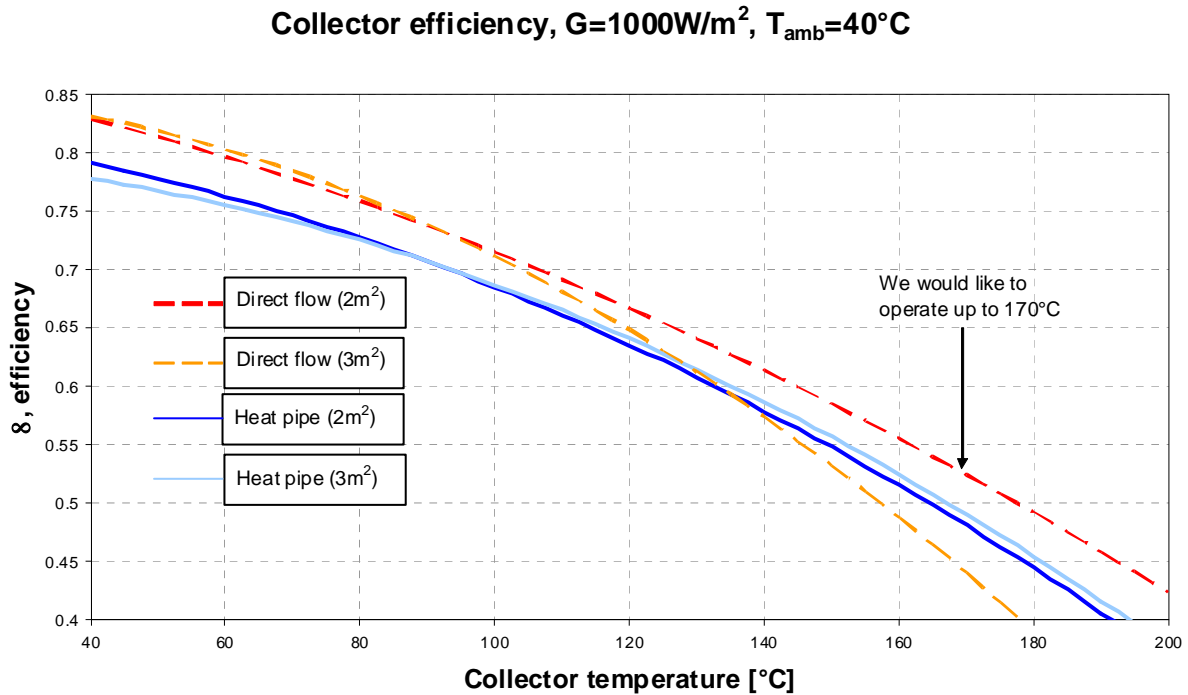


Figure 3. Solar Collector Modeling

Figure 4 shows the output from the $6m^2$ solar collectors in orange for four different levels of irradiance. The heat demand of the refrigeration unit is shown in navy, pink, green and blue for the different cold approach temperatures. The corresponding cooling delivered is shown by the dashed lines, which relate to the right-hand axis. Running the refrigeration unit with a ΔT_{cold} of $15^\circ C$ appear pointless under these conditions; however, it would be more beneficial while the container is cooling down (i.e., the T_{evap} is higher). The figure suggests that more than $6m^2$ of solar collectors will be required in order to provide the necessary cooling.

The evaporator was a critical area of the overall design. There were various technical difficulties/complexities in physically constructing hardware assimilating the ideal evaporator. Instead, designs that limited the amount of complex pipe work, number of valves and associated

control systems were evaluated. The simplest mechanism that was still effective was to have one evaporator that operates at a single evaporating temperature/pressure. The question then was how to arrange the ice bank around the evaporator such that it could transfer heat from the ice to the evaporator and from the air to the evaporator/ice bank combination.

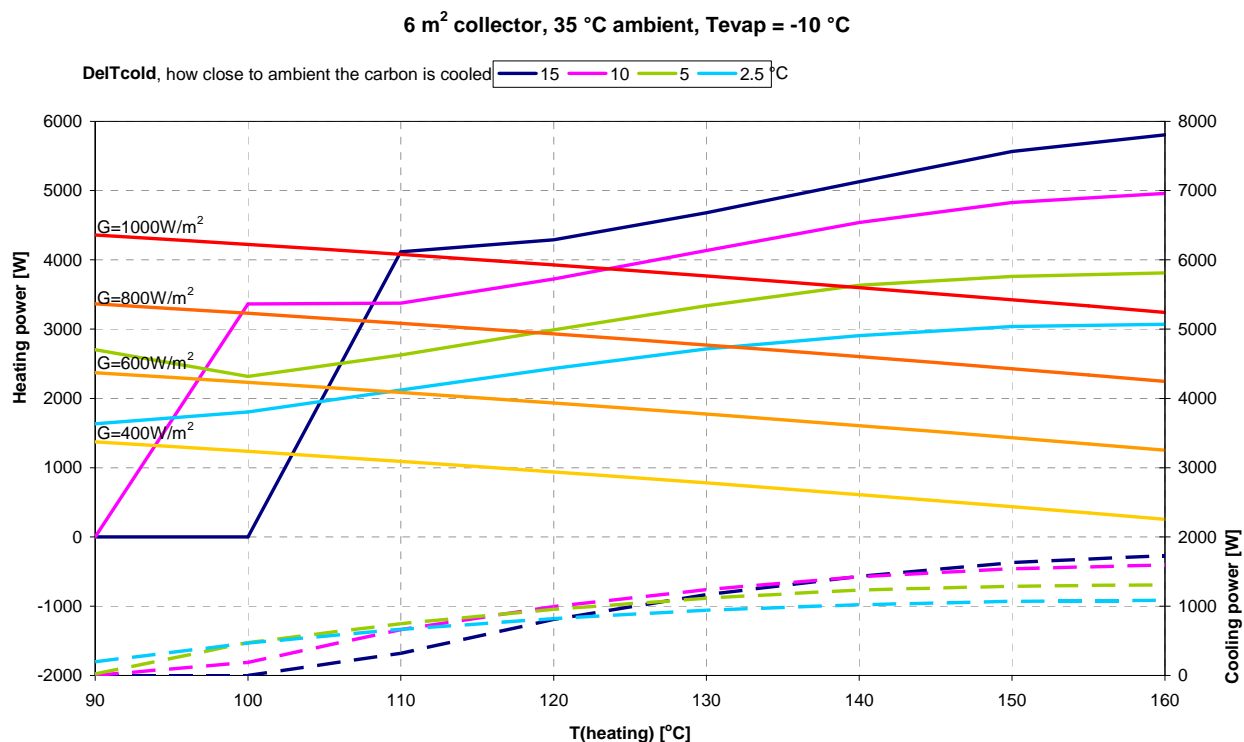


Figure 4. Solar Collector Output, Refrigerator Heat Demand & Cooling Output

2.2.5 Evaporator Specification and Design

Initially, it was believed part of the evaporator should be inside the ice bank, and part should be exposed to the air in the container. This approach would allow heat to be taken from the air in the container directly by the evaporator. However, where the evaporator pulls heat from cannot be controlled; it simply takes most of its heat from the air or water, whichever is the warmer. The construction of an evaporator that was “half-in, half-out” of the ice bank presented a variety of interesting design problems, especially from a construction point of view. After much debate and discussion, it was determined that little advantage would be gained from this arrangement. If the evaporator were built into the ice bank, little difference in performance would likely be experienced other than during the initial chilling of the container from a warm start situation. Under steady-state conditions, the cooling power that can be delivered by the refrigeration unit is determined by the surface area of the ice bank. As long as the unit specified can meet the cooling demands of the application, there should be no requirement for direct contact between

the evaporator and the air within the container. Even so, it would still be beneficial to keep the evaporator as close to the wall of the ice bank as possible.

Load calculations provided a good approximation of the volume of ice required to maintain the container temperature throughout the day and night. Heat transfer modeling allowed the development of the fin design for both the front and the back of the ice bank. The fins were designed to give appropriate air flow regimes on the front and back of the ice bank: on the front the fins were designed to give two separate convective regions at the top and bottom of the ice bank, whereas the back of the ice bank was designed for convection along the full height of the surface. Figure 5 shows the evaporator fully assembled and fitted within the ice bank.

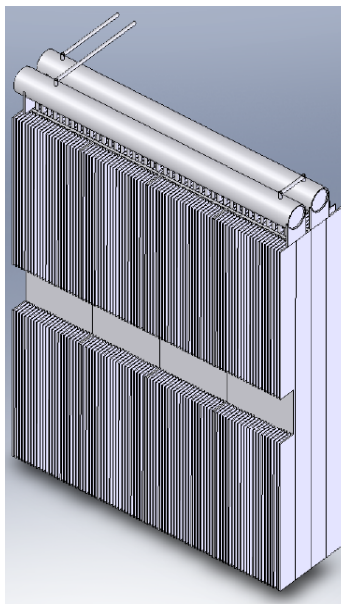


Figure 5. Evaporator Design

2.2.6 Modeling of System Level Performance

The expected performance of the refrigeration system is illustrated in Figure 6 and Figure 7 for steady-state (ice making) conditions with an ammonia evaporating temperature of -10°C . These figures give the performance at ambient temperatures of 30°C and 40°C , respectively. The system was modeled with 8 m^2 of solar collectors, and the heat collected at different levels of irradiance is shown by the orange lines.

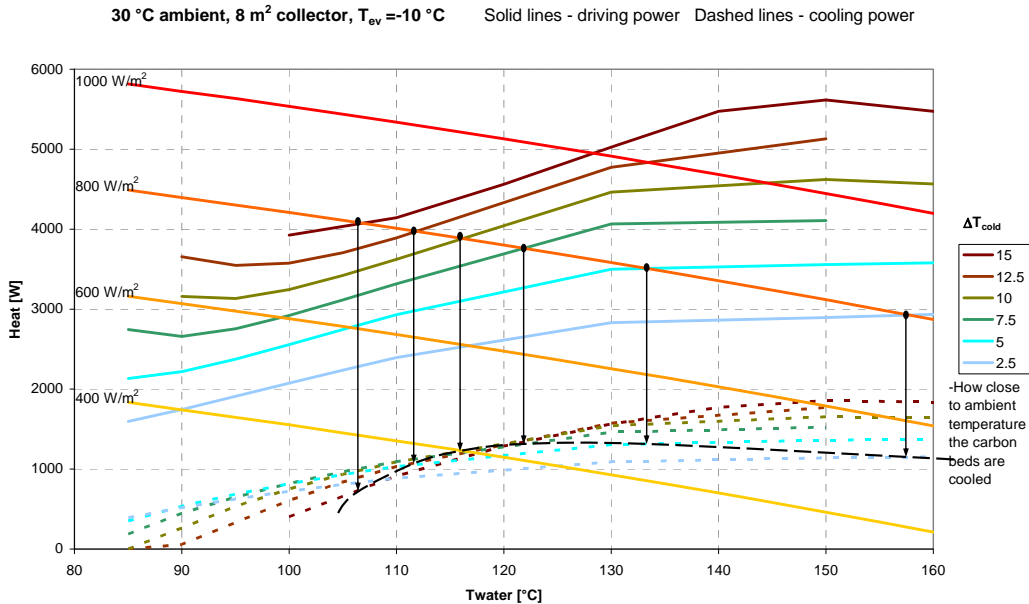


Figure 6. System Modeling – Cooling Power at 30°C Ambient

Given solar radiation, the refrigerator can run with a cycle time chosen to optimize the cooling power delivered to the container. In the figures shown here, the variable ΔT_{cold} is used to represent different cycle times. Longer cycle times result in the carbon beds being cooled more; they will be closer to ambient, with a smaller ΔT_{cold} .

When the insolation is 800 W/m², six operating points can be plotted: Figure 6 shows the refrigerator operating with minimum bed temperatures of 32.5, 35, 37.5, 40, 42.5 and 45°C. Each of these different operating conditions results in a different cooling power being delivered to the container. The cooling power is read by finding the operating point (heating temperature) from the intersection of the collector and refrigerator characteristics and then tracing down to find the cooling power for that cycle (dashed line of same color). By doing this for each of the six different cycles, a cooling curve can be established for the given level of insolation and ambient temperature. The cooling curve is shown in Figure 6 as a black dashed line. At 30°C and with 800 W/m² insolation, the refrigerator delivers the greatest cooling when the carbon beds are heated at 122°C and cooled to 37.5°C. Under these conditions, approximately 1400 W of cooling is delivered to the container.

Figure 7 shows performance for the refrigerator at 40°C. As above, a cooling curve has been drawn. This plot indicates that at 40°C and with 800 W/m² insolation the refrigerator delivers the greatest cooling when the carbon beds are heated at 144°C and cooled to 45°C. Approximately 1100 W of cooling is delivered to the container.

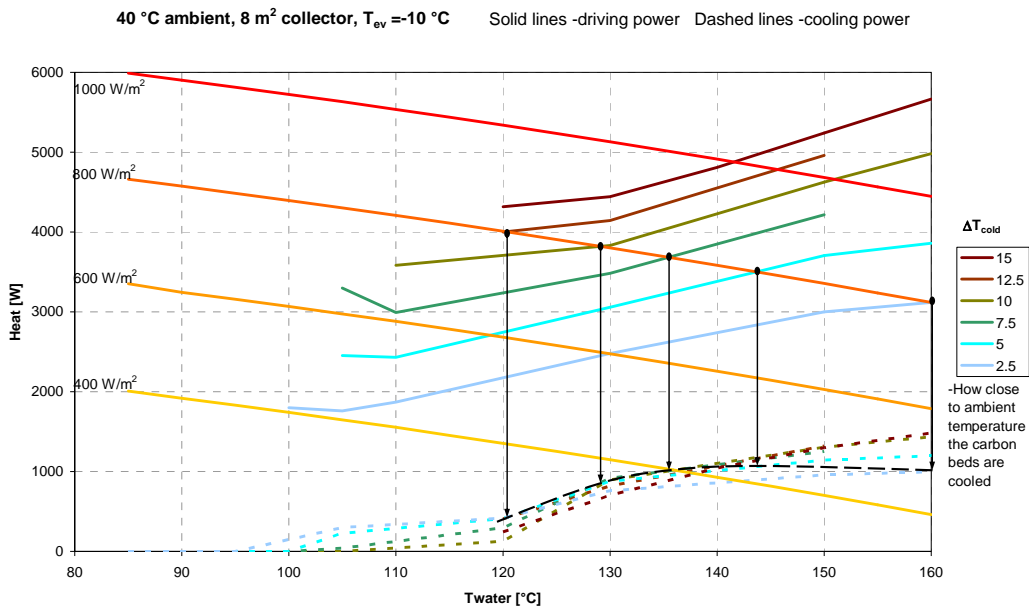


Figure 7. System Modeling – Cooling Power 40°C Ambient

Figure 6 and Figure 7 demonstrate that obtaining a cooling curve for any given condition is not straight forward. The figures show how the cooling power can be optimized by adjusting the cycle time (determined by how close to ambient the carbon beds are cooled). These figures represent the performance at steady-state conditions with an evaporating temperature of -10°C; however, in realistic circumstances the refrigerator will not always be operating under the same conditions, so different cooling curves and performance may be expected. In particular, the performance will be most noticeably different while the container is initially being cooled. During this draw-down period, the evaporating temperature may be much higher, and there would be a corresponding improvement in the performance and cooling power delivered by the refrigerator.

The figures demonstrate that the heat collected by 10 m² of collectors could be utilized even with a high insolation of 1000 W/m². Figure 6 suggests that such an installation operating at 30°C ambient temperature could provide 1850 W of cooling for ice making and even more when the evaporating temperature is higher.

2.2.7 Check Valves

The Swagelok SS-8C-1/3 check valves used in earlier lab cooling systems were proven to be less reliable and not sufficiently robust. Despite its better cracking pressure (1/3 psi corresponding to about 20 mbar and standard leakage of 0.01%), the design of the O-ring seal does not operate well with the pressure and temperature variations of ammonia gas in this application. In fact, the O-ring is often dislodged and the check valve fails to operate properly. Two different valve designs were evaluated.

A check valve manufactured by Parker Instrumentation -- 8AC8L-1/3-T-SS -- was identified as appropriate for the current application. Its design is fairly similar to Swagelok SS-8C-1/3 with

the exception that it has a molded, resilient PTFE seat as opposed to an O-ring. Four of these valves were tested on the lab cooling system with ammonia and have performed as well as the Swagelok ones in term of both COP and cooling production (typical average: 1.5 kW and COP near 0.22).

Another valve evaluated was an RS #RS-237-2470. It is a steel ball-type check valve and a metal-to-metal seal with the advantage of an auto-cleaning seat. Table 2 summarizes the experimental results testing carried out with compressed air under 3.4 bar as recommended by ANSI/FCI 70-2 1976 (R1982). Four of the modified ball check valves were tested on the lab cooling system using ammonia. They performed as well as the Parker 8AC8L-1/3-T-SS in terms of both COP and cooling production (typical average: 1.5 kW and COP near 0.22).

Table 2. Check Calve Evaluation (RS-237-2470) with Compressed Air

Ball Retainer Material	Spring Rate (N/mm)	Stainless Ball Diameter (mm)	Forward Flowrate (m³/h)	Backward Flowrate (m³/h)	Leakage (%)
Nylon	Original	Original	19.764	0.0370	0.187
Nylon	Original	11.1	20.304	0.0120	0.060
Nylon	0.650	10.3	20.520	0.0070	0.034
Aluminum	0.650	10.3	18.432	0.0070	0.038
Aluminum	0.650	10.0	19.512	0.0370	0.019
Aluminum	0.430	10.0	19.296	0.0024	0.013

Although this valve was inexpensive (£25 / €32 each), the initial test evaluation (cracking pressure of 350 mbar, and percent leakage 0.2%) did not match design requirements. Furthermore, the nylon ball retainer could soften under use temperature and increase the seal leakage. A design modification was carried out to improve the valve characteristics: the original ball (11.9 mm diameter) being replaced by a slightly smaller size ball (10.3 mm) after numerous tests with various sizes. To reduce the cracking pressure, different springs were evaluated, and a new spring was selected (spring rate: 0.43 N/mm). A new ball retainer was manufactured in aluminum for lower working temperatures of up to ~100°C, but could also be made in steel for higher working temperatures up to 200°C.

2.2.8 Water Three-Way Valve

The water three-way valve in Figure 1 was an electrically driven ¼ turn valve. The valve body was a ½" ball-valve made in stainless steel and supplied by Swagelok under the reference 3L66RT-050. Its flow coefficient K_v was 5.2 m³/h. The valve was coupled to a 24 VDC electrical motor with a nominal power of 20 W. This motor could produce nominal torque of 5 Nm, enough to turn the valve fully in approximately 1 second.

An off-the-shelf valve that met the requirements would have the following specifications:

Operating ambient temperature: 60°C
Medium temperature: 180°C (water)
Minimum K_v value: 5 m³/h
Minimum rated pressure: 10 bar
Preference Opening time: 1 second (time to cover the 1/4 turn)
Preference size: 1/2" or 3/4"
Preference Type: not permanently powered.

2.3 Carbon Plate Sets

ATMI had been working to enhance the microporosity and gas storage capacity of the carbon monoliths in support of ATMI's existing product line. Three approaches were evaluated during the progress of this work; however, the materials generated from these approaches, when subjected to ammonia adsorption, yielded slow rates of adsorption. It was therefore decided to resort to a fourth procedure—oxidative burn-off. To understand the effect of this treatment, nitrogen micropore volume measurements were obtained, and selected samples were subjected to both low-pressure ammonia adsorption (< 1 bar) and high-pressure ammonia adsorption (~8 bar). These experiments established that the lost porosity that results from inclusion of functional, nonporous additives could be recovered through a final oxidation step.

The properties of the carbon test pieces are reported in Appendix A. The first scale-up of carbon monolith pieces for evaluation was achieved in late April 2008 at the Pennsylvania ATMI manufacturing facility. The pieces represent six different compositions, four pieces of each. The 24 plates were pyrolyzed and activated, and 21 plates were shipped to the University of Warwick for evaluation (four were overly activated and discarded). The properties of the six sets of plates are reported in Table 3. The target properties are also reported.

The permeability measurements are reported as cc/psi/cm²/min and the thermal conductivities as W/m-K. These properties ranked highest in priority for the selection criteria, followed by the carbon density, the BET surface area (Brunauer, Emmett, and Teller), and the two calculations of micropore volume (MPV). The Horvath-Kawazoe (H-K) and Stoeckli values are ways of depicting the average pore sizes of the carbons. The final validation test for the plate materials was, of course, the capacity for ammonia at the two test conditions (40°C and 140°C). The results are shown in Figure 8. As expected, each of the samples showed capacities close to target and the delta capacities close to the 15 wt.% target. Warwick then tested selected plates for permeability, gas capacity and thermal conductivity.

Table 3. Properties of Carbon Plates Submitted for Evaluation

Properties of Carbon Test Plates																	
NewID	Test small		Pieces**	Thermal cond	Weight	Length	Side	Thickness	Density	BETSA	t-MPV	H-K	D-R Eo	D-A Eo	D-A MPV	Exponent	Steeple
	Pieces**	mm															
1614-9-1A1	177	1.83			118.90	111.23	111.37	10.00	0.96								
1614-9-1B1					119.00	110.36	112.49	9.86	0.97								
1614-9-1C1					119.70	111.56	112.39	9.82	0.97								
1614-9-1D1					120.90	111.69	111.77	10.07	0.96	1197	0.442	0.77	25.0089	26.9258	0.484	1.6809	0.79
1614-9-2A1	245	1.38			106.1	111.87	111.64	10.04	0.85								
1614-9-2B1					118.8	111.44	110.94	9.77	0.93								
1614-9-2C1					112.5	112.85	112.84	10.11	0.87								
1614-9-2D1					112.1	112.81	112.06	9.98	0.89	1184	0.436	0.78	25.0342	27.7913	0.484	1.5779	0.79
1614-9-3A1	369	2.04			121.9	111.46	111.86	10.54	0.93								
1614-9-3B1					109.2	111.92	111.35	10.10	0.87								
1614-9-3C1					111.6	110.86	112.60	10.30	0.87	1339	0.493	0.77	25.0179	29.3284	0.563	1.3475	0.79
1614-9-3D1					111	113.44	112.97	10.21	0.85								
1614-9-4A1	169	2.06			119.4	110.60	110.94	10.38	0.94								
1614-9-4B1					119.8	110.88	111.27	9.93	0.98								
1614-9-4C1					120.3	110.92	111.41	9.95	0.98								
1614-19-4D2					113.9	110.72	111.25	9.9	0.93	1299	0.477	0.78	24.0654	25.8361	0.529	1.6679	0.85
1614-19-5A2	133	2.112			110.6	110.18	110.88	9.81	0.92								
1614-19-5B2					116.3	110.29	112.04	10.23	0.92								
1614-19-5C2					113	111.21	110.44	9.77	0.94	1192	0.438	0.78	24.0647	25.4087	0.481	1.7427	0.85
1614-19-5D2					116.2	111.76	110.7	10.23	0.92								
1614-9-6D1	281	2.11			117.8	113.41	114.09	9.80	0.93								
Target Properties	600	1.8							0.95	1050	0.450				0.49		
Stretch	1000	2.5							0.99	1200	0.500				0.52		

Table 22 - Refer to introduction

Note **: Prior to oxidation

Their summary report of this testing is attached as Appendix B. The composition selected based upon the ATMI and Warwick results was the 1614-9-3 material.

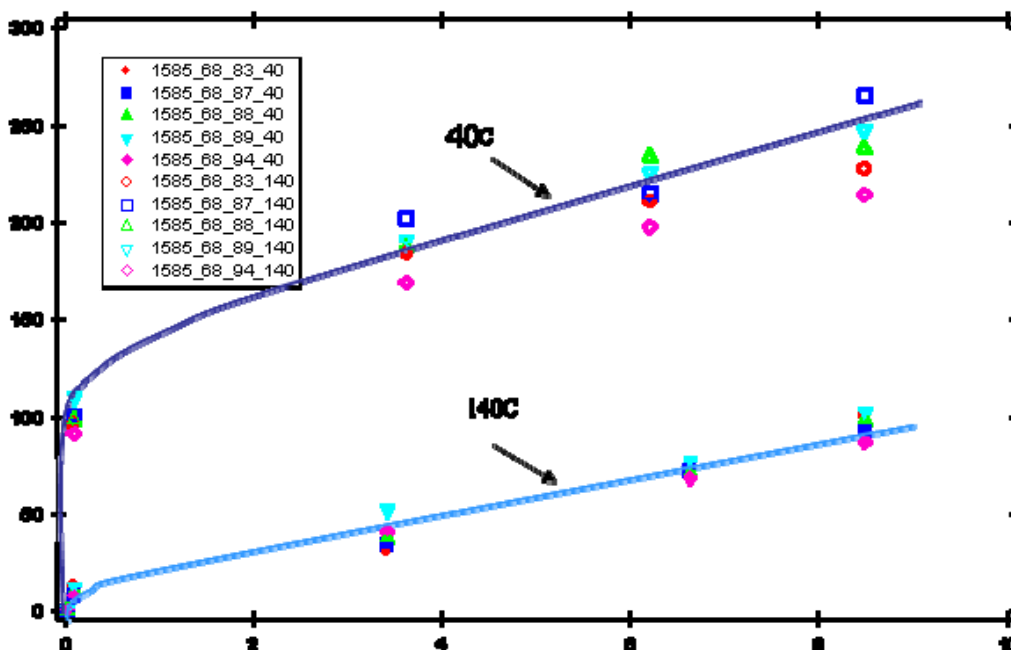


Figure 8. High-Pressure Ammonia Isotherms

2.3.1 Scale-up Production

Although the generators required 12 mm thick plates, initially a decision was made to produce plates 15 mm thick to allow for milling down to final size just prior to insertion into the generators. This approach would accommodate the potential for some plate warpage during pyrolysis. The scaled-up mix of powders were blended to ensure uniform composition and then pressed into 62 plates. These plates were then subjected to pyrolysis and to a CO₂ activation step to enhance pore volume, surface area and permeability. Of the 62 plates, 40 were pyrolyzed in a tube furnace while 22 were pyrolyzed in a conveyor furnace. The latter was attempted since much flatter plates could be generated in the conveyor furnace. However, these plates responded very differently to the activation step and became over activated when treated to the same conditions as the tube-furnace material. Over activation results in very poor physical strength and stability of the plates.

The 40 test plates from the tube furnace pyrolysis were activated in two batches, one batch of 24 and one of 16. Selected samples from test plates were then analyzed for porosity properties, and all of the plates were shipped to the University of Warwick for surface milling to ensure perfect flatness and insertion into the two generators. Based upon the size of the generator slots, it was estimated that between 38 and 40 plates would be necessary to fill the two generators. The surface properties of the sampled plates matched or slightly exceeded the properties of the target 3C test plate analyzed earlier at Warwick and declared to be the most favored of the test plates analyzed by them (Table 4). These results suggested that the "A" plates and some "B" plates be used. The "C" plates were only to be used as a contingency in the event of, for example damage in transit, the others plates were insufficient to complete the generator fill.

During late 2008, various machining procedures were attempted to reduce the thickness of the plates: milling, lapping, sanding, and grinding combinations all failed to result in smooth-sided plates 12-mm thick. The carbon surface became pot-holed and when inserted into a single cell test frame to evaluate the thermal contact conductance, the carbon showed decidedly poor performance due to poor thermal contact with the walls. However, several of the 15-mm plates did respond well to sanding. Their pedigree indicated that they were among those plates which received a lesser degree of oxidation-activation (11% burn-off vs. 15% burn-off for the majority of the plates).

Table 4. Properties of First Batch of 15 mm Thick Plates

Sample ID	1614-9-3C	A	B	C
Test #	0026	0025	0035	0036
Surface Area BET m²/g	1180	1284	1149	1084
Micro Pore volume 't' ml/g	0.426	0.46	0.41	0.39
Slit Size Horvath-Kawazoe nm	0.57	0.57	0.57	0.55
Dubinín-Rad. Eo	26.34	26.13	26.21	28.65
Dubinín-Astakhov Eo	26.97	26.73	27.13	29.43
Micro Pore Volume D-A ml/g	0.480	0.52	0.47	0.44
Exponent	1.822	1.81	1.77	1.85
Slit width (Stoeckli) nm	0.72	0.73	0.73	0.63
Density g/cc(average of plates)	0.87	0.87	0.84	0.73
Number of plates		24	16	22

In December 2008, work began to re-make the plates. They were fabricated directly to the 12-mm final thickness target, and plans progressed to process them in the ATMI conveyor furnace to ensure as flat a plate as possible (the conveyor furnace was not fully commissioned at the time the plates were fabricated in July).

Unfortunately, the stock of one carbon additive, the carbon beads, used to produce the first set of plates was insufficient for a second production of plates, and the original vendor was unable to supply a new batch. A second supplier was sought. When samples of beads from the new supplier were received, they were incorporated into test pieces and subjected to finishing. It was found that these coupons did not possess the necessary strength and were rejected. Experiments were undertaken to understand the weakness of the plates, and a modified set of specifications for the beads was defined. A batch of beads from the new vendor was ordered, and experiments commenced to identify the necessary bead content to meet the permeability target.

In parallel to the efforts focused on re-making the plates, sanding of the stronger plates continued along with experiments to determine whether the sanded surface could have its thermal contact conductance improved through high-thermal-conductivity coatings. The application of such coatings is common in the semiconductor field where removal of heat from semiconductor devices is often of paramount importance. Early experiments indicated that a much smoother surface could be generated using this coating procedure. As satisfactory results were obtained using a commercially available high thermal conductivity epoxy resin to enhance thermal contact conductance, more of this epoxy was purchased and shipped to the University of Warwick to be applied to the surfaces of the carbon plates prior to installation into the two generators.

A new mix composition with new beads resulted in the preparation of an initial 60 mixes ready for pressing in late January. Problems were experienced immediately with the press used for this task, so a number of the plates had to be discarded. Once the pressing problems had been overcome, an additional 24 mixes were prepared at Danbury and shipped to the Pennsylvania manufacturing location for subsequent successful pressing. The plates were to be pyrolyzed in the conveyor furnace early in February 2009, but more problems arose when trying to bring the furnace back on-stream (it had been shut-down since October 2008 due to market conditions). A test of a number of the pressed plates was started on February 25th, 2009, and a separate test was begun in one of the batch tube furnaces in Danbury with the test plates lying horizontal rather than standing vertical. The latter test proved unsuccessful. On discharge from the furnace, the pyrolyzed plates were clearly warped. Thirty-five of the plates that had been loaded into the conveyor furnace in February all exited badly warped as well. Because the warping also occurred in the 100% polymer plates included in the conveyor furnace run, the fault appeared to lie with the pressing operation. The staff in Pennsylvania then conducted an extensive series of pressing tests with 100% polymer to find the root cause of the problem. These plates were subsequently fed into the conveyor furnace and yet again, when discharged, all were warped.

Concurrently, a test was performed in the Danbury tube furnace, with pressed polymer-mix plates, which are known to warp, but this time weight was applied during the pyrolysis in an attempt to maintain the plate flatness. This test was successful, and plates subjected to a certain weight force were discharged quite flat-sided. Since the pressing problem had not been resolved by March 27th, it was decided to press the remaining mixes and subject the plates to pyrolysis with weight applied. Four pilot tube furnaces were applied to this task during April, and although problems were experienced with the off-gas scrubber at Danbury delaying completion, the plates were finally discharged during week 17. These plates along with plates from previous tests were carefully screened for flatness, and pieces exhibiting reasonable flatness were selected for further work. This effort constituted sanding the side faces with intermittent checks by laying them on a flat steel surface followed by cutting the edges to produce as flat-sided and as tightly packed set of pieces as possible to fill a single slot in the generators. The dimensions of the slots were 143 mm deep by 139 mm wide, and the carbon sets were cut by hand to achieve these dimensions. The sanding was successful, as it had been learned that if sanding was attempted prior to final activation, a reasonably smooth-sided plate could be produced.

Because many warped reject plates were available in March, tests were completed with them to confirm the CO₂ activation step in one of the Danbury tube furnaces. These activation conditions were then applied to the 24 sets of carbon (along with the 12 test pieces) during week 18, and the final material packed and shipped to the University of Warwick for installation in the two generators. The average weight of each set was in excess of 200 grams, suggesting that the final loaded weight of carbon in the generators would achieve the target 2 kg of carbon per generator.

Characterization data for the 12 test pieces are shown in Table 5 and Table 6. Some benefits of increased permeability with the latest test plates were evident over the target material and that of the A plate produced in 2008. The thermal conductivities were close to target values but exhibited significant variability depending on the location of the test coupon in the sample.

Some inhomogeneity in the distribution of the high conductivity fibers was most likely responsible for this variability.

Table 5. Thermal Data for Test Pieces of Finished Plates

Sample ID	Edge face or internal	% Burn off	Thermal Conductivity				Heat Capacity			
			25C	50C	75C	100C	25C	50C	75C	100C
A-Plate target		12.91	1.720	1.768	1.805	1.834	1.069	1.11	1.163	1.208
X1a	internal	14.21	0.986	1.097	1.09	1.190	0.957	0.896	0.819	0.867
X1b-1	internal	14.21	1.256	1.391	1.374	1.460	1.113	1.094	1.003	1.062
X1b-2	internal	14.21	1.291	1.393	1.399	1.469	0.95	0.979	0.974	1.028
X1c	internal	14.21	0.810	0.875	0.883	0.949	0.875	0.793	0.769	0.812
X1d	Edge face	14.21	0.840	0.936	0.882	0.934	1.065	1.08	0.917	0.941
X1e	internal	14.21	1.075	1.198	1.207	1.259	1.177	1.156	1.066	1.105
X2b	internal	18.5	2.513	2.584	2.721	2.736	1.028	1.037	1.106	1.139
X3a-1	Edge face	21.5	0.636	0.689	0.751	0.808	0.826	0.852	0.905	0.953
X3a-2	Edge face	21.5	0.717	0.771	0.785	0.847	0.985	0.944	0.935	0.997
X3b	internal	21.5	2.318	2.363	2.399	2.439	1.056	1.108	1.161	1.220
X5a	internal	19.9	1.483	1.629	1.614	1.690	1.147	1.131	1.018	1.082
X5b	Edge face	19.9	0.997	1.139	1.123	1.197	1.112	1.078	0.972	1.023
X5c	internal	19.9	1.288	1.397	1.378	1.448	1.127	1.025	0.960	1.018
X6a-1	internal	14.1	1.301	1.379	1.445	1.517	1.004	1.049	1.090	1.144
X6a-2	internal	14.1	1.320	1.403	1.411	1.500	1.109	1.073	1.065	1.127
X6b	internal	14.1	1.232	1.326	1.333	1.434	1.056	1.092	1.067	1.140
X7b	internal	19.2	0.931	1.005	1.056	1.123	0.958	0.945	0.969	1.020
X10b	internal	21.7	2.031	2.054	2.071	2.107	1.228	1.239	1.266	1.317

Table 6. Selected Characterization for Plate Test Pieces

Test pieces	Burn-off %	NH3 capacity	DARCY	40psi perm	BET SA	t-MPV	DA-MPV	Stoeckli
Target	14.35	0.189 g/g	1.145	368.9	1180	0.426	0.48	0.72
A-plate	12.91	0.186 g/g			1284	0.46	0.52	0.73
X1	14.21				1214	0.447	0.499	0.81
X2	18.48		2.0743	611.9	1104	0.409	0.438	0.73
X3	21.50		1.99	531.3	1169	0.425	0.476	0.73
X4	22.70		2.08	823.9	1120	0.409	0.455	0.75
X5	19.86		2.664	796.3	1343	0.487	0.542	0.83
X6	14.10	0.183 g/g	0.7303	318.9	1129	0.414	0.452	0.77
X7	19.16		1.0832	476.89	1156	0.421	0.464	0.81
X8	22.39		0.9573	286.91	1199	0.436	0.479	0.74
X9	25.30				1275	0.462	0.502	0.93
X10	21.65		1.1751	517.01	1326	0.467	0.536	0.84
X11	20.40		1.1059	464.95	1234	0.449	0.494	0.79
X12	17.96		2.6237	1270.4	1175	0.431	0.462	0.84

2.3.2 Generator Construction

Each generator was designed to support nine stainless steel shims with internal ½ mm diameter hollow flow-through sections with the shims ganged together via stainless steel U-bars 12-mm thick. To ensure a leak-free seal, the shims were nickel-brazed to the U-bars. The challenge was then to weld water manifolds to each side of the generator. Previous attempts to weld a generator with a stainless-steel filler resulted in the weld bead cracking, perhaps as a consequence of the higher temperature and interaction with the nickel present between the shims.

As a result of the problems experienced when brazing the generator, it was decided to fit the manifolds using mechanical fasteners and O-rings to seal the system. This technique had been used previously, but under slightly different operating conditions. The advantage of using this method to fit the manifolds was that this procedure would not damage the seal in the generators in any way. The disadvantage was that it would add thermal mass to the generators that would affect the transfer of heat to and from the carbon. Figure 9 and Figure 10 show one of the two generators machined to allow the manifolds to be fitted with O-ring seals.

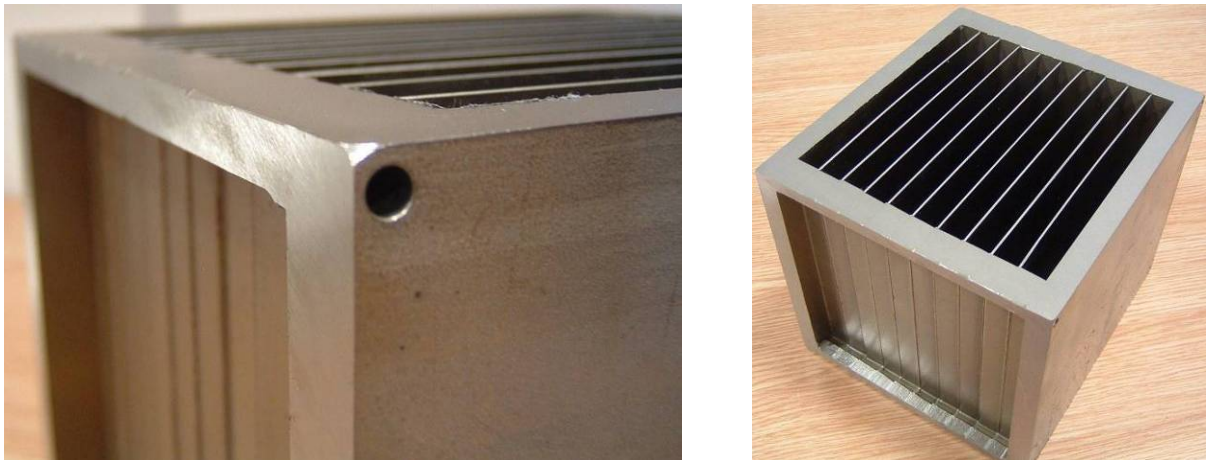


Figure 9. One of the Generators Machined to Receive Manifolds with O-ring Seals

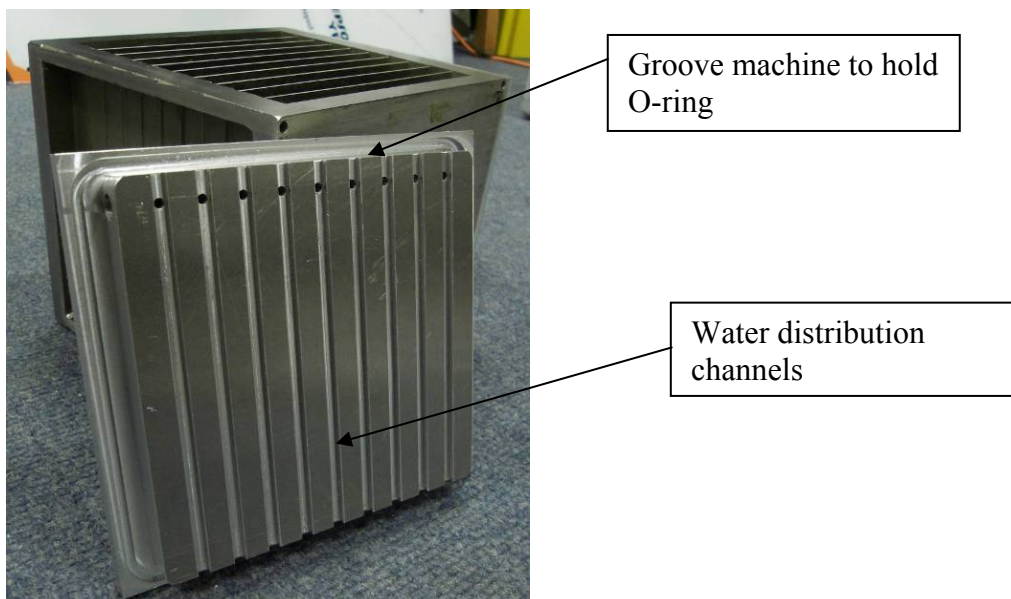


Figure 10. Water Manifold Plate

The two generators with O-ring seals were then pressure tested. Testing was first done with inert gas (argon) up to 8 bar. Unfortunately, one of the generators (Gen 2) leaked under these conditions; gas escaped from the brazed joint between one end plate and the adjoining U-bar. The other generator (Gen 1) passed the inert gas test and was further tested with pressurized water up to 26 bar. The generator held this pressure for 60 hours without any leak or associated

reduction in pressure. It was then taken to over 30 bar to ensure that it would withstand this elevated pressure. Generator 2 was re-welded.

Machining the water manifolds was fraught with difficulties. Initially these problems were the result of errors in programming the CNC machine (computer numerical control), which resulted in incorrect geometries. However, when the plates were almost complete, it was found that it was incredibly difficult to machine the final groove for the O-ring. This problem was caused by the fact that the face in which the groove was to be cut was about 15 mm below the top of the piece. The small tools required for this job underwent considerable flexing when trying to cut the already work-hardened steel. This flex caused the tools to chatter and move around, cutting a wider groove than desired before snapping.

After much discussion, it was decided that the easiest way to overcome the problem was to machine the manifold plates from aluminum rather than stainless steel. The softer material did not cause the tools to flex in the same way, and it was then possible to machine the plates reasonably quickly.

Access for the water supply and return pipes presented a small problem, and there was concern about whether welding them to the manifold plates would cause unacceptable distortion. However, after discussion with the technicians, the pipes were welded onto the plates, and there was no discernable distortion to the sealing faces of the plates.

A second challenge was to find a way of clamping the manifold plates into position. The solution is shown in Figure 11. A second plate was used to clamp the manifolds using 18 bolts to provide an even clamping force across the face of the plate. The second plate is supported by the bracing rods, which hold the plate so that the bolts can be tightened to force the manifold against the generator.



Figure 11. Generator showing Bracing Rods & Clamping Bolts

Both generators were then pressure tested for leaks on the water side (around the new manifolds, Figure 12) by pressurizing both the ammonia and water sides of the generator with compressed air at 7 bar. Both sides of the generator had to be pressurized, as pressurizing only the water side would cause the shims to inflate and rupture because there was no carbon packed inside the generators at this point in time. The ammonia side of each generator had already been tested for leaks. The leak tests revealed small leaks in both generators through the brazed connection between the U-bars, into the cavities that were used to carry supporting rods during firing. These cavities were then filled with silicone, and the generators were re-tested.



Figure 12. Generator Undergoing Preliminary Pressurization to 3 Bar

2.3.3 Plate Installation

Work in June 2009 focused on covering the flat-sided carbon plates with the high thermal conductivity epoxy coating (Cotronics Duralco 132) and packing the carbon into the leak-tested generators. The carbon plates were arranged as shown in Figure 13, but the large plate was cut into three strips so as to allow gas to pass easily into and out of the carbon. Although the permeability of this new carbon was good, the team felt that this process would remove only a small amount of carbon with the benefit of assuring good dynamics for gas adsorption or desorption. When packed, the pieces of carbon had clean open surfaces along their entire length to allow gas to freely move in and out. This feature avoided the problem of the residual epoxy fouling the top surface and preventing the passage of gas.

The leaking generator was taken for metal spraying to produce a fresh layer of stainless steel over the small hole that had formed in the sealing face of the generator. This repair resulted in slight deformation to the face that seals the ammonia side, which was then ground flat. Unfortunately, the new sprayed metal face on the water side gave rise to additional problems

because the quality of the sprayed metal was not sufficiently high, making it impossible to achieve a perfect surface finish. After a couple of unsuccessful leak tests at high pressure, a thicker O-ring and silicone sealant were found to do a satisfactory job at sealing the manifold and holding air and water within the pressurized generator.



Figure 13. Carbon Plates ready for Loading into Generator

The second generator was then loaded with carbon. The two generators were packed with carbon plates. The properties of the plates are summarized in Table 7, and the mass of carbon and epoxy in each generator is included in Table 8.

Table 7. Baseline, Target, and Achieved Properties

	SDS3 base	Target	Achieved
General Data			
Density g/cm ³	1.12	0.95	0.894
Heat Capacity, J/ g-K (25, 100C)	0.842,1.01	1	1.069,1.131
Transport Properties			
Permeability (Warwick measured) m ² (x 10 ⁻¹⁴)	0.086	>25	28.3
Thermal Conductivity (298K) W/m-K	0.823	1.8	2.04
Adsorption			
BET Surface Area m ² /g	1040	1050	1339
Micropore Volume, ml/g			
t-plot	0.378	0.45	0.49
Dubinin-Astakhov	0.386	0.47	0.56
Alpha-S	0.415	0.49	0.56
NH ₃ at saturation kg/kg (kg/m ³)	0.241	0.26	0.26(90)

Table 8. Loading Data for Generators

Mass (g)	Total	Steel	Carbon	Epoxy
Generator 1	9306	7106.5	1852.43	347.07
Generator 2	9349.5	6999	1931.65	418.85

2.3.4 Leak Testing

Once the carbon had been loaded into the generators, the generators were then clamped into the retaining flanges with all manifolds in place for pressure testing. A slight leak was found on the top plate (ammonia side) of one generator, but this leak was almost entirely eliminated by the use of a slightly thicker O-ring. After leak testing was completed, the generators were mounted onto the heat pump testing rig shown in Figure 14. The processes involved in testing the generators are described in detail in the next sections.



Figure 14. Laboratory Test Rig

2.3.5 Carbon Drying

The generators were connected to a vacuum pump and pumped out at 140°C for approximately 6 hours. The plot in Figure 15 shows the measured carbon temperature during drying.

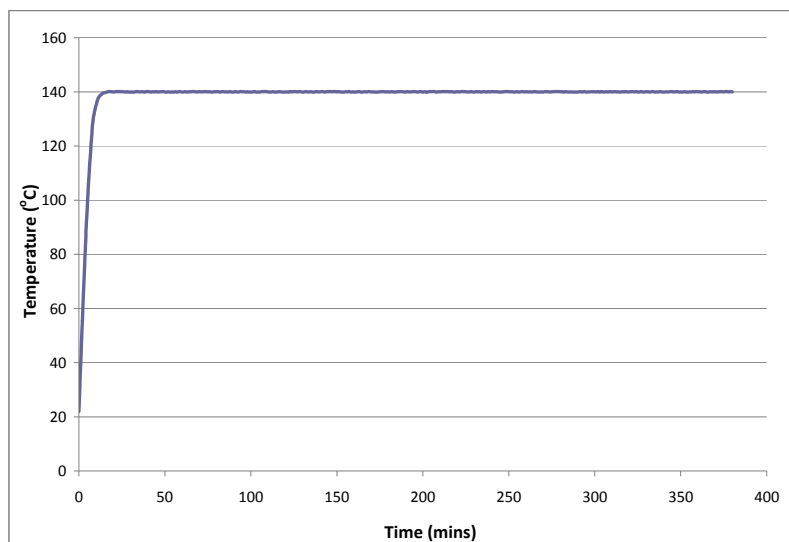


Figure 15. Bake-out of the Carbon Plates

2.4 Generator Testing in the Laboratory

2.4.1 Ammonia Charging

The generators were filled with a total of 800 grams of ammonia and then sealed and allowed to reach ambient temperature. The expected concentration of ammonia was then calculated from the measured temperature and pressure using the Dubinin-Astakhov equation and compared to the actual concentration. The results are summarized in Table 9.

Table 9. Ammonia Charging

Generator 1 Temperature	19.5	°C
Generator 2 Temperature	19	°C
Generator 1 Pressure	2.94	bar
Generator 2 Pressure	2.92	bar
Ammonia Total Charge	0.8	kg
Total Carbon Mass	3.6	
Concentration	0.22	kg kg ⁻¹
Mean Generator Temperature	19.25	°C
Mean Generator Pressure	2.93	bar
Mean Saturation Temperature	-10	°C
$T/T_{sat}-1$	0.1112	
x_0	0.2599	kg kg ⁻¹
k	5.8413	
n	1.8	
Calculated Concentration (D-A Equation)	0.23	kg kg ⁻¹
Difference, Concentration	0.01	kg kg ⁻¹
Difference, Mass	36	g

2.4.2 Laboratory Testing

The sorption generators were tested on a heat pump test rig available at the University of Warwick. In this case, the capacity of the generators was measured in terms of the heat output of the condenser rather than the cooling output of the evaporator.

The heater controller was set to 140°C, and the control software was set to run 3, 4 and 5 min cycle times with a basic cycle (i.e., no heat recovery). Mass recovery was carried out for 4 seconds at the end of each half cycle. The 4 minute cycle time yielded the highest condenser mean heat output. The test conditions are given in Table 10.

Table 10. Test Conditions

Parameter	Value	Unit
Condenser Water Inlet Temp	15.1	°C
Condenser Flow Rate	10	l/min
Evaporator Air Inlet Temp	21.3	°C

The heat input to the generators was too high to enable the 10 kW heater to maintain 140°C. The generator water inlet and outlet temperatures are shown in Figure 16 for the 4 minute cycles.

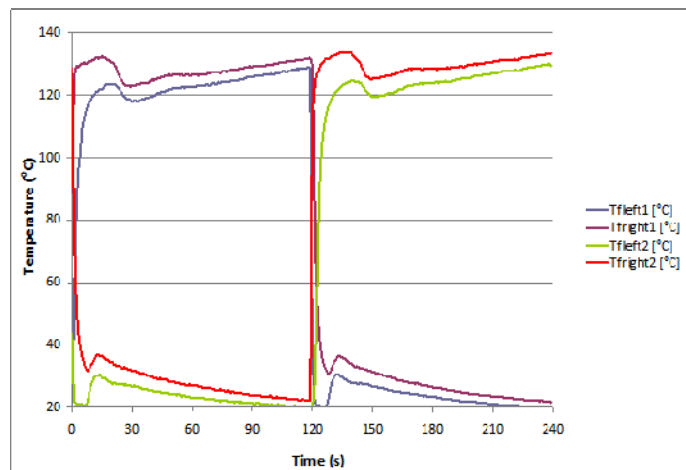


Figure 16. Generator Water Temperatures

The curves in Figure 17 plot the measured carbon temperatures for the 4 minute cycle. It can be seen that the measured temperature swing is significantly lower for Generator 2. This result is most likely an experimental artifact due to poor contact between the thermocouples and the carbon. In fact, later experiments show that Generator 2 performs better than Generator 1. Measurement of the carbon temperature frequently causes difficulties, but it is merely for interest and plays no part in the performance analysis (although it may be useful for determining the cause of poor performance).

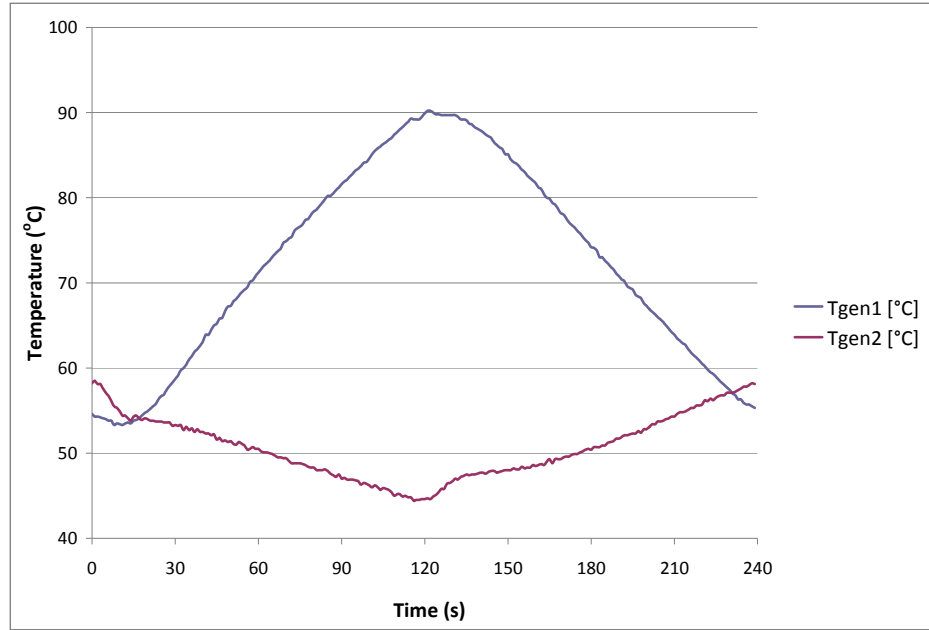


Figure 17. Measured Carbon Temperatures

Figure 18 plots the condenser heat output for the 4 minute cycles:

- Mean condenser heat output during heating of Generator 1: 1192 W
- Mean condenser heat output during heating of Generator 2: 1357 W

The condenser heat output is higher during the heating of Generator 2, most likely the result of better thermal contact between the shims and carbon in Generator 2, which had straighter shims. Figure 19 shows the generator pressures.

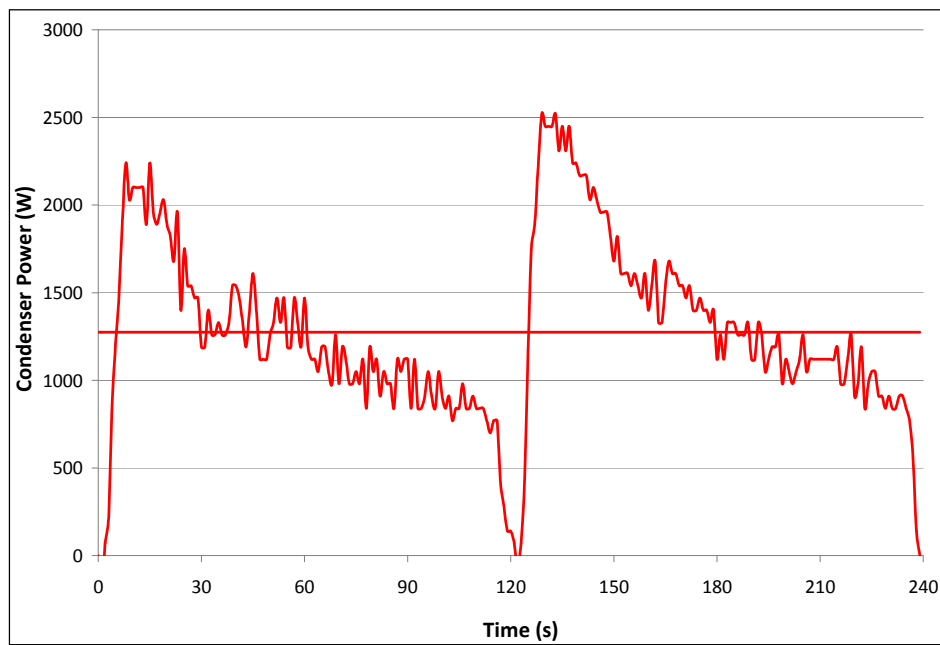


Figure 18. Condenser Heat Output

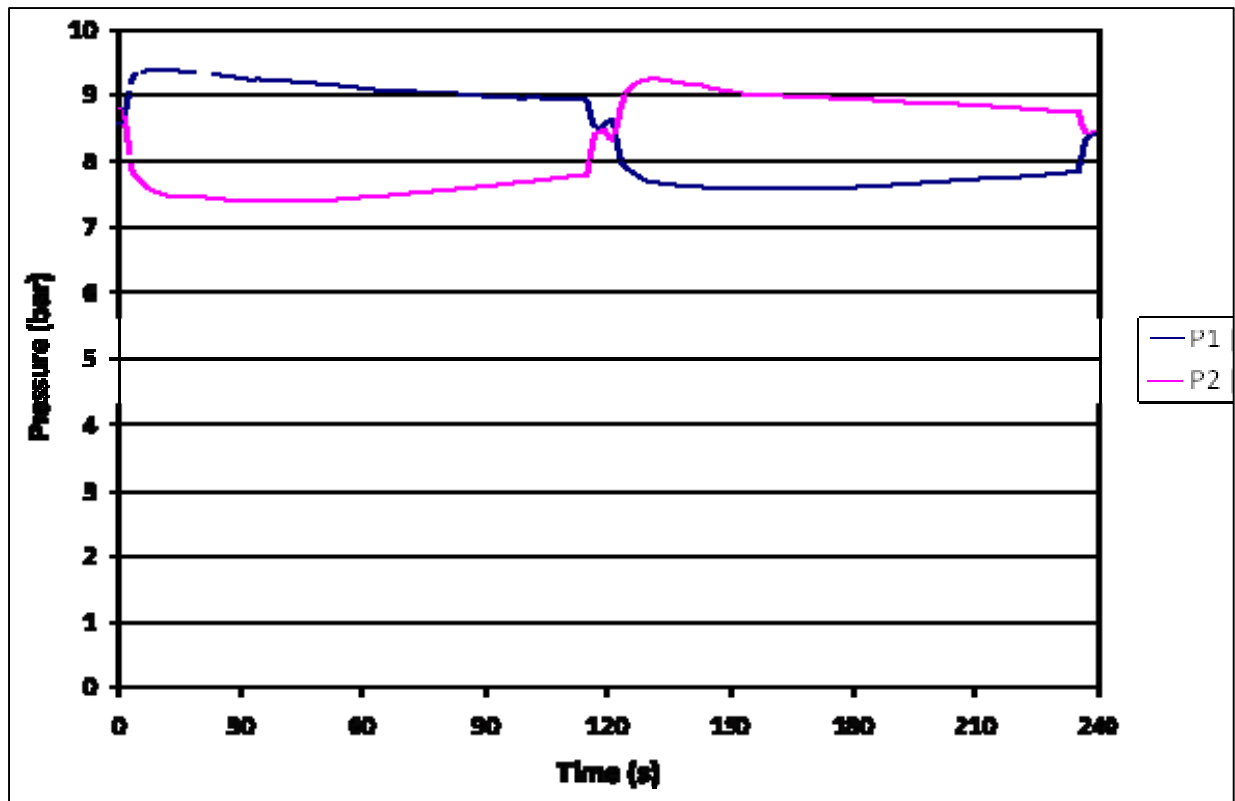


Figure 19. Generator Pressures

2.5 Frame Fabrication

2.5.1 Frame and Ancillary Equipment

While the testing of the generators in a laboratory provided some assurance the projected degree of cooling might be achieved during final operation of the system, much work was still necessary to fabricate the support frame with the generators.

The evaporator was completed and fitted inside the QuadCon along with a water tank. The water tank was purely a safety precaution for this alpha unit and designed to absorb ammonia in the event of system over-pressurization (e.g., resulting from a pump or fan failure). The support frame was constructed and the condenser, cooler, pumps, valves, etc. mounted in position. The hot and cold water systems were plumbed. Integration of the refrigeration system to the QuadCon container is shown in Figure 20 and Figure 21.

Although an early plan was to install a float in the condenser that would control flow from the condenser to the expansion valve, difficulties were experienced with the operation of this system. The final choice was an electronic level detector which would open and close a valve when a sufficient volume of liquid ammonia had appeared in the condenser.



Figure 20. The Frame Connected to the QuadCon



Figure 21. Other Views of the Frame

Also seen in the figures is the generators fitted to the frame, and the plumbing for the ammonia completed. A small water-heated evaporator was fitted to the frame unit in order to test the control systems prior to mounting the frame onto the QuadCon.

2.5.2 Testing the Equipment in the Assembled Frame

Initial tests were run to ensure the joints were all good and that the control algorithms worked. The ammonia side was pressure tested in the lab to eliminate any remaining leaks before the frame was moved outside for charging with refrigerant. The small water-heated evaporator which had been fitted to the frame was left in place so tests could be carried out with a smaller ammonia charge. Testing with the evaporator inside the QuadCold required significantly more ammonia (the evaporator in the QuadCold had already been leak and pressure tested).

Initial tests highlighted some problems with the control algorithm for the unit. The tests were conducted under less than ideal conditions and delivered a measured cooling of 0.5 kW. It was hoped that further tests with better operating conditions and improved control would yield higher cooling capacity.

The attachment of the frame to the QuadCon meant removing the water-heated evaporator from the system and making final connections with the evaporator in the QuadCon. The emergency water tank can be seen in the QuadCon in Figure 22, and the evaporator in place in Figure 23.



Figure 22. Emergency Water Tank in the QuadCon



Figure 23. Evaporator in Place

Prior to shipping the system to ATMI/Danbury, a short 8-hour test was conducted using a heated load produced by an electric hot water heater (120°C) and approximately 10 liters of water in the evaporator ice-bank. The results are shown in Figure 24. Unfortunately, the flows of ammonia through the Coriolis mass-flow meter could not be recorded during this test because the transmitter ordered with the meter (subsequently replaced) could not download data to the computer. Nevertheless, from the results of this test, the belief was strong that the two generators would achieve the target air temperature of 5°C in the QuadCon and would make ice, provided the driver water temperature from the solar thermal collectors reached at least 120°C.

Following this test, the ammonia was discharged from the system and replaced with 1-bar argon, the two sections separated and the entire system packaged and shipped to Danbury.

Once in Danbury, the entire system was moved into a storage building. A safety review was then developed by the ATMI team with the assistance of the University of Warwick during meetings on January 14-15, 2010. A copy of the safety review is attached to this report as Appendix C. Piping and instrumentation diagrams (P&ID) for the water and ammonia systems are included. Electric control and wiring diagrams are attached as Appendix D. Images of the computer screens are attached as Appendix E.

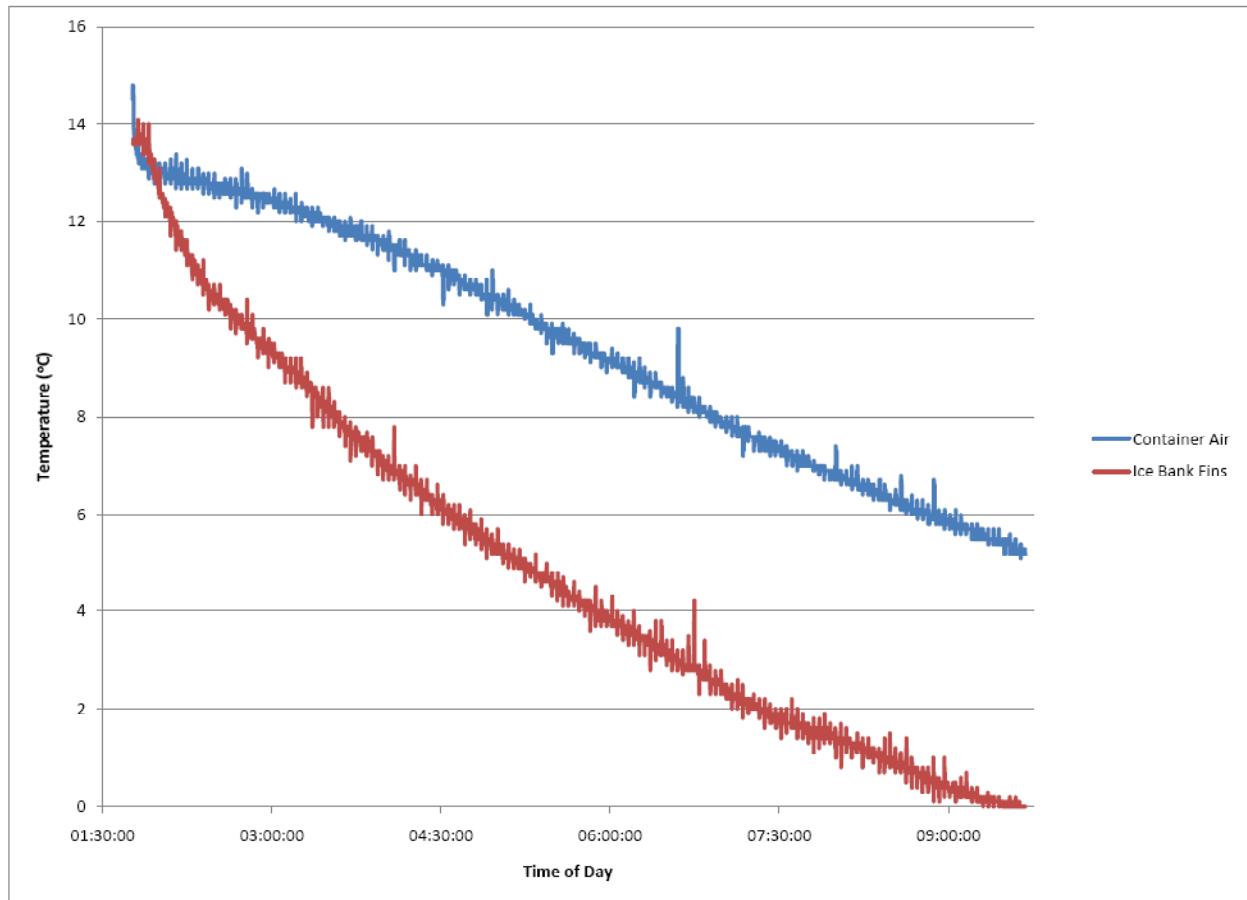


Figure 24. Testing of the System -- Temperatures Inside the QuadCon

3. Field Testing

Following meetings on January 14-15, 2010, with Stan Shire and Steve Metcalf from the University of Warwick, and Alex Schmidt of NSRDEC, details of the integration of the refrigeration units with the solar power systems and their commissioning, operation and decommissioning for transport were compiled (Appendix F).

The entire system with tools for assembly was shipped from Danbury on January 21 for delivery at the Sundanzer, Tucson Arizona test site on January 28. Soon after arrival, Dr Shaun Wilson and Shkelqim Letaj began orchestrating commissioning of the two units, installation of the photovoltaic panels to provide the parasitic power to the system, and the Thermomax solar–thermal panels to provide hot water as the main energy input. Both sets of solar panels had been constructed at the Danbury site during the previous summer and tests undertaken to ensure the effectiveness of their energy supply. Photographs of the system on the Tucson site are shown in Figure 25, Figure 26, and Figure 27.



Figure 25. Photovoltaic Panels on Roof of SunDanzer



Figure 26. Solar Thermal Panels at QuadCon Adsorption Refrigeration System



Figure 27. QuadCon with Refrigeration Unit

3.1 Commissioning and Bake-Out of the Carbon

As the commissioning progressed it was quickly realized that the generators on the ammonia side were no longer leak-tight. On further examination, it was evident the welds on both ammonia manifolds had failed. Later discussions regarding this issue suggested the damage had occurred during movement of the frame to the outsource company for packaging prior to shipment. Repair of the welds required removing the top brazed steel plate from each generator, thus exposing the carbon. The plates and manifolds were then removed, a temporary cover placed over the generators and their carbon plates, and the manifolds brought back to Danbury for repair. Modifications were also made to the mounting plates so that the piping system could be fed through enlarged holes in the mountings. Both manifolds were strengthened, re-welded and shipped back to the Sundanzer test site.

Wilson, Jones and Letaj completed the reassembly of the equipment at the test site by March 1st and began a bake-out of the carbon in the generators using the hot water supply from the solar panels. Bake-out was difficult because the water temperatures were limited to less than 140°C and could only be realized by the automatic cycling of valves from cold water to hot water at an ultimate vacuum of ~ 0.17 Torr. When the welds failed in the ammonia manifolds, the thermocouples that had been inserted into the carbon were also lost; hence, the actual temperature achieved in the carbon during the bake-out procedure is unknown, but probably did not exceed 100°C. In the original plan, the full bake-out was to have been completed at the University of Warwick during the lab test, after which the ammonia would have been removed and replaced with argon and the carbon would have remained air-free until being charged with ammonia at the test-site. Nevertheless, the bake-out at the test-site was carried out for over two days until the vacuum level stabilized.

Don Carruthers and Steve Metcalf (University of Warwick) arrived on March 2nd and assisted in the ammonia charging of the system. Because the evaporator would accommodate a significant volume of ammonia, the evaporator was chilled with ice-water while the ammonia cylinder was heated to transfer a total of 6 kg of anhydrous ammonia into the system.

3.2 Solar-Powered Adsorption Refrigerator Operation

Operation of the system began on March 3rd. The control software automatically activated the pumps, fans and valves once sufficient solar energy was detected at the solarimeter. Because this control point could be pre-selected, the start of the system was activated at a solar radiation level greater than 150 W/m². Almost immediately, it was realized that two additional components had failed. One of the water buffer tanks (there are three) began to leak water through the bladder air valve, implying leaking of the bladder. This unit was removed and the line to it capped off. Also, the ability for refrigerant material recovery was inactive due to the failure of a coil that activated a solenoid valve located in the ammonia line between the two generators. A replacement coil was ordered; it arrived and was installed on March 11th. From then on, material recovery could be added into the cycle time

A second problem was then experienced: a high-temperature shut-off switch had been set to trigger redirection of the hot water flow from the generators to cooling coils in the water cooler. Unfortunately, when this happened during the first few days of operation, the entire system shut down on several occasions. This issue was subsequently corrected by software changes; but until the change was made, operators had to take special care to adjust processing conditions once the water temperatures approached 140°C.

The primary action to avert the shut-down was to reduce the heating period in the cycle time (e.g., 240 s to 120 s) and eliminate the heat recovery period. During much of the first seven days the heat period was maintained at 180 s, the material recovery period at 0 s and the heat recovery at 60 s. Once the material recovery valve circuit became operational, a period for this recovery could be included in the cycle time. At the beginning of each day, before the sunlight reached the solar detector, the temperatures of the evaporator and the air temperature in the QuadCon were noted. On March 4th the internal temperatures were 14 & 18.6°C at 8:17 am, and following a high solar day when the system shut-down automatically at 5:00 pm, the evaporator ice-bank temperature had dropped to 5.8 & 5.9°C. The air temperatures in the QuadCon on the morning of March 5th were 9°C, but following a day of good solar radiation, the ice bank temperatures were still not close to freezing temperatures at 6°C and 8°C.

When it was quite apparent that the temperatures in the ice-bank/evaporator were not reaching freezing by March 6th, the Coriolis meter -- which measured the mass flow of liquid ammonia from the condenser to the expansion valve and evaporator -- was adjusted so it could output the cumulative ammonia flow. This flow was subsequently recorded on an hourly basis.

Calculations were then made to establish what the internal temperatures might be from ammonia vaporization at the quantities being reported by the Coriolis meter. The heat removal required to cool 50 L of water from 14°C to 0°C would be 2940 kJ, and the heat removal to freeze the 50 kg of water would be 16,678 kJ, giving a total of 19,618 kJ. Because the enthalpy of vaporization of ammonia is 1371.2 kJ/kg, it would take 14.3 kg of ammonia vaporization to fully freeze the 50 L. In a nine-hour solar input during a good day, it would require ~1.5 kg of ammonia per hour. This amount was significantly higher than the Coriolis meter was reporting.

It was therefore decided to remove water from the ice-bank/evaporator to more closely match the conditions reportedly used by Steve Metcalf during the final Warwick test (i.e., 10 L vs. the 60 L

believed to be in the ice-bank). On March 7th, water was drained from the ice-bank/evaporator with the discovery that not 60 L but close to 200 L of water was in the ice-bank. A cooling capacity of at least 3 kW would be required to freeze such a large volume of water so the possibility of generating efficient cooling in the QuadCon -- from heat transfer tubes to water to aluminum fins -- was quite impossible. With only 60 L in the 200 L chamber, 2/3 of the tubes would not be in contact with water and therefore not in contact with the fins. This discovery at such a late stage was very disappointing. It was a fundamental design flaw in the system that could not be corrected without a major rebuild of the evaporator. Nevertheless, the unit was operating well each day so a decision was made to continue operations, monitoring the liquid ammonia generation as changes in solar radiation occurred and changes in heat period, mass recovery period, heat recovery period and total cycle times were made and studied.

3.3 Daily Operations: Changing Process Conditions and Monitoring Ammonia

With 46 L of water charged to the ice-bank, daily operation of the system was monitored by the supervising team member who recorded the hourly/part-hourly liquid ammonia generation. The software collected the following set of data every 10 s: the time (EST), ambient temperature, water temperature into Generator 1, water temperature out of Generator 1, water temperature into Generator 2, water temperature out of Generator 2, Thermomax water temperature in and Thermomax water temperature out, two recordings of air temperature in the QuadCon, the temperature of the evaporator at the top and at the bottom, the temperature of the liquid in the condenser, the pressure in Generator 1 and the pressure in Generator 2, the pressure in the condenser, the pressure in the evaporator, the water pressure, the cooling power (W), the solar radiation level (W/m^2), the ammonia flow in kg/hr. The entire computer-generated data logging is too large to be contained within this report.

The operational conditions are reported as the cumulative Coriolis data in Appendix G. The software recorded the following data: date, time (EST), cumulative ammonia, incremental change, heat cycle (s), mass recovery (s), heat recovery (s), cumulative total ammonia for the day, operator initials, time period (local time), elapsed time (min), solar radiation (W/m^2), ammonia average (g/min), ammonia flow efficiency $[(\text{g/hr})/(\text{W/m}^2)]$, average temperature of the evaporator, average temperature of the condenser, average pressure of the evaporator, average pressure of the condenser, cooling power, L (kJ/kg), cooling (kW), the temperature of the Thermomax collectors in and out, the solar thermal efficiency ratio, ambient temperature, and the temperature of the Thermomax collectors out minus the ambient temperature.

3.4 Evaluation of Changes in Process Conditions

From March 13th, operations were fairly uneventful; this provided an opportunity to evaluate the influence of the heat, materials recovery and heat recovery periods on the performance of the unit (Table 11).

Table 11. Changes in Operational Settings During March 13 – 28

Day	Date	Heat input Btu/hr	Material recovery Btu/hr	Heat Recovery Btu/hr
Sa	3/13/2010	120	10	2C
Sa	3/14/2010	150	10	2C
M	3/15/2010	180	10	2C
Tu	3/16/2010	210	10	2C
W	3/17/2010	300	10	2C
TH	3/18/2010	240	10	2C
F	3/19/2010	300	10	2C
Sa	3/20/2010	300	10	2C
Sa	3/21/2010	300	10	2C
M	3/22/2010	300	6	1C
M	3/22/2010	300	6	1C
Tu	3/23/2010	240	6	1C
W	3/24/2010	250	4	6
Th	3/25/2010	280	4	6
F	3/26/2010	276	4	6
Sa	3/27/2010	216	4	0
Sa	3/28/2010	276	4	6

4. Results

4.1 Conditions for Maximum Ammonia Generation

Days that experienced the highest production of liquid ammonia were those with initially the longest heat periods. During the midday hours of March 20 and 21, the solar radiation reached values in excess of 750 W/m^2 , and because the water temperatures reached nearly 140°C , the heat periods were necessarily reduced from 300 s to 195-210 s and the heat recovery period eliminated completely. This change naturally resulted in shorter cycle times and the largest generation of liquid ammonia in the condenser: more than 7 kg for the day and in excess of 1.2 kg for the hour. Temperature and pressure cycles for 2:00 pm (MT) are shown in Figure 28 and Figure 29. Unfortunately, these conditions did not have a significant effect on the temperatures in the QuadCon (Figure 30).

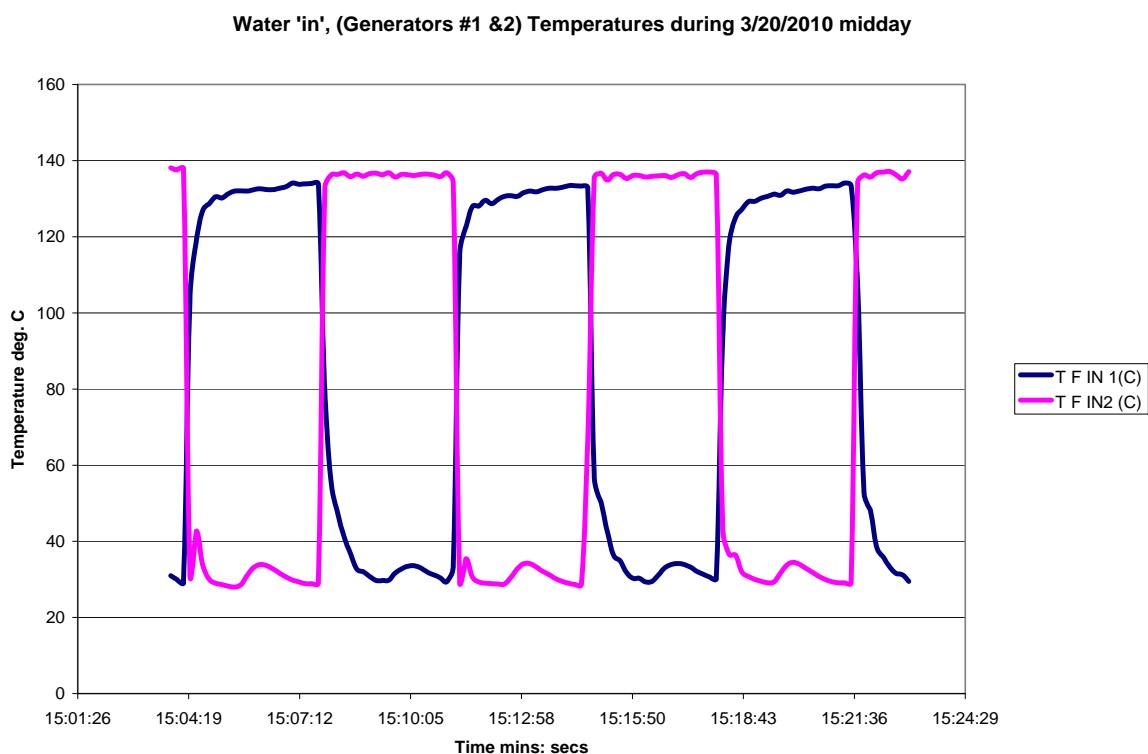


Figure 28. Water Temperatures on 3/20/2010

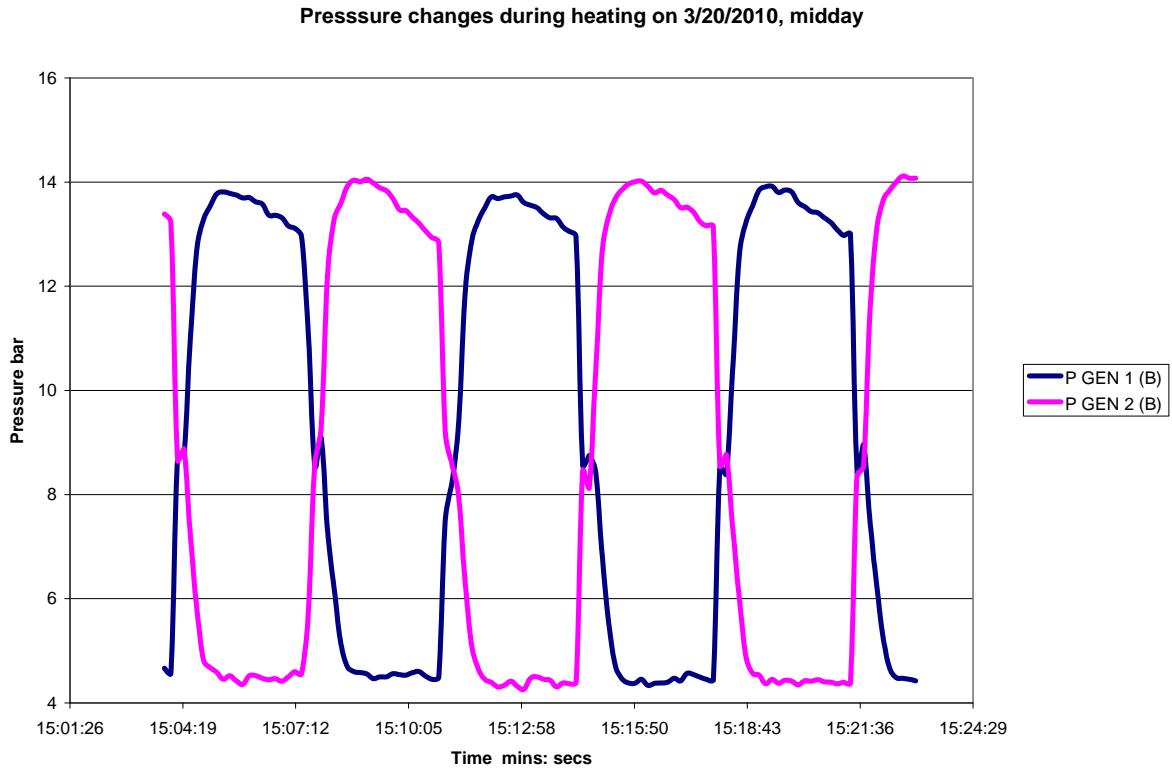


Figure 29. Pressures in Generators 1 & 2 During Operation 3/20/2010

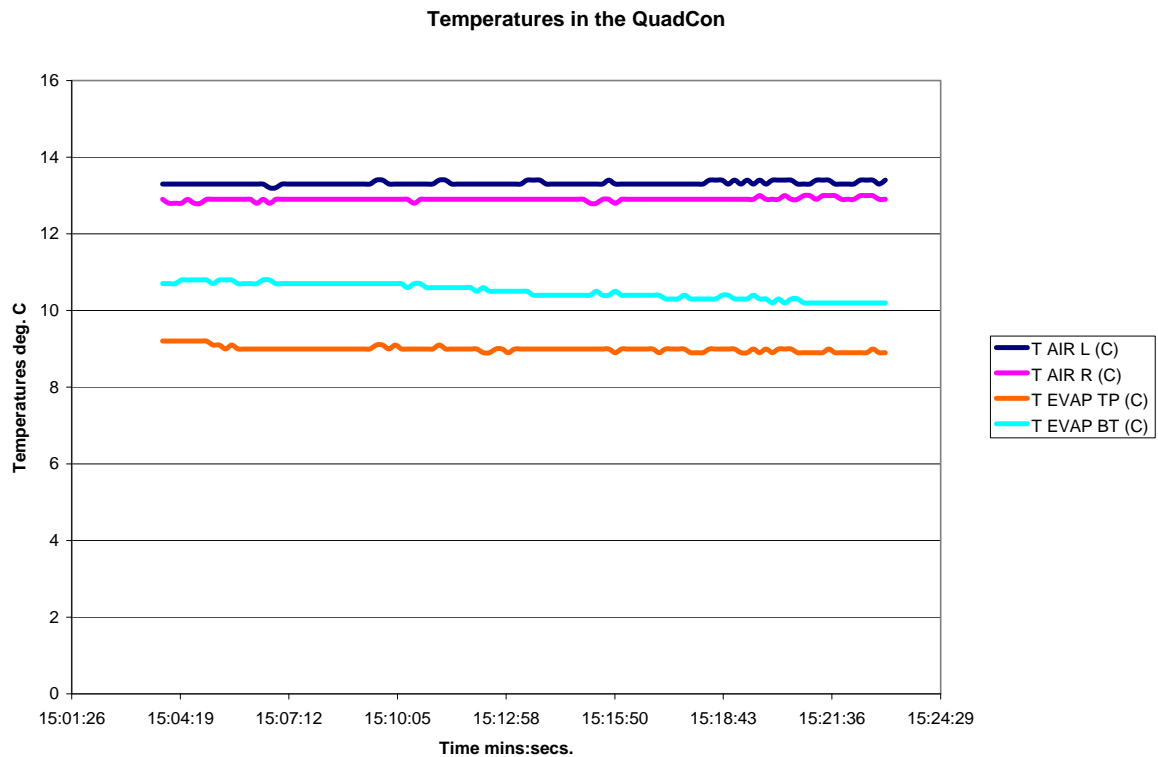


Figure 30. Temperatures in the QuadCon on 3/20/2010

The calculated values for cooling power, Q , are provided using Equations (1) through (4):

$$Q = m \times L \times 1000 \quad (1)$$

where m is measured in kg/s and L is measured in kJ/kg and given by the following:

$$L = -0.009T_{\text{ev}}^2 + 1.095 T_{\text{ev}} + 1264 - 4.8T_{\text{cond}} \quad , \quad (2)$$

where

$$T_{\text{ev}} \equiv T_{\text{evaporator}} = [2748.3/(11.515 - \ln P_{\text{ev}})] - 273 \quad , \quad (3)$$

and

$$T_{\text{cond}} \equiv T_{\text{condenser}} = [2748.3/(11.515 - \ln P_{\text{cond}})] - 273 \quad . \quad (4)$$

Under the most advantageous conditions on March 20th and with a 6.8 minute cycle time, the enthalpy of vaporization of ammonia under the operating conditions, $L = 1150$ kJ/kg, and the cooling power Q (as reported in the cumulative Coriolis spreadsheet) was only near 400 W, far removed from the 1500 W expected but quite close to the 0.5 kW reported by Warwick in the next to final test. Hence, regardless of the poor performance of the evaporator, the cooling power was significantly lower than expected.

4.2 Conditions Which Produced the Coldest Temperatures in the QuadCon

Following repair of the solenoid valve, March 12th was the first day when conditions allowed all three parameters to be set: heat period (HP), material recovery (MR) and heat recovery (HR). The heat period was the time for hot water to be fed to the generator. The material recovery was a process whereby high pressure ammonia in the hot generator was allowed a sudden expansion into the low pressure, cold generator. The cool carbon could adsorb ammonia at quite a high pressure with an increase in the total ammonia capacity of the carbon. The heat recovery involved pumping water from the hot to the cold generator prior to the hot water coming from the collectors. While some useful data were generated on March 12th, and indeed evaporator temperatures did drop below 2.5°C during the switch from "180, 10, 20" to "120, 10, 0", the system was more stable later.

A careful analysis of all data revealed operating conditions during the day on March 15th generated not only a significant volume of ammonia but also produced among the lowest evaporator temperatures achieved during the entire 28-day operation -- temperatures as low as 3.1°C. The selected conditions for that day were a 180 s heat period, 10 s material recovery and 20 s heat recovery for a total of 7 min cycle times. During a 40-min period starting at 1:12 p.m. local time, the heat recovery was eliminated to ensure temperature control of the generators. The hours preceding these low temperatures at the evaporator experienced some of the highest solar conditions (as high as 770 W/m²).

Because the evaporator temperatures were being recorded from thermocouples situated on the aluminum fins and not in the water/ice bath, it is possible ice was being produced (Figure 31, Figure 32, and Figure 33). However, regardless of the low evaporator temperature, the air

temperatures in the QuadCon continued to rise during the day. Much of this increase was attributed to the fact that the constant sunlight on the steel exterior of the QuadCon brought skin temperatures up as high as 56°C while ambient temperatures were still in the high 20s. One solution to this radiant heating would be to situate the photovoltaic panels in front of the QuadCon and thereby lower the radiant heat on the insulated container.

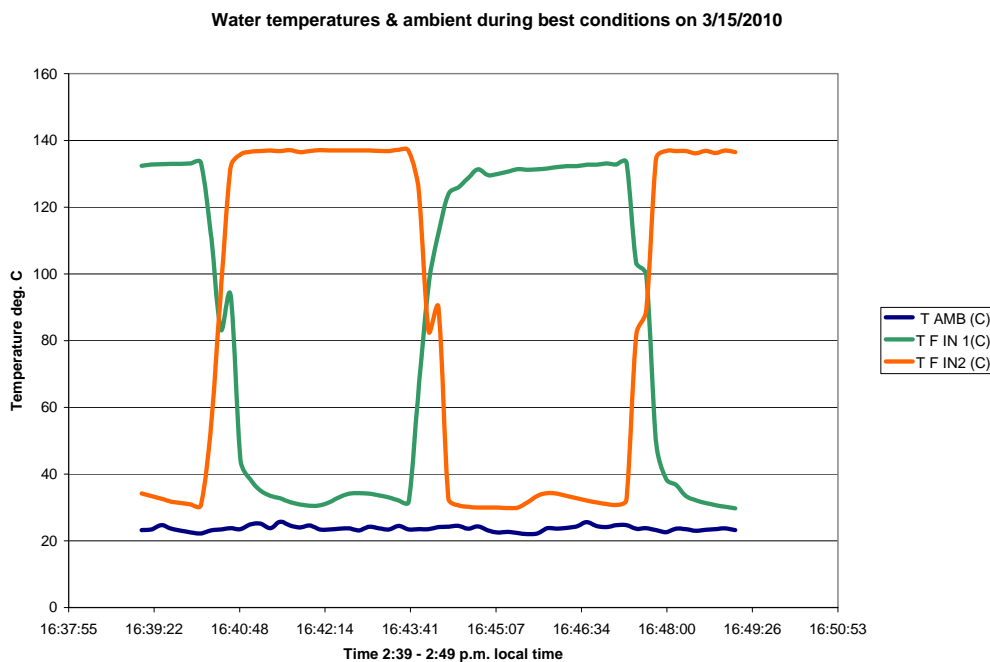


Figure 31. Best Conditions HP = 180 s, MR = 10 s, and HR = 20 s

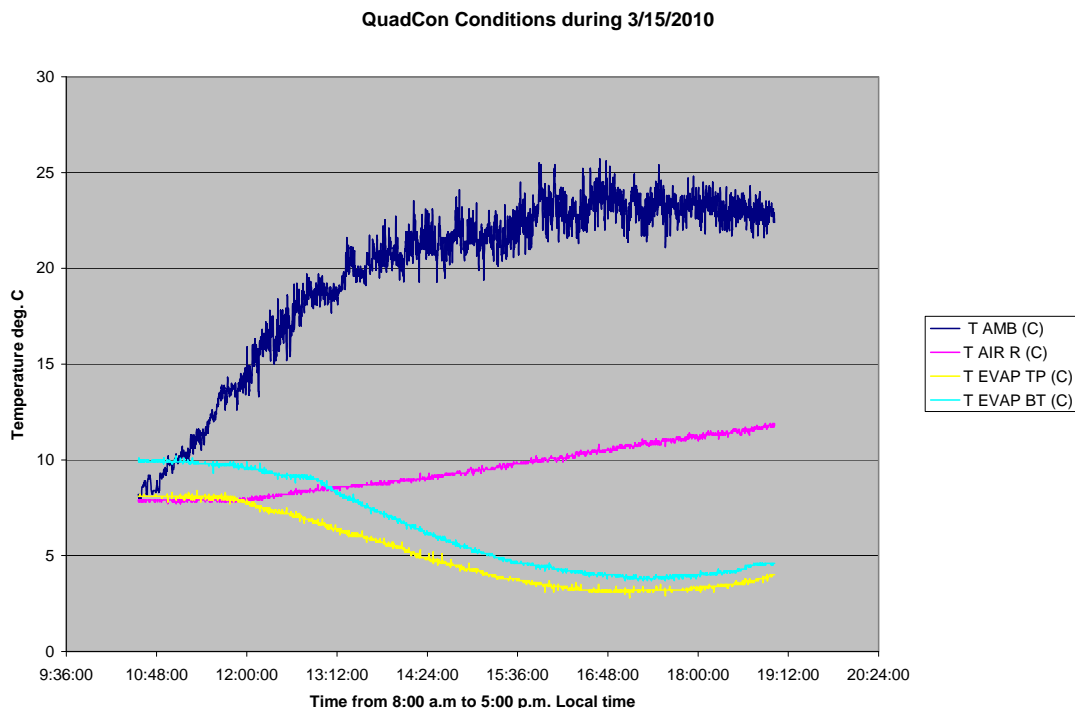


Figure 32. Results for Conditions HP= 180 s, MR = 10 s, and HR = 20 s

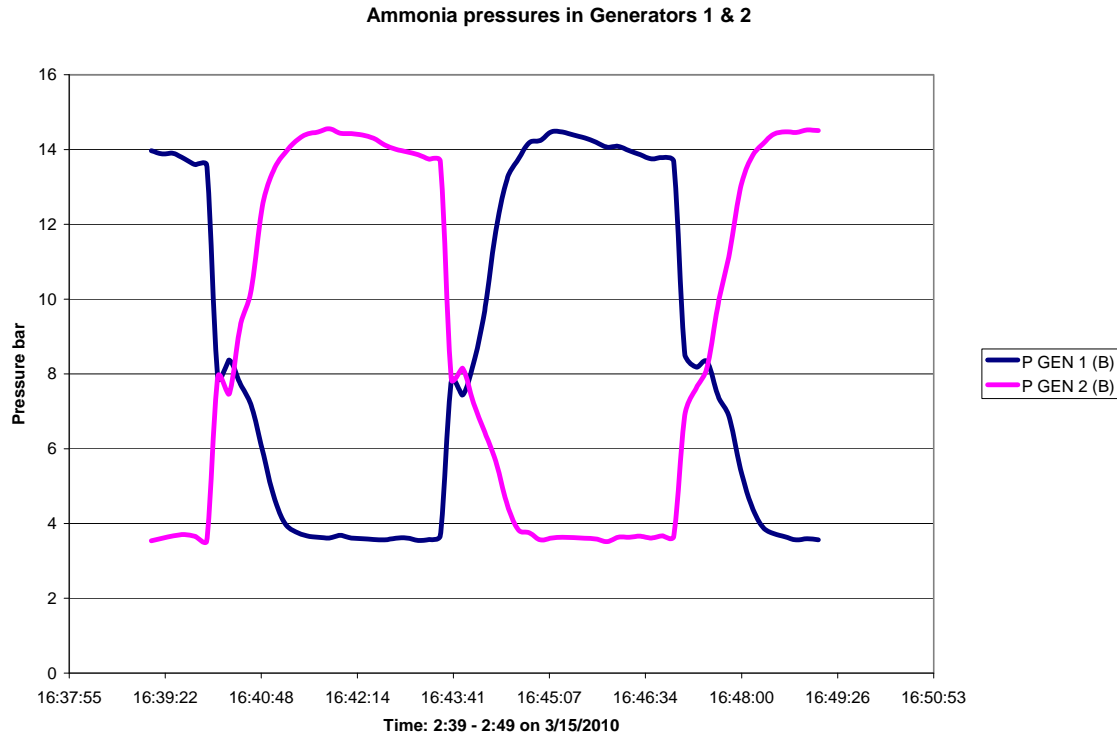


Figure 33. Best Conditions HP = 180 s, MR = 10 s, HR = 20 s

4.3 Best Operations

The computer control of the automated system worked extremely well. If the project were to be re-activated, algorithms would be included in the software to automatically change the heat period, material recovery period and the heat recovery period in response to the high heat conditions during the midday sun. These changes to the settings had to be made manually by the operators during the test periods.

Both the solar thermal collectors and the solar voltaic panels worked extremely well. Had the generators been able to accommodate higher temperatures, the heat supply from the collectors would have dramatically improved the COP of the system.

4.4 Discussion Regarding Ultimate Performance

4.4.1 Temperature Limitations

During the typical eight hours of daily solar radiation, the average solar intensity at the Sundanzer site in March was barely 650 W/m^2 (peaking at $750 - 800 \text{ W/m}^2$), which was significantly lower than had been expected. Nevertheless, target water temperatures near 140°C were reached for at least 3 hours of the 8 hours of sun contact. Because it had been demonstrated early in the program that 120°C water could not lift the temperature of the carbon in the thermal mass of the generator above 90°C , the ammonia release between a temperature not much higher than this (from the 138°C water) and $\sim 30^\circ\text{C}$ would have been significantly less than targeted. Hence, the much lower ammonia desorption would translate into much lower enthalpies from evaporation and lower subsequent cooling.

It was originally expected the carbon would reach temperatures higher than 140°C (Figure 3), but the ultimate design of the generators with O-ring manifolds on both the ammonia-side and the water-side prevented operation with water temperatures above 140°C and heat transfer from the water shims to the carbon was not as efficient as desired. Critoph had emphasized in earlier presentations that it was essential to reduce the mass of the generators from those that had been used in TOPMACS developments, and the way to accomplish this task was to weld manifolds onto both the ammonia and water sides [8]. However, after numerous failed attempts to weld the water and ammonia manifolds to the generators without causing leaks, the clamping design was adopted with O-ring seals. This approach added a significant mass of steel (and hence thermal mass) to each generator, which meant that during every cycle, heat was being dispersed throughout the mass and away from the carbon, thereby limiting the heat transport to and from the carbon.

From the beginning, efforts were made to maximize contact between the carbon and the shims -- the thin steel separators through which the water flowed. This effort required carbon plates and shims to be extremely flat such that neither bowed in any way. An early statement from Warwick, subsequently confirmed by the Tucson testing, was that the two generators were not equal in performance: one released much more ammonia during desorption than did the other, and Warwick believed this discrepancy was related to the straighter shims in the generator that produced more ammonia. In addition, although the first batch of plates was extremely flat sided, the final set had warped during pyrolysis, and much effort was spent selecting pieces and sanding them to achieve reasonable levels of flatness.

4.4.2 Condition of Carbon

It is difficult to explain why the two generators performed quite well on the University of Warwick test rig with one generator indicating as much as 1350 W of average cooling power (Figure 18) translating into a 700 W/kg specific cooling power (SCP), while in contrast when tested on the frame and later when fully operational achieved only ~110 W/kg SCP and 400 W per two generators. This level of cooling fell well shy of that anticipated based on the load calculations in Table 1. If the problem is related to the treatment of the carbon following the test rig activity, the question arises, "Was it not possible to valve off the carbon after ammonia had been drawn off, keeping the carbon air-free before installation in the frame?" Certainly the best bake-out conditions for the carbon could only be achieved on the test rig. The bake-out conditions on the frame were limited by the hot/cold water cycling. If the generators had been valved off when disconnected from the test rig and then installed on the frame, the carbon could have been preserved air-free. Close examination of the generators on the test rig and later on the frame does not show close-off valves.

Was the issue of the failed welds the cause of a much degraded carbon adsorbent? Certainly it was difficult to raise the temperature of the carbon to achieve a reasonable level of bake-out prior to start-up using the hot-water/cold-water cycling of the system. Had there been no exposure of the carbon to air following the test on the test rig, the condition of the carbon almost certainly would have been significantly improved for later use.

4.4.3 Evaporator Sizing Issue

A large problem was that the evaporator in the QuadCon was improperly sized. The original plan was for the evaporator ice bank to have a total volume of 60 L. The initial design reported in the second summary report of November 2007 showed a single rectangular containment volume between two sets of fins into which was included a third set of 40 fins plus the 40 evaporator tubes and a single ammonia header tubular vessel. The total ice-bank volume of that containment vessel was about 90 L less than the volume taken up by the 40 fins and 40 tubes, so a real volume close to 60 L would be expected. In the third summary report from December 2007, the final design of the evaporator was shown to be very different with two rectangular containment vessels, two ammonia header tubular vessels, and front and rear sets of fins. The water content of the two rectangular vessels when filled in Tucson showed an ice-bank of nearly 200 L. Major modifications of this evaporator would be necessary for proper use in a QuadCon.

4.4.4 Overall Coefficient of Performance

A calculation of cooling power in Table 12 at the various average solar intensities allows the computation of COPs for the entire system. These results are plotted in Figure 34 against the heat periods. Because the solar intensity is reported as a W/m^2 and the system has $10 m^2$, the COPs for the system are significantly lower than expected.

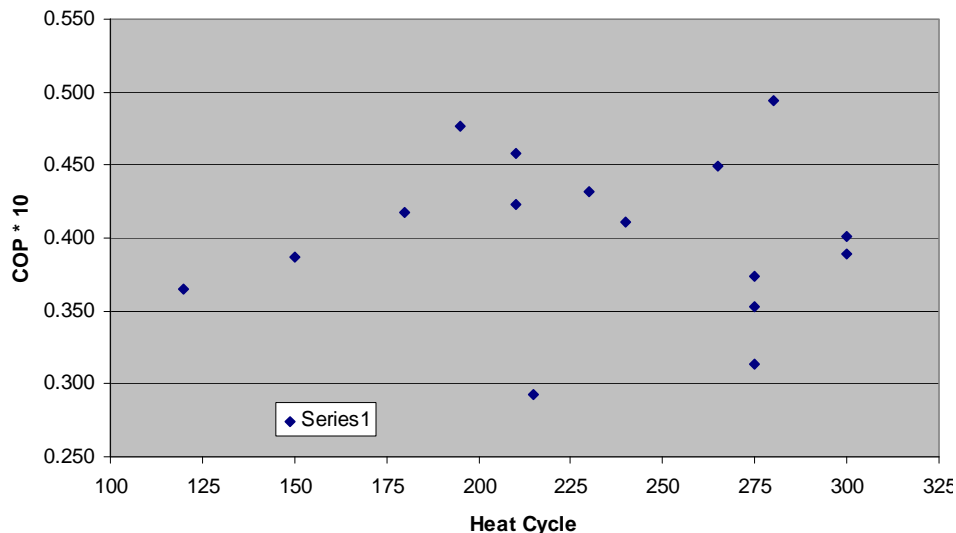


Figure 34. Coefficient of Performance vs. Heat Cycle Period (in seconds)

Table 12. Changes in Operational Settings During 3/12 – 3/28

			AMBIENT CONDITIONS		TOTAL PERFORMANCE			SPECIFIC / NORMALIZED PERFORMANCE		
			Average Solar Intensity, W/m ²	T_ambient_avg, C	Cumulative NH ₃ , kg	Average Coding Power, W	Average T_evap, C	NH ₃ Flow Efficiency, (g/hr) / (W/m ²)	Coding power / Solar Intensity, W / (W/m ²)	T_amb-T_evap
F	3/12/2010	482	652.7	18.1	58045	227.5	4.31	1.107	0.349	13.79
Sa	3/13/2010	483	608.9	20.52	59743	222.2	6.39	1.219	0.365	14.13
Su	3/14/2010	484	654.6	17.95	63275	253.1	7.79	1.198	0.387	10.16
M	3/15/2010	486	637.6	19.92	68785	266.4	5.72	1.332	0.418	14.20
Tu	3/16/2010	487	622.6	23.64	67299	263.1	7.71	1.331	0.423	15.93
W	3/17/2010	489	647.7	26.53	66623	251.8	10.04	1.262	0.389	16.49
TH	3/18/2010	492	605.8	26.03	6629	248.9	10.83	1.334	0.411	15.20
Fr	3/19/2010	492	484.7	21.77	509	194.3	11.73	1.281	0.401	10.04
Sa	3/20/2010	501	615.09	20.89	736	282	9.67	1.433	0.458	11.22
Su	3/21/2010	494	589.05	22.06	7271	281	7.96	1.499	0.477	14.10
M	3/22/2010	448	623.65	25.35	53725	227	9.37	1.154	0.364	15.98
M	3/22/2010	353	655.71	23.92	52795	283	9.45	1.369	0.432	14.47
Tu	3/23/2010	85	482.17	21.4	11369	238	15.22	1.664	0.494	6.18
W	3/24/2010	497	605.7	20.18	72802	272	10.04	1.451	0.449	10.14
Th	3/25/2010	502	602.36	23.89	64026	225	9.09	1.270	0.374	14.80
Fr	3/26/2010	507	597.01	22.59	56041	211	10.58	1.111	0.353	12.01
Sa	3/27/2010	500	621.6	21.24	48646	182	10.07	0.939	0.293	11.17
Su	3/28/2010	507	632.42	24.34	53151	198	10.43	0.995	0.313	13.91

5. Conclusions

Through a partnership with research staff at the University of Warwick School of Engineering, Coventry, U.K., ATMI undertook materials development, product design, fabrication, and site testing of a Solar-Powered Adsorption Refrigeration system with the goal of providing refrigeration to a QuadCon insulated container. The system operated safely without any external electric power for a period of 6 weeks at the Sundanzer test location in Tucson Arizona in March/April 2010. While many aspects of the system functioned well, the unit did not completely meet target performance. The final testing was foreshortened when it was realized that certain components were not meeting an expected performance level.

During the 2 ½ years of this project, which included both new materials and new equipment development, a great deal was learned about the features of adsorption refrigeration technology that influence the final efficiency of a system. The goal of the project was to achieve in the QuadCon a consistent 5°C air temperature during both day and nighttime operations and during conditions which necessitated door openings during the day. Attempting to move straight from materials development to a fully functioning unit without the usual intermediate development of smaller-scale prototype units was an ambitious route to our final goal. However, we attempted to apply modern modeling routines to bridge the gap and allow for a rapid transfer of theory to practice. While the modeling assisted the design basis, achieving the specifications derived from the modeling was difficult and in some cases not possible (e.g., targeting a moderate generator mass that relied on successful welding of the water and ammonia manifolds).

The Solar-Powered Adsorption-Refrigeration QuadCon did not achieve the target level of refrigeration for reasons enumerated in the previous chapter. Had the target level of cooling been reached, it would have been an easy task to monitor the side-by-side energy demand of an electrically-powered QuadCon to confirm the energy benefits.

6. Recommendations

The primary focus to improve the system must be to better manage the thermal dynamics of the generators.

- The generator design must be modified to ensure better intimate contact between the carbon plates and the heat-exchanger plates (engineered flat-sided heat-exchanger plates).
- The generator design must be modified to eliminate the need for clamping systems (i.e., include welded water and ammonia manifolds).
- The carbon plates must be improved. One way to achieve this improvement would be to enhance the permeability of the plates without the use of bead additives and hence achieve flatter-sided monolith blocks. Such action could allow for thinner carbon plates and hence easier heat transfer dynamics.
- The evaporator would need to be completely rebuilt to accommodate only the targeted amount of water in the ice-bath (60 L).
- A new control strategy, not based on a fixed cycle time but on a fixed temperature difference ΔT_{cold} (generator in adsorption phase vs. ambient), is needed to optimize the cooling.
- The manifold system in the frame should allow for a proper high-temperature ($\sim 180^\circ\text{C}$) high-vacuum bake-out of the carbon before use.

The secondary focus should be to reduce the size of the condenser and water-cooler heat-exchangers with an overall attention to smallness in the ancillary equipment necessary for the system to function effectively.

Finally, the exterior steel skin of the QuadCon in the direct sunlight prevented effective use of the QuadCon insulation. A fiber-glass reinforced plastic shell, as used in larger refrigerated containers, would be advantageous to minimize radiation heating of the QuadCon. Positioning of the photovoltaic panels to cover much of the sunlit side of the QuadCon might achieve the same result.

This document reports research undertaken at the U.S. Army Natick Soldier Research, Development and Engineering Center, Natick, MA, and has been assigned No. NATICK/TR- 11/016 in a series of reports approved for publication.

7. References

1. Tiron, R., *The Hill*, 10/15/2009, "\$400 per gallon gas to drive debate over cost of war in Afghanistan."
2. Critoph, R.E., *Solar Energy*, 41, 1, (1988) 21-31, "Performance Limitations of Adsorption Cycles for Solar Cooling"
3. Critoph, R.E., *Applied Thermal Engineering*, 16, 11 (1996) 891-900, "Evaluation of Alternative Refrigerant-Adsorbent Pairs for Refrigeration Cycles".
4. Critoph, R.E., *Carbon*, 27, 1 (1989) 63-70, "Activated Carbon Adsorbent Cycles for Refrigeration and Heat Pumping".
5. Wang, R. Z., Oliveira, R.G., *International Sorption Heat Pump Conference, June 22 -24, 2005, Denver, CO, USA*. P.1 – 21 "Adsorption Refrigeration – An Efficient Way to Make Good Use of Waste Heat and Solar Energy".
6. Yong, Li, Wang, R.Z., *Recent Patents on Engineering*, 1, (2007) 1 – 21, "Adsorption Refrigeration: A Survey of Novel Technologies".
7. Tamainot-Telto, Z., Critoph, R.E., *Applied Thermal Engineering*, 21 (2001) 37 – 52, "Monolith carbon for sorption refrigeration and heat pump applications".
8. Critoph, R.E., *IEA Conference, Alkmaar, 9-10 October, 2007*. Presentation: "TOPMACS Plate Sorption Reactor".

Appendix A - Results of Testing Carbon Samples

Test samples of carbon with additives to improve permeability and thermal conductivity were evaluated and the results are presented in the following tables.

Sample ID	Total Additives	Density	BET SA	t MPV	Flow @ 40 psi	Thermal Conductivity
	%				cc/psi/cm2/min	W/m-K
1585-48-58	8	0.973	1032	0.383	86.24	1.125
1585-48-59	9	0.964	1033	0.384	87.20	0.915
1585-48-60	10	0.985	1021	0.379	78.76	1.285
1585-48-61	11	0.981	1018	0.379	88.10	1.423
1585-48-62	12	0.956	1002	0.372	102.36	1.403
1585-48-63	13	0.934	996	0.369	127.16	1.364
1585-48-64	14	0.962	990	0.367	107.35	1.663
1585-48-65	16	0.961	956	0.375	143.12	1.651
1585-48-66	9	0.965	1034	0.382	88.900	1.114
1585-48-67	11	0.979	1004	0.373	84.240	1.322
1585-48-68	13	0.933	1002	0.372	97.290	1.527
1585-48-69	15	0.966	995	0.370	108.030	1.528
1585-48-70	17	0.963	981	0.363	131.430	1.489
1585-48-71	18	0.927	944	0.350	211.130	1.382
1585-48-72	19	0.924	949	0.351	156.430	1.450
1585-48-73	20	0.893	947	0.350	368.910	2.042
1585-56-74	13 sandwich				129.520	
1585-56-75	14 sandwich				181.240	
1585-56-76	16 sandwich				257.590	
1585-68-77	18 sandwich				169.25	
1585-68-78	19 sandwich				222.33	
1585-68-79	20 sandwich				193.36	
1585-68-80	10	0.940	1024	0.379	90.180	1.015
1585-68-81	12	0.961	1001	0.371	97.320	1.109
1585-68-82	14	0.989	995	0.369	107.790	1.329
1585-68-83	16	0.996	978	0.363	129.690	1.472
1585-68-84	18	0.994	960	0.356	137.990	1.536
1585-68-85	19	0.983	955	0.353	177.360	1.828
1585-68-86	20	0.946	931	0.345	171.820	1.656
1585-68-87	21	0.955	930	0.344	244.900	1.379
1585-68-88	12	0.993	1003	0.371		1.770
1585-68-89	13	0.951	988	0.367	100.240	1.363
1585-68-90	14	0.994	994	0.368	88.714	1.236
1585-68-91	16	0.959	967	0.358	99.271	2.343
1585-68-92	19	0.981	936	0.348	169.110	2.051
1585-68-93	20	0.970	923	0.342	132.750	2.112
1585-68-94	22	0.949	921	0.341	176.680	1.706
1585-68-95	24	0.947	888	0.329	281.270	2.105

Additive levels of individual components are concealed for these structure-property studies, which are performed outside the scope of the current contract

Effect of Oxidation									
Origl. ID	Sample ID	% burn off	Density	BET SA	t-MPV	Permeability	Orig'l Permeability	Permeability change	Original Conduct.
HF-01-114	HF01-114	0	1.120	1050	0.388	20.00	20	0	0.819
1493-45D	1585-72A	13.14	0.889	1248	0.463				
1493-45B	1585-72B	9.95	0.913	1142	0.423				
1585-56-66	1585-72C	3.3	0.971			112.87	88.9	23.97	1.114
1585-41-56	1585-73A	4	0.958	1033	0.383	96.18	84.106	12.078	1.877
1585-41-49	1585-73B	3.5	1.023	1065	0.395	105.68	78.81	26.87	1.25
1585-41-50	1585-73C	4.55	0.998	1048	0.386	82.75	64.44	18.31	1.382
1585-41-51	1585-73D	4.41	0.985	1033	0.382	74.73	67.62	7.11	1.35
1585-41-52	1585-73E	3.35	1.006	1053	0.39	84.09	84.13	-0.04	1.139
1585-41-53	1585-73F	7.54	0.964	1046	0.385	83.91	79.77	4.14	1.663
1585-41-54	1585-73G	5.54	0.967	1088	0.402	76.73	69.131	7.599	1.639
1585-41-55	1585-73H	8.61	0.962	1060	0.391	96.92	80.934	15.986	1.485
1585-48-63	1585-73I	4.6	0.957	1022	0.378	142.79	127.16	15.63	1.364
1585-48-58	1585-73J	5.04	0.918	1088	0.402	93.89	86.235	7.65	1.125
1585-48-62	1585-73K	7.28	0.945	1054	0.39	117.94	102.36	15.58	1.403
1585-48-61	1585-73L	8.85	0.947	1070	0.395	101.13	88.09	13.04	1.423
1585-48-64	1585-73M	5.52	0.965	1089	0.4	156.20	107.35	48.85	1.663
1585-48-60	1585-73N	5.76	0.974	1083	0.401	85.86	78.76	7.104	1.285
1585-48-65	1585-73O	8.33	0.930	1027	0.379	164.05	143.12	20.93	1.651
1585-48-59	1585-73P	10.22	0.947	1144	0.422	110.75	87.20	23.549	0.915
1585-56-68	1585-73Q	8.76	0.894	1220	0.45		97.29		1.527
1585-56-67	1585-73R	11.15	0.933	1160	0.427		84.24		1.322
1585-56-73	1585-73T	7.23	0.810	985	0.364		368.91		2.042
1585-56-70	1585-73S	8.23	0.932	1171	0.432		131.43		1.489
1585-56-69	1585-73V	8.52	0.911	993	0.366		108.03		1.528
1585-56-71	1585-73U	6.92	0.915	1063	0.392		211.13		1.382
1585-68-91	1585-73W	9.1	0.938	1044	0.386		99.27		2.343
1585-68-81	1585-73X	7.88	0.916	1151	0.426		97.32		1.109
1585-68-85	1585-73AA	7.86	0.916	989	0.365		177.36		1.828
1585-68-95	1585-73Z	10.49	0.844	983	0.359		281.27		2.105
1585-68-87	1585-73BB	4.86	0.928	978	0.361		244.9		1.379
1585-68-93	1585-73Y	6.82	0.920	1022	0.378		132.75		2.112
1585-68-83	1585-73DD	14.3	0.874	1146	0.421		129.69		1.472
1585-68-92	1585-73CC	8.15	0.938	996	0.367		169.11		2.051

Appendix B - Permeability Test Results

Permeability test results for the series of carbon plates submitted to the University of Warwick are listed in the below tables. Potential cooling capacity assumes generator temperature of 160°C, cold-side temperature of 40°C, and evaporator temperature of -10°C.

Sample	Gas	T _{amb} (°C)	T _g (°C)	μ (Pa.s)x10 ⁻⁵	K _a (m ²)x10 ⁻¹⁴	B x 10 ⁸
LM127	Air	16.3	16.4	1.7838	3.6065	6.6152
1614-9-3B1	Air	22.7	22.8	1.8162	15.3376	3.3976
1614-9-4B1	Air	-	-	-	N/A	N/A
1614-9-5B2	Air	22.8	22.6	1.8148	10.0942	2.4454
1614-9-6D1	-	-	-	-	N/A	N/A

Table 2: Axial permeability

Sample	Gas	T _{amb} (°C)	T _g (°C)	μ (Pa.s)x10 ⁻⁵	K _r (m ²)x10 ⁻¹⁴	B x 10 ⁸
<i>Diverging Flow</i>						
LM127	Air	18.9	18.9	1.7967	34.4550	0.4421
1614-9-3C1	Air	23.4	22.8	1.8189	28.2767	0.2274
1614-9-4C1	Air	22.8	21.7	1.8105	3.9159	6.3837
1614-9-5D2	Air	23.2	23.7	1.8206	4.6697	0.6734
1614-9-6D1	Air	23.3	23.1	1.8174	11.2596	0.4541
<i>Converging Flow</i>						
LM127	Air	18.6	18.6	1.7949	34.9080	0.4863
1614-9-3C1	Air	23.7	22.8	1.8206	27.4765	0.1379
1614-9-4C1	Air	22.4	22.3	1.8138	3.8236	3.8310
1614-9-5D2	Air	23.2	23.7	1.8205	4.8238	3.6529
1614-9-6D1	Air	23.4	22.6	1.8149	11.9899	0.0604

Sample	Density (kg/m ³)	ΔX (kg NH ₃ /m ³ carbon)	Potential cooling production with 2 minute cycle time (kW)
LM127	750	64	1.7
1614-9-3C1	894	90	2.4
1614-9-4C1	N/A	N/A	N/A
1614-9-5D2	997	107	2.8
1614-9-6D1	932	82	2.1

This page intentionally left blank

Appendix C - Safety Review

C-1 Background

The U.S. Army currently uses commercially-available refrigerated containers -- the QuadCold manufactured by Charleston Marine Containers, Inc. -- for their need to store food, medications, and other goods. The QuadCold is outfitted with a conventional, electrically-powered, vapor-compression cycle.

The goal of this experiment is to gather data to compare performance of an alternative -- ATMI's Solar-Powered Absorption Refrigeration System (mounted in a QuadCon) -- with that of the QuadCold that uses electricity provided by a diesel generator.

ATMI's proof-of-principle test unit will be sent to an alpha test site at Sundanzer Development, Inc., Tucson, Arizona. The ATMI safety review for operation of the adsorption refrigerator at Sundanzer is presented below.

Review Title: Operation of the Solar-Powered Adsorption Refrigeration System

Purpose/Description: To evaluate the performance of the modified Solar-Powered QuadCon refrigerator, and compare the results with the existing, off-the-shelf military refrigeration system.

Review Author: Shkelqim Letaj

Group: ATD

Expiration Date: 03/10/2011

Serial Num:
SLEJ-7WRRLB

Version Number: 1

Issue Date: 03/10/2010

Status: Final

C-2 Safety Issues

C-2.1 Chemical (Starting, Intermediate and Final Products)

<u>Substance</u>	<u>Quantity</u>	<u>Hazard</u>	<u>TLV/IDLH/UEL/LE</u>
1) Ammonia (NH ₃) 2) Helium (He) 3) Steam	1) 6 kg 2) 49 L Cyl 3) 15 Gallons	1) Toxic, and Corrosive 2) Pressurized inert gas, Asphyxiant 3) Press.= 60 psi, Temp = 140 C	<u>L</u> 1) 25 ppm TLV, 300 ppm IDLH 2) > 81 % 3) N/A

C-2.2 Electrical

<u>Equipment</u>	<u>Voltage</u>	<u>Operating Current</u>	<u>Fuse Current</u>
1) System Control Enclosure	1) 24 VDC	1) < 20 A	1) 20 A
2) Data Acquisition Enclosure	2) 120 VAC	2) ~8 A	2) 10 A
3) Photovoltaic Control Enclosure	3) 24 VDC	3) < 60 A	3) 60 A
4) Photovoltaic Panel	4) 28 VDC	4) 7.8 A	4) 10 A
5) QuadCool	5) 400 VAC (3P)	5) 8.1 A (Max)	5) 10 A

C-2.3 Physical: (heavy objects, sharp objects, hot surfaces, etc.)

Both QuadCold and QuadCon units are very heavy and so require forklift capability to move onto transport assets or relocate onsite. Moving of the QuadCon will be done by third party at the test location. The modified QuadCon uses solar collectors to heat water to temperatures of 140°C, and pressurize to 65 psi. When doing any repair, the system solar collectors should be covered with tarps to block solar input until the water temperature drops below 60°C. There may also be a need for compressed gas cylinder use, in which case operators should follow ATMI's high-pressure gas cylinder handling procedures (ATMIDBY-ESOP- 0013). The solar collectors are made of glass to retain a vacuum, so care should be taken and tough gloves should be worn when handling these tubes to minimize the risk of cuts.

C-3 Emergency Procedures

C-3.1 Circuit Box Area, Location, and Breaker Number

- Photovoltaic Panels - Panels will be energized all the time, there is no circuit breaker. (Refer to PV wiring diagram)
- Photovoltaic Control Enclosure - CB-01, CB-02, CB-03, CB-04, CB-05, F-01, and GFP (Ground Fault Protection) .(Refer to PV wiring diagram.)
- Water Heater - F1 and F2
- Refrigerator Control Enclosure - F1

C-3.2 Full Emergency Shut-Down

Because unit will be installed in Tucson, AZ, this will not be available.

C-3.3 Operator Emergency Shut-down

- Depress "Emergency Machine Off" (EMO) on control box. This will shut down power to the system. However, depending upon the hot water temperature, power may be automatically reactivated to the relay for the thermostat which operates valve #9, the pump #1 and the cooler fan. This safe condition would ensure that when the thermostat reaches the high limit it will activate the pump, valve and cooling fan sending hot water from the solar collectors to the high-temperature coils in the cooler, bringing the temperature of the solar collector water down.

- Under an emergency shut-down condition, immediately cover the Thermomax solar collectors with tarps to minimize further heating.

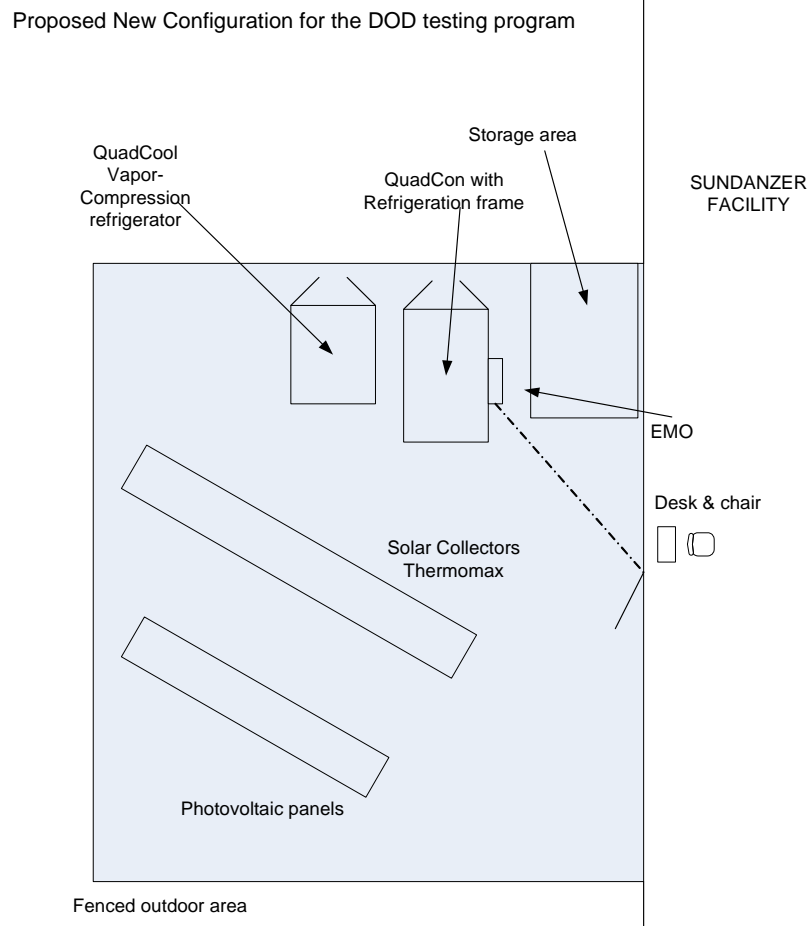
C-3.4 EMO Testing Verification:

I, the author, have tested the EMO and found that the EMO works as stated above.

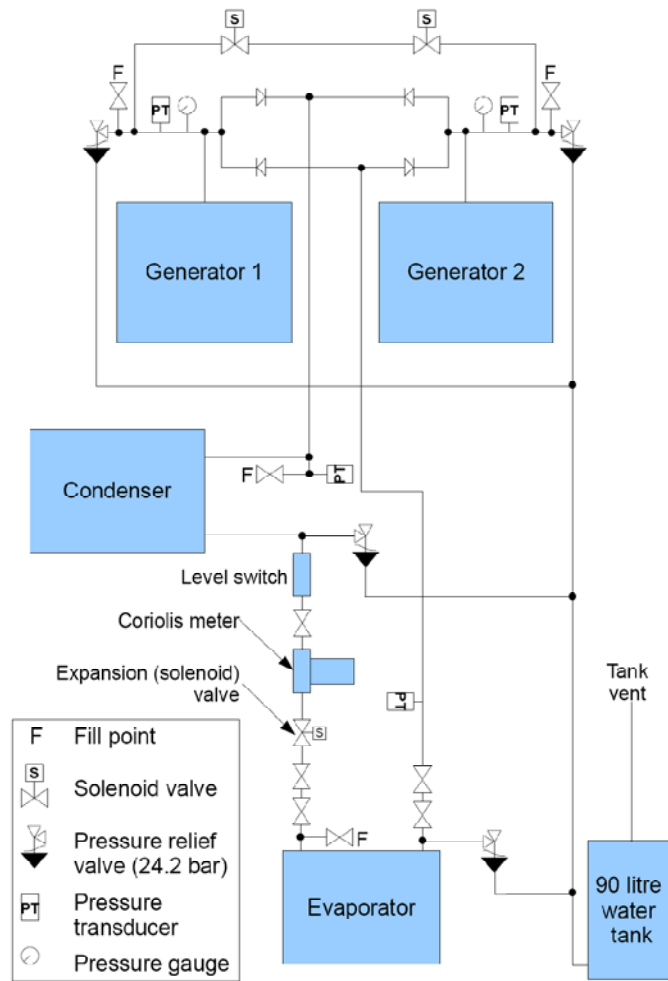
Signed, Shkelqim Letaj on 02/18/2010 05:41:55 PM

C-4 Diagrams/Schematics

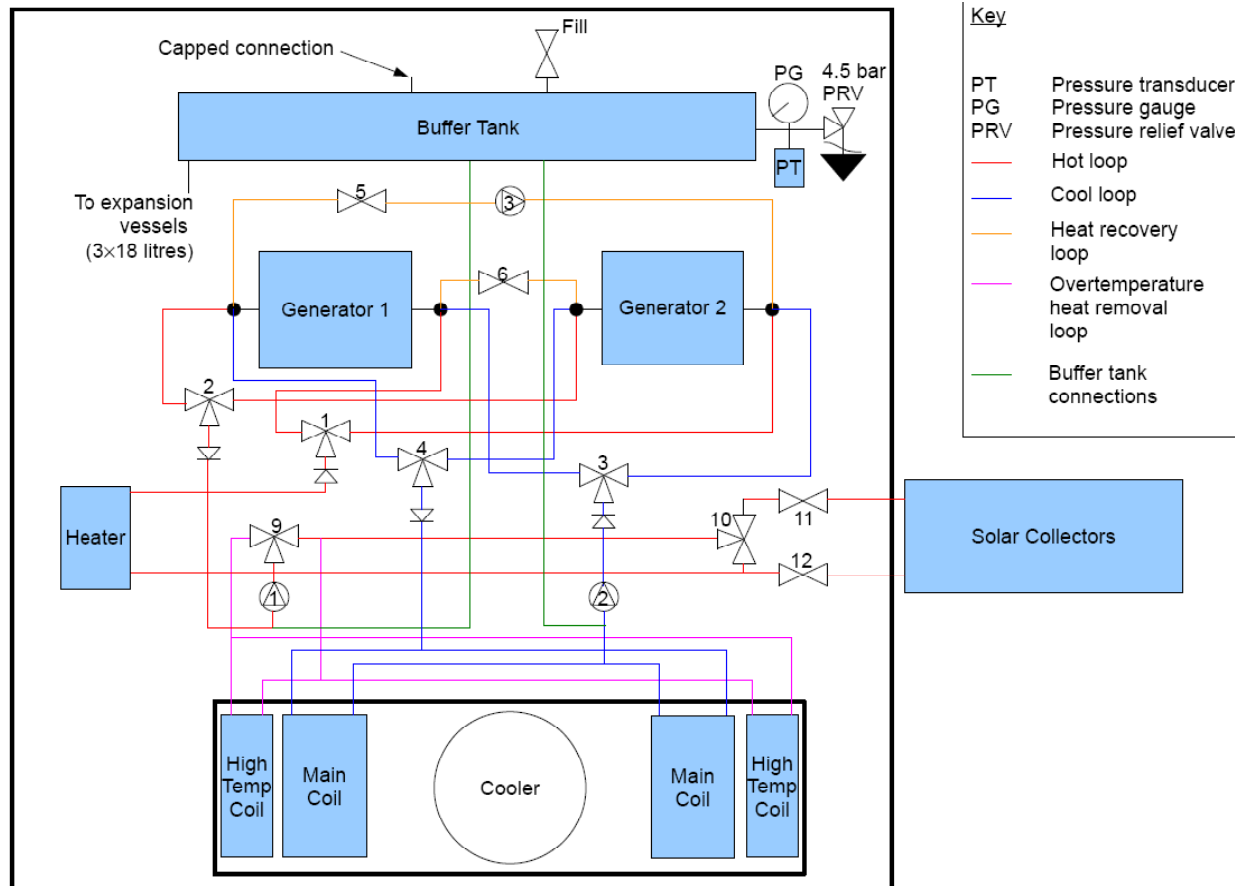
C-4.1 Room Map



C-4.2 Refrigerant (Ammonia) Manifold Piping and Instrumentation Diagram



C-4.3 Water Manifold Piping and Instrumentation Diagram



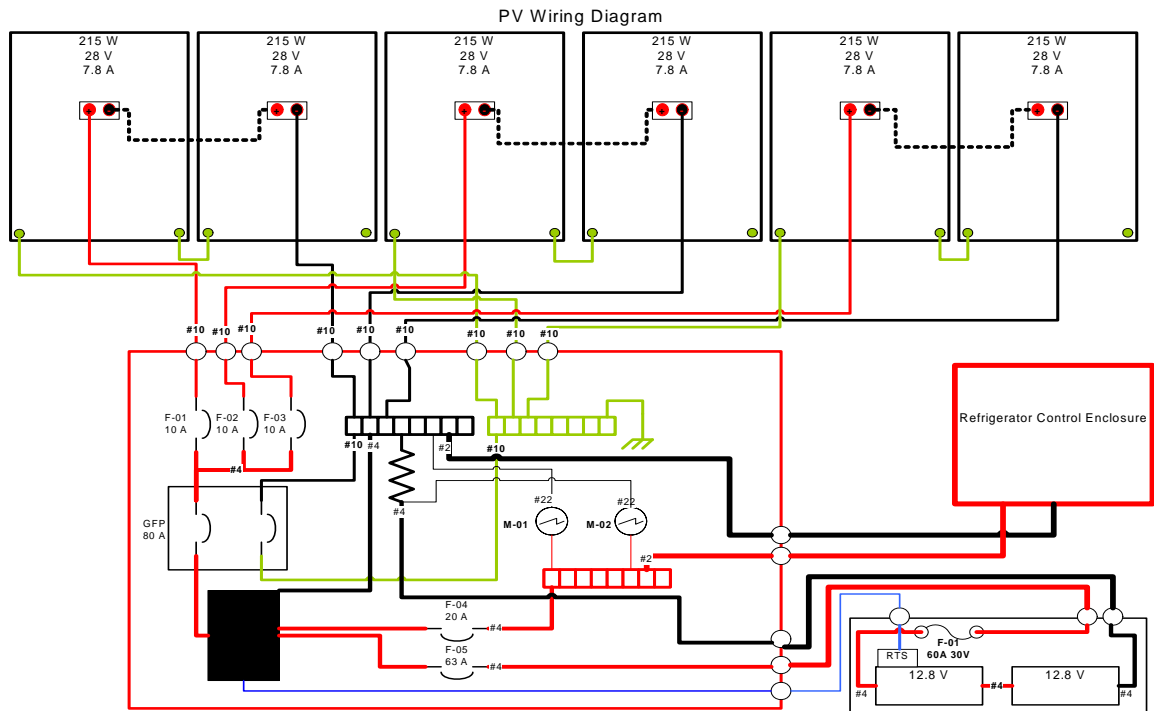
Valves

- 1 Hot water flow valve. 3-way L-port ball valve with 24Vdc actuator.
- 2 Hot water return valve. 3-way L-port ball valve with 24Vdc actuator.
- 3 Cool water flow valve. 3-way L-port ball valve with 24Vdc actuator.
- 4 Cool water return valve. 3-way L-port ball valve with 24Vdc actuator.
- 5 Heat recovery valve 1. Ball valve with 24Vdc actuator.
- 6 Heat recovery valve 2. Ball valve with 24Vdc actuator.
- 7 Mass recovery valve 1 (ammonia). 24Vdc solenoid valve.
- 8 Mass recovery valve 2 (ammonia). 24Vdc solenoid valve.
- 9 Overtemperature valve. 3-way T-port ball valve with 24Vdc actuator. Diverts hot flow to the high temperature coil in the cooler when a thermostat detects that the water temperature has exceeded the maximum value (can occur during high insolation if the machine cannot use all of the heat from the collectors).
- 10 Collector bypass. 3-way L-port ball valve. Manual. Bypasses the collector connections when the machine is used with the electric heater only.
- 11, 12 Solar collector isolating valves. Manual ball valves.

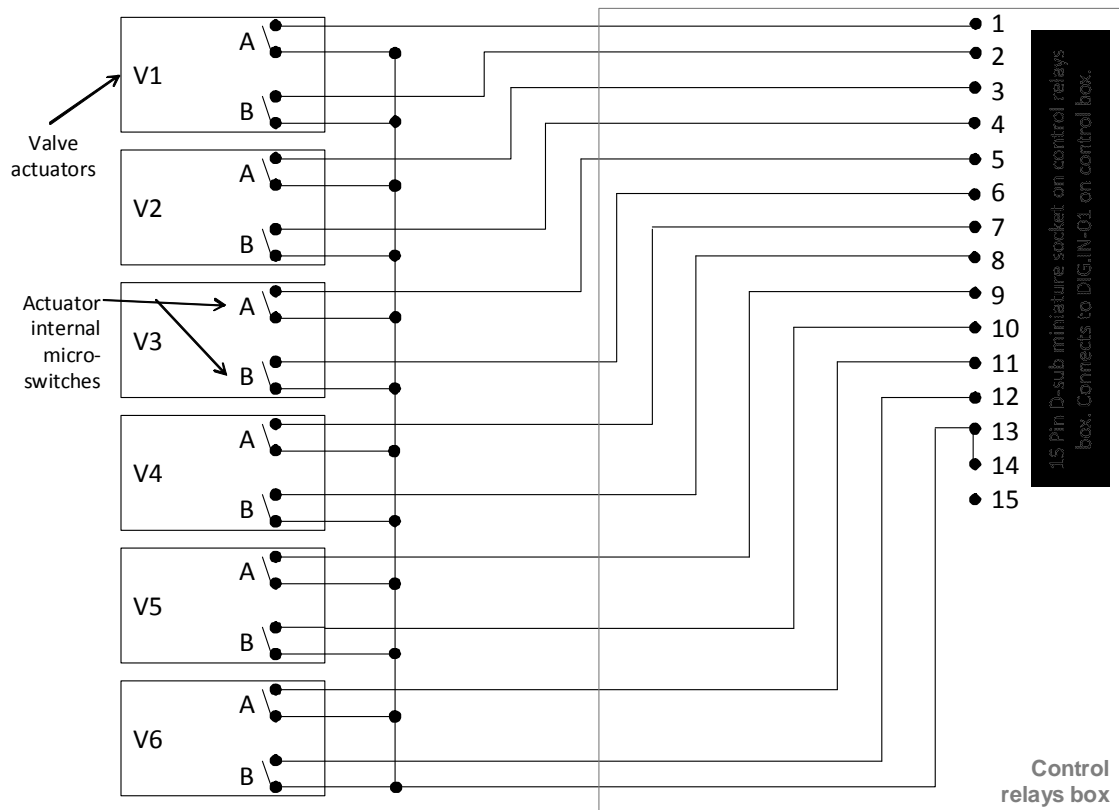
Pumps

- 1 Hot water pump
- 2 Cool water pump
- 3 Heat recovery pump

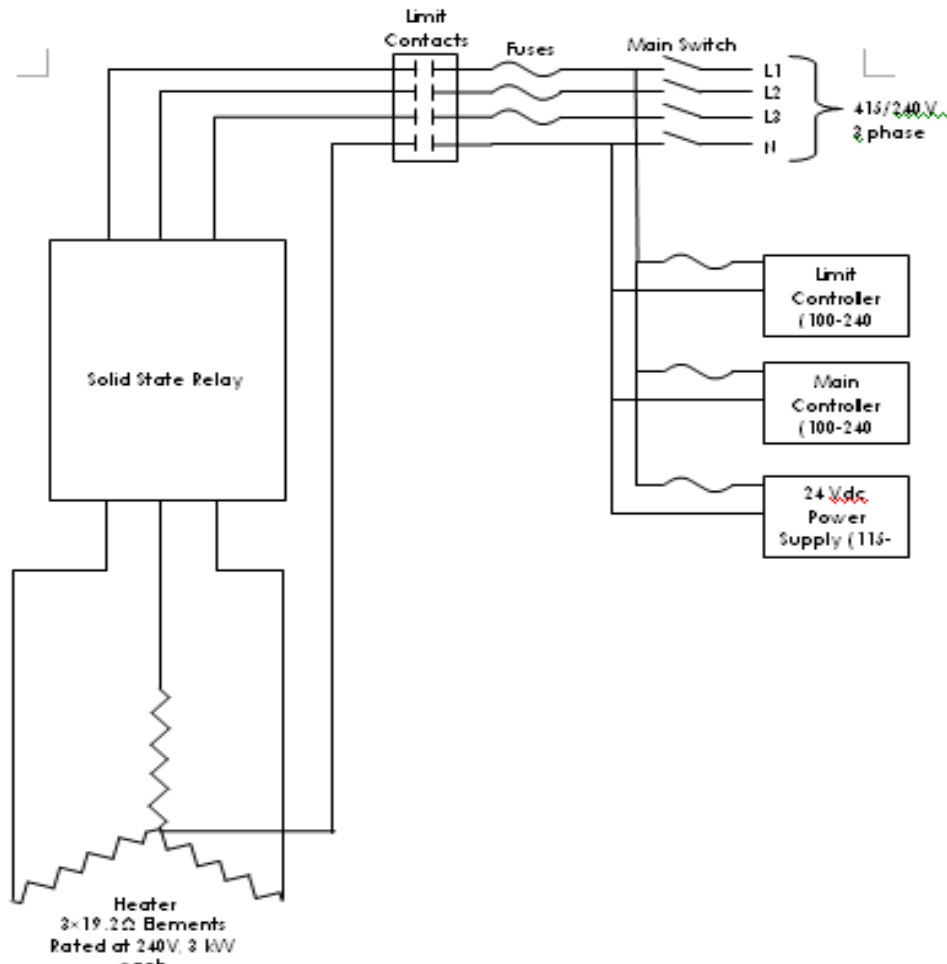
C-4.4 Photovoltaic Sub-System Electrical



C-4.5 Refrigeration Unit Electrical



C-4.6 Electrical Water Heaters Used During Shake-Down Testing



C-5 Potential Hazards and Solutions

Ammonia (NH₃) Leak - To prevent this potential hazard before filling the system with Ammonia, the operator must perform a leak check of the system by pressurizing the system to 30 bar (300 psi), and then performing a leak down test to see if the system is losing pressure which would indicate a leak in the system. Another potential leak scenario is if the pressure of the system goes above the pressure rating of the pressure release. If the system is over-pressurized the pressure release outlets go directly to a water tank scrubber. The pressure relief valve (one of the 3) will open and direct the ammonia to the 90 liter water tank in the QuadCon.

Water Line Over Pressurization - Over-pressurization due to over-heating of the system is another potential hazard which could result on a burst of the water line, solar tube, or any other component where water flows. To prevent this from happening the system is equipped with expansion vessels that would prevent the pressurization of the system. In addition, the system has emergency cooling coils that will be activated if the temperature of water goes above the preset limit (thermostat controlled). Another measure of protection is the water/steam pressure release valves that are installed in the system that open and discharge onto the pavement if the above equipment cannot control the pressure and the temperature of the system.

Broken Glass - Solar collector tubes are insulated by a glass jacket (vacuum barrier) so care should be taken when handling these tubes because they are very fragile.

Photovoltaic Panels - These panels should be covered when working with wiring because panels will produce electricity even if they are not installed. Building up the charge in these panels could cause lethal shock and burn hazard. To reduce the risk of electrical shock or burns, modules may be covered with an opaque material during installation.

Electrical Wires - Wires will run from the photovoltaic control enclosure to the refrigerator control enclosure that carry up to 60A current that could cause a lethal electrical shock. These wires will run through conduit to prevent any damage, however care should be taken when working around these wires.

Tripping - Because there are wires and water lines running from one sub system to another, care should be taken when walking around due to number of trip hazards. Cable and hose protection systems will be used in areas where personnel walks frequently.

Hot Water Line Burst - In event of water line burst this can potentially cause an unsafe situation if operator is near when the steam is discharged. Cable and hose protection systems will be used in areas where personnel walks frequently to minimize this hazard.

Solenoid Valve Failure - If the solenoid valves fail in an open position, there would be no cooling. If they fail in a closed position, efficiency would suffer. Either condition presents no danger.

Suspicion of Lost Ammonia - If the operator suspects a loss of ammonia, the system should be emptied, the system pressurized, leak tested, repairs made as necessary, then the system can be refilled.

Sensing Lost Power to Ammonia Level - The sensor is a vibrating leaf type level control. The Coriolis meter will report a zero flow and cause an alarm condition.

C-6 Potential Incidents and Operator Response

The following compares incidents that require a simple operator shutdown vs. more dramatic measures such as building evacuation. However, this testing is outside.

The following situations will require the operator to shut down the system and fix the problem:

- 1) Very minor ammonia leak from fittings and welds on the gas manifold. System should be pumped out and leak checked to ensure the leak was fixed.
- 2) One or both pressure release valves in the ammonia manifold open.
- 3) Minor or major leak from water manifold.

The following situations will require the operator to shut down the system and request assistance:

- 1) Major ammonia leak from the fittings and welds on the gas manifold.

- 2) Employee injury.
- 3) Anytime the operator feels it is necessary

C-7 Environmental Issues

Hazardous Gas - Gaseous ammonia (NH_3) will be present.

Gaseous/Liquid Effluent & Abatement - There is a 90 L tank that will be filled with water to react with ammonia. Hot water will be present during operation.

Hazardous Aqueous Waste - The liquid ammonia can be neutralized using acetic acid (vinegar), and disposed of as non-hazardous waste. Alternatively, follow hazardous waste procedure ATMIDBY-ESOP-0005.

Hazardous Solid Waste - N/A

Spill Plan/Worst Case Scenario - The worst case scenario is a release of 6 kg of ammonia into atmosphere. This would not be a reportable quantity according to federal and most state regulations. The MDA Scientific Gas Analyzer will monitor the system to alert the operator and put the system into safe state.

C-8 Miscellaneous

C-8.1 Operational Procedures

C-8.1.1 Initial Installation at Test Site

- Installing the Thermomax Solar Collectors
- Install collectors facing the sun with an angle of $\sim 48^\circ$ from horizontal.
- Cover the collectors with tarpaulin.
- Install the photovoltaic panels and the junction power box and batteries.
- Cover the panels with tarpaulin.
- Install a relay and power to valve #9, pump #1, and the water cooler fan, which would become activated when the thermostat reaches a critically high temperature.

C-8.1.2 Connecting the Refrigeration System to the QuadCon

- Move the QuadCon in the designated area so that the doors face the north-west fence line about 6 feet from the fence.
- Remove all wooden shipping-protection pieces and remove the frame from the pallet.
- Remove the side panels from the frame.
- Raise the frame from the pallet using a fork truck, then locate the frame on a pallet jack.
- Maneuver the frame on the pallet jack towards the cut-out at the rear of the QuadCon, taking care not to move too quickly.
- When close enough, connect the heater connection plug to the socket on the left-top corner of the cut-out.

- Move the frame into the cut-out, allowing ~2" clearance all around.
- From above the cut-out, connect the braided plastic hose from the pressure relief valves near the generators to the plastic T-coupling.
- The braided plastic hose that emerges from the rear of the QuadCon is connected to the water reservoir below the cut-out. Add approximately 60 liters of water to the reservoir.
- Connect the two (green) thermocouples (TCs) to the TC leads from the electric heater.
- Connect the four yellow thermocouples to the extension TC cables.
- Connect the liquid line connection on the rear of the QuadCon to the liquid line connection which is capped off above the generators.
- Open both valves on either side of the connection.
- Connect the steel-braided flexible hose from the evaporator suction line on the rear of the QuadCon to the suction line connection point above the generators on the refrigeration unit (both fittings have ball-valves).
- Open both ball valves on either side of the connection.
- Remove the four flared connection caps -- three from the frame system and one from the rear of the QuadCon.
- With all four valves closed at those connection points, connect the four flared-connections to the four flexible hoses from the vacuum manifold.
- Install the Electrical Control Box on the side of the QuadCon.
- Connect a grounding wire to the grounding points and the ground at the Sundanzer Plant.
- Install the solar meter horizontally on the roof of the QuadCon.
- Insert all of the tagged DIN (German Institute for Standardization) plugs into the sockets on the Control Box.
- Insert all the yellow thermocouple connections into the Control Box.
- Replace the sheet steel siding on the Coriolis side of the frame
- Run 3/4" copper tubing from the outlet and inlet of the Thermomax Solar Collectors to the 3/4" Swagelock fittings on the Coriolis side of the frame
- Pull wiring through steel conduit from the PV panels to the QuadCon Control Box.
- Connect electric power from the junction box from the Photo Voltaic panels to the control box.
- Install foam insulation on the 3/4" copper pipe and cover the pipe with protective guards to ensure the pipe does not get damaged.
- With the top sheet metal cover of the frame removed, access is possible to the water fill valve. An automatic air valve can be plumbed into the water buffer tank alongside this valve.
- Begin to fill the Thermomax solar collectors with water. When filled (with the trap still in place), open the water valves #11 and #12 at the connecting points on the refrigeration frame.
- Start water flow and measure flow rate and temperature.
- Direct the line from the pressure relief valve on the solar collector water to the ground.
- Top off the water through the water fill valve on the buffer tank.

- Install rain covers over the Control Box, the ventilation slats on the Frame top and the open cut-out at the rear of the QuadCon.
- Install the MDA Scientific Gas Analyzer in a location, close enough to the ammonia lines in the refrigeration frame to ensure detection of an ammonia leak.

C-8.1.3 Commissioning

- Using the fill manifold evacuate the manifold and then open each of the four shut-off valves in the refrigeration system and evacuate the entire system of the dry argon and trace ammonia left. The exhaust from the pump should be directed into a water reservoir to dissolve up any ammonia that had desorbed from the carbon following the shake-down runs in U. of W.
- Now pressurize the manifold and system using dry nitrogen from a pressurized cylinder at 15 bar (220 psi) to check for leaks. Leave the pressurized system open to the pressure gauge, overnight and check the following morning that the pressure has not dropped.
- Place the ammonia cylinder on a weigh scale to monitor exactly how much ammonia is being added.
- Cool down the evaporator by connecting hoses to the red-handled valve connectors below the evaporator and the outflow hose reaching over the side and into the cold compartment (two compartments) and pumping cold water from a constant temperature bath.
- Evacuate the system again to < 1 mbar vacuum.
- Close the vacuum valve to the system and open the ammonia cylinder (on the weigh scale) to begin filling the cooled evaporator and the generators.
- Once ~6 kg of ammonia have been added, close the ammonia valve, close the four valves on the frame and QuadCon.
- Pump out and cycle purge the manifold with the pump exhaust continuing to discharge to the water bucket.
- Disconnect manifold
- Cap-off fill ports.
- The system is now ready to operate.

C-8.1.4 Operation

- After connection of the PV power to the control box and with all systems ready to start, remove the tarp from the PV panels and allow current to flow.
- Once power is supplied to the control box, remove the tarp cover from the Thermomax solar collectors. The pumps should be operating and water flow should be noticeable at the flow meters.
- At the laptop computer set a cycle time (suggested start might be 5 minutes).
- Allow the system to reach steady state, monitoring all thermocouple points, Coriolis ammonia flow, solar meter, ambient temperature, temperature of the condenser, evaporator, ice formation, air temp in the QuadCon, hot water temperature from the solar collectors, water pressure and ammonia pressure

- Depending upon the degree of success at the 5 minute cycle time, adjust the time up or down with the range of 2–6 minutes.
- Continue the data generation until enough conditions have been achieved which would allow the generation of an algorithm to control cycle time depending upon reaching a constant cooling power. This is expected to take 1-2 weeks assuming no serious malfunctions.
- Cooling Power = Coriolis mass/sec... kg/sec x λ latent heat kJ/kg
- Cooling Power = kg/sec x 1336.97 kJ/kg
- Once the algorithm has been decided, apply to the control system and allow system to function with auto varying cycle time dependent on the solar insolation, the Thermomax water temperature, the ambient temperature and the ammonia pressure.
- Install the 2nd QuadCool and monitor its performance and power requirement alongside the ATMI QuadCon.
- Continue the test work for at least 2-3 weeks, of steady state operation.

C-8.1.5 Decommissioning

- Begin the decommissioning early in the morning of the shut-down day.
- Cover up the solar panels -- Thermomax and photovoltaics.
- Switch off the electric power from the batteries.
- Close water valves and drain the solar collectors.
- Disconnect lines from the collectors to the QuadCon frame.
- Remove four caps at the ammonia fill positions and connect the flexible hoses from the vacuum manifold.
- Evacuate the manifold with a valved connecting line to a 55-gallon drum of water (water scrubber), open the four ammonia valves and crack open carefully the valve to the water scrubber, letting the ammonia escape gradually into the scrubber.
- Neutralize the ammonia in the 55-gallon drum with vinegar.
- Once the pressure reaches atmospheric pressure, close the scrubber valve and begin pumping down the ammonia (with the exhaust of the pump directed into the water scrubber).
- Pump down to < 1 mbar then close the vacuum line to the manifold and gradually open the nitrogen line, filling the system with dry nitrogen to atmospheric pressure.
- Close all four fill valves on the frame and QuadCon and cap off the fill ports.
- Remove the Coriolis meter and replace with a single 1/4" SS tube with Swagelok fittings.
- Disconnect the cables to the Control Box,.
- Dismantle the box and store separately.
- Close the two valves which connected the frame liquid ammonia line to the QuadCon evaporator liquid ammonia line.
- Disassemble the frame and QuadCon connection. Disconnect the liquid lines and cap off.
- Using the pallet jack pull the frame away from the QuadCon and disconnect the electrical lines to the heater control box.
- Using a fork-lift, raise the frame up onto the wooden shipment pallet.
- Clamp the frame in place on the wooden pallet.

- Ship the QuadCon, frame, Control Box, laptop computer, Thermomax collectors and frame, photovoltaic panels and frame to U.S. Army at Natick, MA.

C-8.2 Personal Protection

C-8.2.1 Buddy System

When doing maintenance work on the system, the operator should have a "buddy", or s/he should let one of her/his colleagues know that they are working on the system so can be checked on periodically.

C-8.2.2 Personnel Protective Equipment (PPE)

Operators will always wear Z87 rated safety glasses when working around the refrigeration unit. Nitrile gloves should be worn when handling any liquid solutions that reacted with ammonia. SCBA (Self Containing Breathing Apparatus) should be worn when filling and removing ammonia from the system.

C-8.3 Safety Interlocks/Measures

C-8.3.1 Hard Interlocks

Ammonia Manifold - There are four pressure release valves in the ammonia manifold that would open if pressure exceeds 350 psi (24.2 bar). Pressure release valve outlets are routed to a 90 liter water tank that is used to react with any ammonia released.

Water Manifold - There are four pressure release valves in the water manifold. The first pressure release is connected to the buffer tank in case the pressure increases in the manifold, and the second pressure release is connected on the solar panels to prevent over pressurization if valves #11 and 12 are closed (refer to water manifold diagram).

C-8.3.2 Soft Interlocks

Ammonia Pressure Monitoring - If ammonia pressure goes above preset limit (lower than the rating of pressure release valves), software will put the system into a safe state with all valves closed and will turn on a fan to cool off the system until the pressure goes below the preset limit.

High Temperature Coil - System is equipped with high-temperature coil used if the water temperature of the water goes above preset temperature. When the sensors measure a higher water temperature than the preset value, it will open valve #9 (refer to water manifold diagram) so water will flow through to the high-temperature coils to cool off the water.

C-8.4 Critical Equipment and Safety-Related Maintenance

C-8.4.1 MDA Scientific Gas Analyzer

Personnel using this system should be familiar with handling of hazardous compressed gases, Kitigawa colorimetric tube testing, and MDA gas analyzers. Operator should be familiar with this safety review and all procedures involved with this operation of this

system. System uses high electrical current sources that require training to understand the hazards that come from this.

The MDA equipment must be optically verified monthly. The MDA tape should be checked daily to ensure it does not run out while system is running. When using MDAs, ensure correct ChemKeys and Chemcassettes are used.

Critical Equipment Name	Location	Equipment Calibration / PM record or checklist (please attach)	PM Frequency	PM Requirements (not required if Equipment record or checklist is attached)
MDA	Sundancer lot	14KEQP #0389	Monthly	Perform reading verification using manufacturer supplied color stains. Use ATMIDBY EWI-0009 Unit is used as a secondary detection device, supplemental to the house MDA. It is not used to verify concentrations, nor is it used on a regular basis. It is used as a yes/no instrument to indicate system leaks during operation with the advantage of a quicker response time than the house MDA. Only primary monitor requires calibration

C-9 Review Signatures and History

Electronic Notification List:

FEC:	Trainees:
Matt Donatucci	Shkelqim Letaj, Shaun Wilson, Edward Jones, Donald Carruthers, Joe Sweeney, Ed Sturm

Full Review Signatures:

Name:	Shaun Wilson	Ed Sturm	Edward Jones
Date:	02/22/2010	03/08/2010	03/08/2010

Name:	Donald Carruthers
Date:	01/25/2010

Minor Process Change Approval: (chairperson only)

Chairperson: Shaun Wilson

Last Signature: Full Review finalized by Laura Hiscock on 03/10/2010, version 1

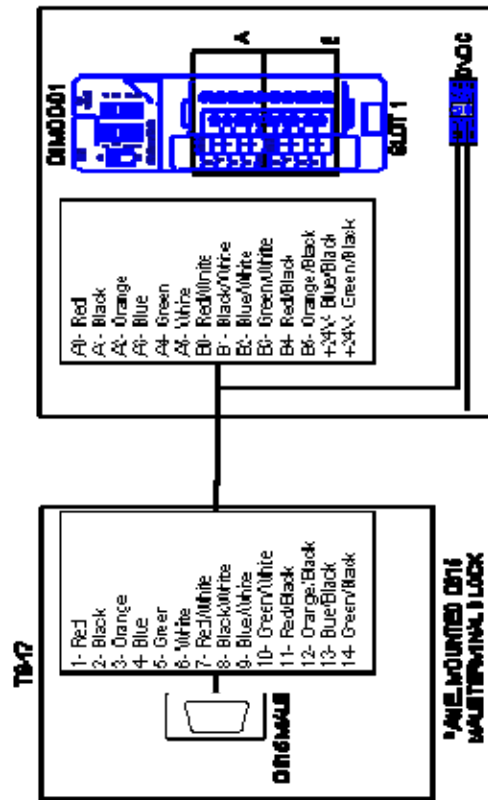
Change History:

Date	Version	Changes Made
03/08/2010	1.0	Original document version

Full Review Approved by Laura Hiscock on 03/10/2010 - version 1
Created by Shkelqim Letaj on 10/12/2009

This page intentionally left blank


Rev.	Description	Date
1	UNAPPROVED	4/8/2010



 ATMI <small>Advanced Thermal Management Inc.</small>		* Commercial Drive Danbury, CT 06810, USA (203) 269-7122 Fax: (203) 269-7122 E-Mail: info@atmi.com		Page: 11
Order: General Aircraft Ion Refill order Sys Ion (SP-AP) Message - Control Endocrine Digital h		Order Date: 04/18/2012 Order No: 8 Order Date: 04/18/2012 Order No: 8		Order Date: 04/18/2012 Order No: 8
Order Date: 04/18/2012 Order No: 8		Order Date: 04/18/2012 Order No: 8		Order Date: 04/18/2012 Order No: 8

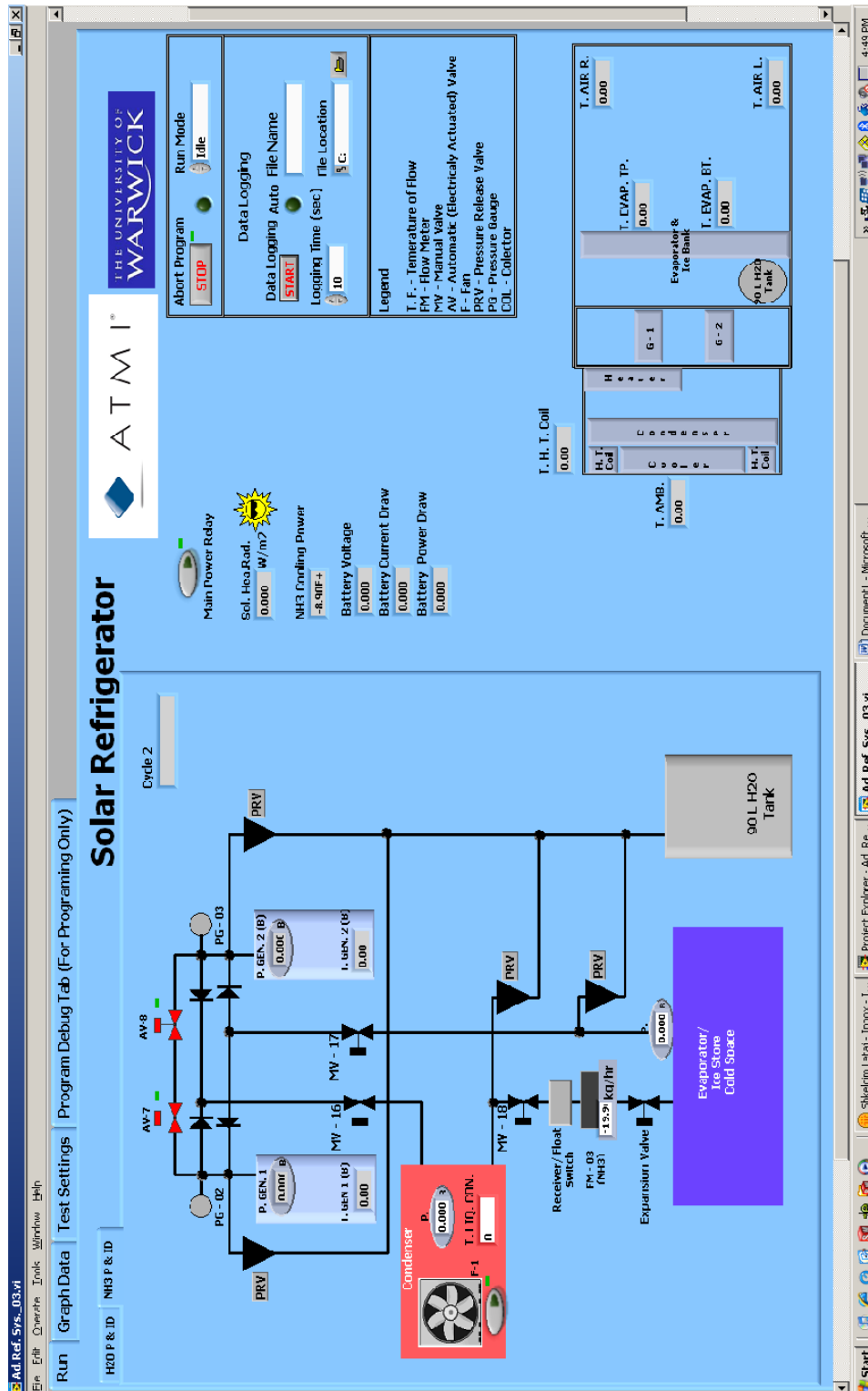


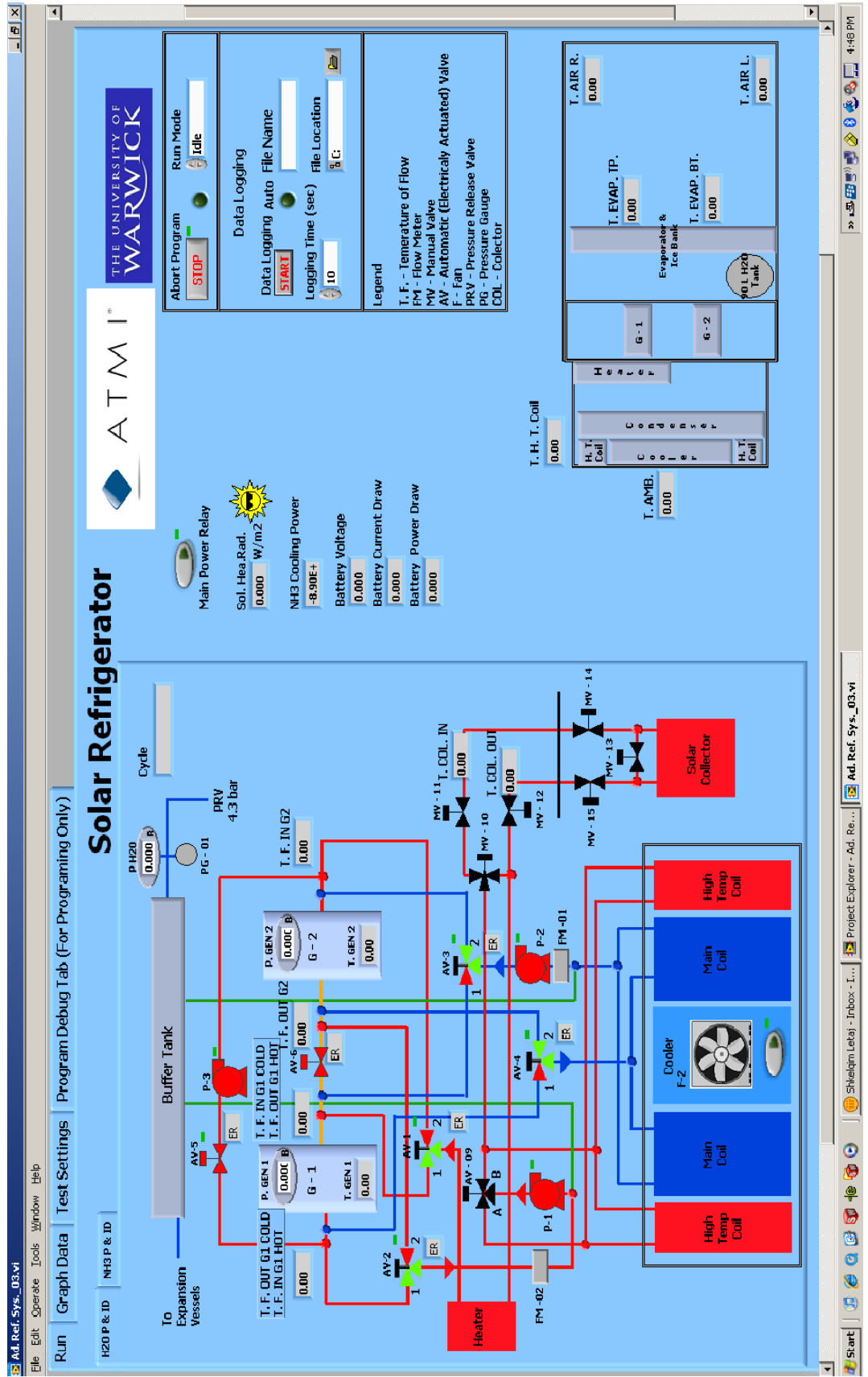
AWLOG IN OUT		
01	94424	041 A05
02	94425	94426
03	94427	94428
04	94429	94430
05	94431	94432
06	94433	94434
07	94435	94436
08	94437	94438
09	94439	94440
10	94441	94442
11	94443	94444
12	94445	94446
13	94447	94448
14	94449	94450
15	94451	94452
16	94453	94454
17	94455	94456
18	94457	94458
19	94459	94460
20	94461	94462
21	94463	94464
22	94465	94466
23	94467	94468
24	94469	94470
25	94471	94472
26	94473	94474
27	94475	94476
28	94477	94478
29	94479	94480
30	94481	94482
31	94483	94484
32	94485	94486
33	94487	94488
34	94489	94490
35	94491	94492
36	94493	94494
37	94495	94496
38	94497	94498
39	94499	94500
40	94501	94502
41	94503	94504
42	94505	94506
43	94507	94508
44	94509	94510
45	94511	94512
46	94513	94514
47	94515	94516
48	94517	94518
49	94519	94520
50	94521	94522
51	94523	94524
52	94525	94526
53	94527	94528
54	94529	94530
55	94531	94532
56	94533	94534
57	94535	94536
58	94537	94538
59	94539	94540
60	94541	94542
61	94543	94544
62	94545	94546
63	94547	94548
64	94549	94550
65	94551	94552
66	94553	94554
67	94555	94556
68	94557	94558
69	94559	94560
70	94561	94562
71	94563	94564
72	94565	94566
73	94567	94568
74	94569	94570
75	94571	94572
76	94573	94574
77	94575	94576
78	94577	94578
79	94579	94580
80	94581	94582
81	94583	94584
82	94585	94586
83	94587	94588
84	94589	94590
85	94591	94592
86	94593	94594
87	94595	94596
88	94597	94598
89	94599	94600
90	94601	94602
91	94603	94604
92	94605	94606
93	94607	94608
94	94609	94610
95	94611	94612
96	94613	94614
97	94615	94616
98	94617	94618
99	94619	94620

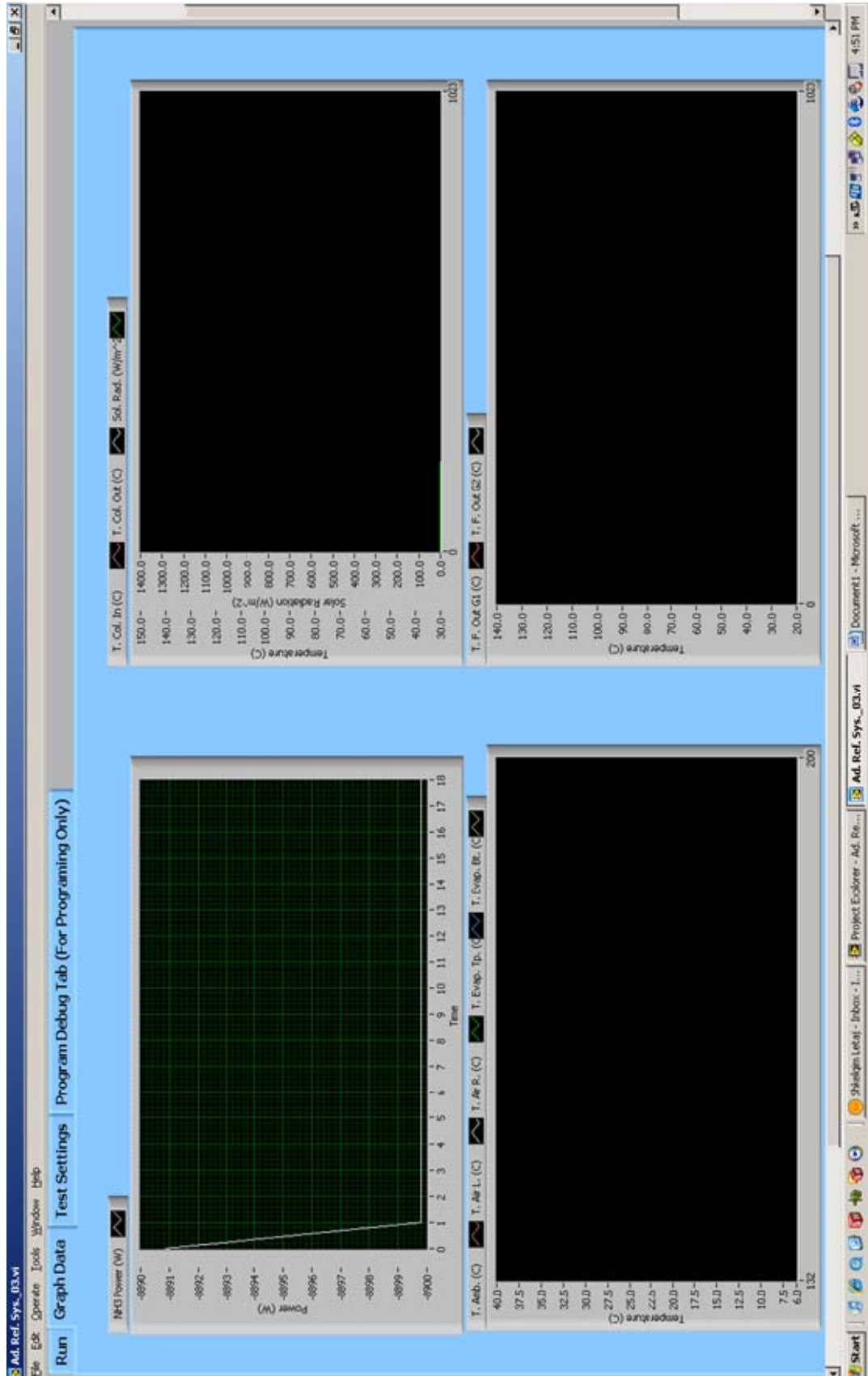
 ATMI <small>Advanced Thermal Management Inc.</small>	7 Commerce Drive Danbury, CT, 06810, USA <small>Phone: 203.734.1132 Fax: 203.734.2033</small> <small>Email: info@atmi.com</small>	Solar Powered Adaption Refrigeration System (SPARS) With Diagram - Control Enclosure Adapter Cable 01	7 Commerce Drive Danbury, CT, 06810, USA <small>Phone: 203.734.1132 Fax: 203.734.2033</small> <small>Email: info@atmi.com</small>
--	--	--	--

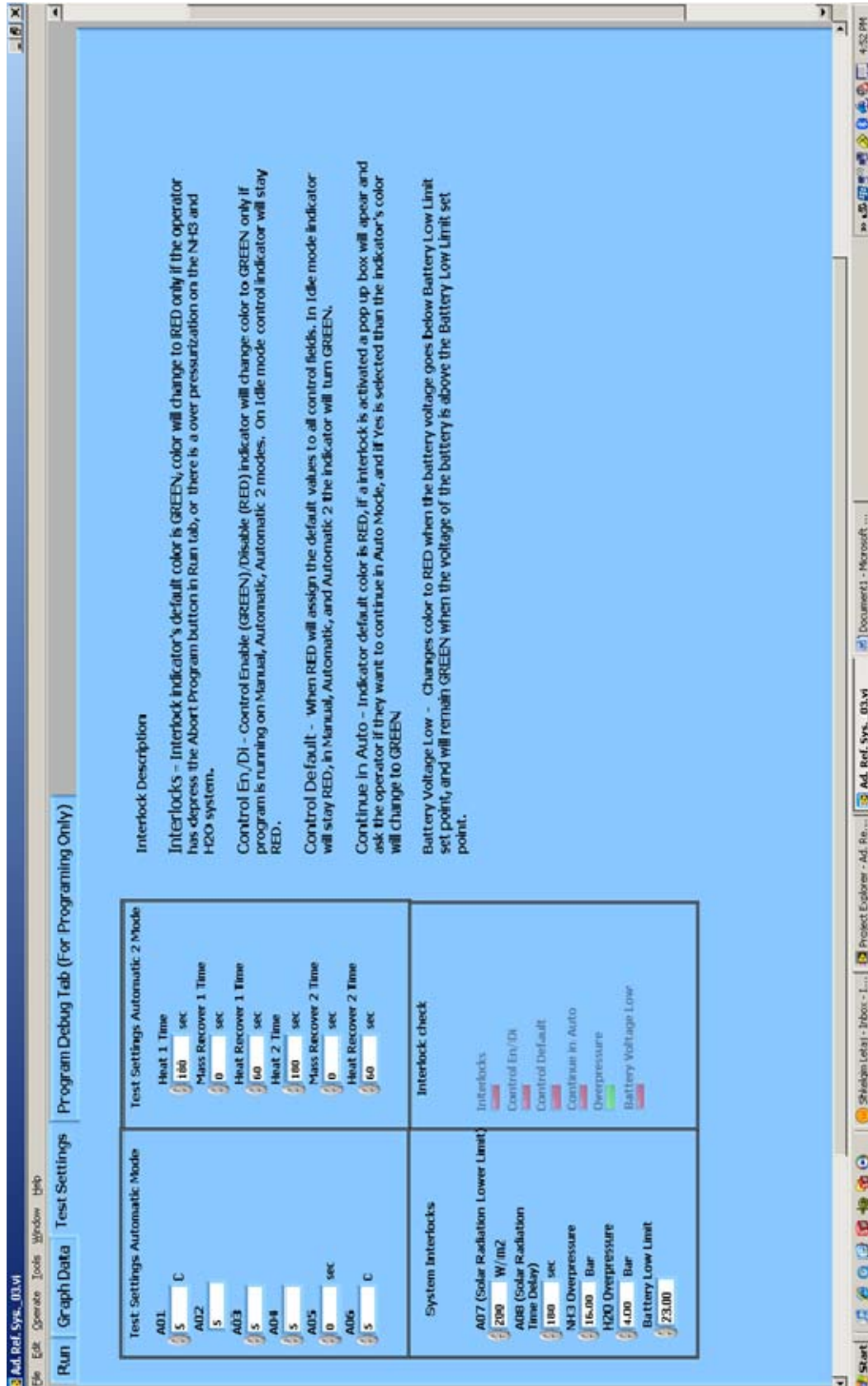
This page intentionally left blank

Appendix E - Images of Video Monitor Screens









This page intentionally left blank

Appendix F - Solar-Powered Adsorption Refrigerator Commissioning

Ammonia Charging

Total ammonia charge: minimum 2 kg, maximum 6 kg

For commissioning, a greater quantity will be required in case of any problems which require the system to be emptied and refilled.

All connection points for evacuating and filling the ammonia system have ¼" AN flare fittings (see picture). We generally use ammonia compatible charging hoses with steel fittings (see picture) for evacuating and charging. Note that copper or copper alloys cannot be used with ammonia. An ammonia charging manifold would be desirable (without one ammonia must be released to purge lines of air). A balance with a resolution of 10 g will be required to fill the system with the correct quantity of ammonia, which must have a range suitable for the size of ammonia cylinder used. An ammonia compatible vacuum pump will be required for evacuating the system. A vacuum of 1 mbar or less is sufficient. For ammonia filling, ice is required in order to condense ammonia in the evaporator. Approximately 30 kg of ice should be sufficient.



¼" AN flare fitting



Ammonia charging hose

To summarise, ammonia charging requires:

- Ammonia charging hoses with ¼" AN flare fittings (×3 minimum, 2 m or more in length)

- Ammonia charging manifold
- Ammonia cylinder containing 15 kg minimum
- Ammonia proof vacuum pump (1 mbar or less)
- Balance, 10 g resolution, capacity to suit ammonia cylinder
- 30 kg ice

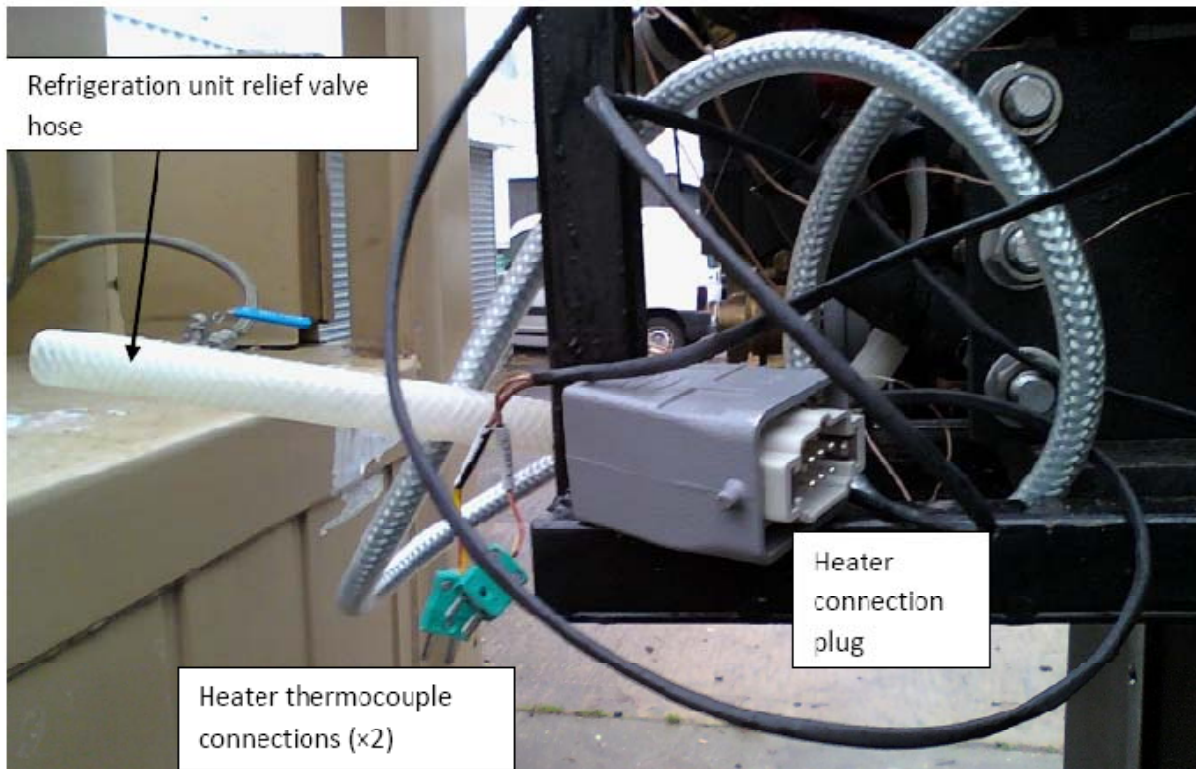
Electrical Systems

Heater Control Box

A hand drawn wiring diagram for the heater control box is included in 'Heater Control Box.jpg'. The heater control box is located in the container 'cut out'. The power is supplied through the 35A Harting socket located on the front of the box. The matching plug was shipped inside the container. Pin 1 should be connected to live and Pin 2 to neutral. The voltage is 240 Vac. The heater itself has 3 elements and would draw 38A at 240V if all 3 were connected. This exceeds the 35A rating of the socket. One of the 3 heater fuses (fuses 3, 4 and 5 on the diagram) has therefore been removed in order to draw only 26A, and only 2 elements will operate. You may wish to disconnect the wiring to one of these 3 fuse holders (Warwick could supervise this during the commissioning visit).



Heater Control Box



Heater Connections

The heater is mounted on the refrigeration unit. It is connected by a 16A Harting plug (see above picture) and a socket located on the side of the heater control box. The heater has a control thermocouple and a safety limit thermocouple which are connected under a weatherproof cover on the side of the heater control box.

Control Relays Box

The control relays box is mounted inside the refrigeration unit under a removable panel (see picture). A hand drawn wiring diagram is included in 'Control Relays Box.jpg'. The 24Vdc input is connected by a red (positive) and a black (negative) lead on the underside of the box which are terminated in 4 mm shrouded plugs.

DIN sockets are located on the underside of the box for connection to the PLC enclosure. The PLC enclosure can be mounted on the container using the two mounting bolts shown in the picture.

the valve after again ensuring that the valve is closed. The line can then be connected. This line must be completely insulated otherwise cooling will be lost.



The second ammonia connection is the suction line from the evaporator. This is connected by a stainless steel braided hose which remains permanently connected to the container (see picture below). It has a ball valve with a plugged tube on the end of it. The plug must be removed after ensuring that the ball valve is closed. The handle has been removed from this ball valve to prevent accidental opening when the unit contains ammonia. Handles are provided in the technical manual holder on the container. The picture shows the ball valve in the closed position, with the handle perpendicular to the axis of the valve. The handle should never be permanently connected to the valve during connection of the line whilst the unit contains ammonia, as the handle can easily be knocked and the valve opened.

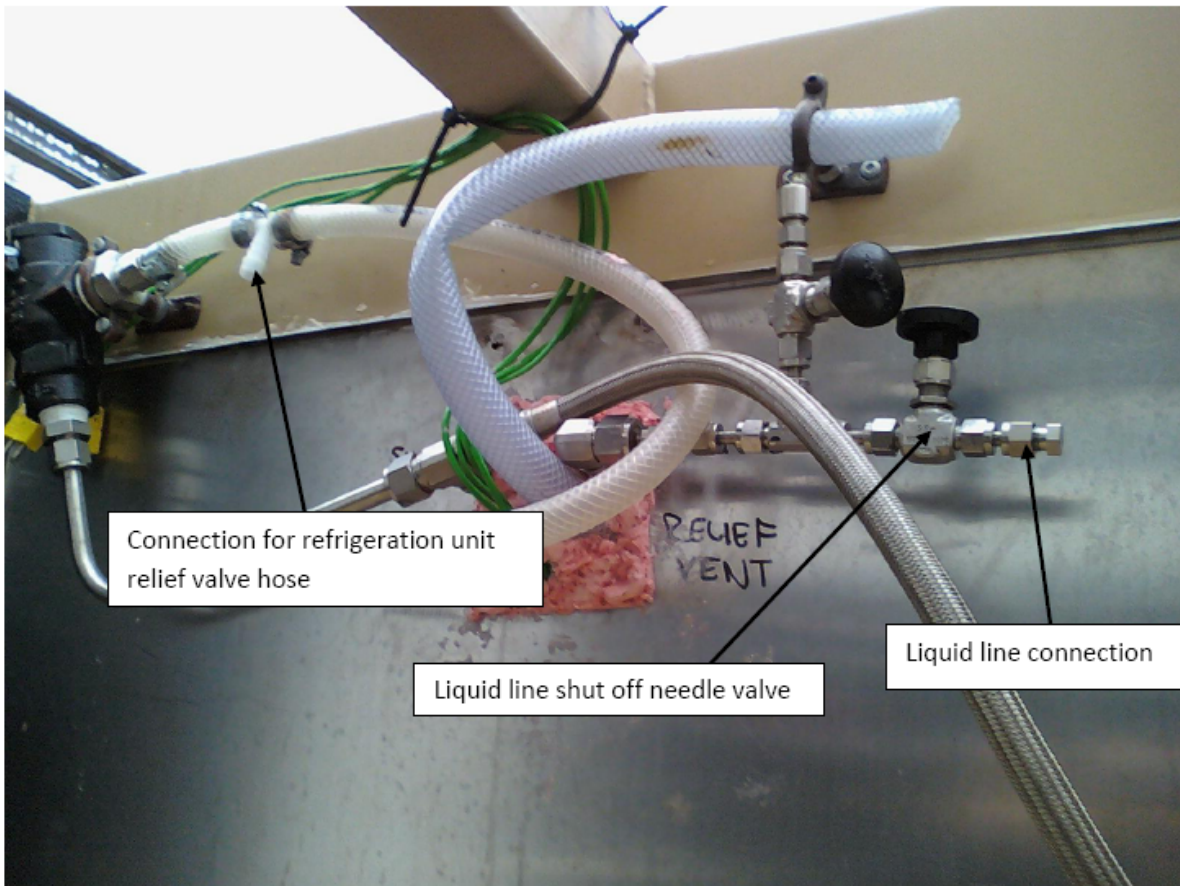
This hose connects to the ball valve on the refrigeration unit shown in the picture. This ball valve has a cap which must be removed after again ensuring that the valve is closed.



Connection Instructions

- 1 Before the refrigeration unit and container are placed together, the heater plug and the two heater thermocouples must be connected to the heater control box (they cannot be easily accessed when the overhanging section of the refrigeration unit is placed inside the container cut-out).

- 2 A pallet truck or fork lift truck should be used to place the refrigeration unit against the container as shown in the previous picture. A manual pallet truck is safer as there is less risk of damaging the overhanging section of the refrigeration unit as it is placed inside the container cut-out. Clearance between the refrigeration unit and container cut-out is tight (~2 inches) so care must be taken. The refrigeration unit cannot be lifted very far off the ground before the pipework on the overhanging section contacts the container.
- 3 The pressure relief valve hose on the refrigeration unit must be connected to the hose which leads to the water tank inside the container (see picture below) and secured with a hose clip.



- 4 Two ammonia connections must be made between the refrigeration unit and the container. The first is the liquid line to the evaporator. The above picture shows the liquid line connection on the container. The plug in the end of the tubing must be removed and retained. IF THE EVAPORATOR ALREADY CONTAINS AMMONIA THEN THE NEEDLE VALVE MUST BE CLOSED (TURNED CLOCKWISE) BEFORE REMOVING THE PLUG. The unit was shipped from the UK empty of ammonia. This line connects to the needle valve on the refrigeration unit shown below. The cap must be removed from the end of



Extension leads for all of the 15 thermocouples on the refrigeration unit are terminated with plugs for connection to the PLC box and are located under the removable panel which covers the control relays box (together with the pressure transducer and coriolis meter connection cables). The coriolis meter transmitter is also located on this side of the refrigeration unit. To access this to make the necessary changes the entire side panel should be removed (access to all of the connections will also be easier with this removed).

- 6 The connections for the solar collectors are located under the removable panel which covers the control relays box. Cut-outs are provided in the removable panel for the pipes (see picture on page 4). The upper connection is the inlet to the collectors. The lower connection is the return from the collectors. They are $\frac{3}{4}$ " Swagelok tube compression fittings. They are shut-off by two ball valves, which again have their handles removed to prevent accidental opening.

This page intentionally left blank

Appendix G - Summary Tables for Solar-Powered Adsorption Refrigerator Site Test

Date	Time	Cumulative NH3	Incremental change (kg)	Heat Cycle	Mass Recovery	Heat Recovery	Cumulative Total NH3 for Day (kg)	Who	Time Period	Elapsed time (min)	L_avg (W/m^2)	NH3_avg (g/min)	NH3 Flow Efficiency (g/hr)/(W/m^2)	T_evap.avg	T_cond.avg	P_evap.avg	P_cond.avg	L (KJ/Kg)	Qdot (kW)	T_col in	T_col out	Solar thermal efficiency ratio	T_amb avg	T_col,out T_amb
3/6/2010	3:30	27.6638																						
	4:00	27.7910	0.2272	180	0	60																		
	4:30	28.0793	0.2883	180	0	60																		
	5:00	28.5133	0.4340	180	0	60																		
	5:30	28.8348	0.3215	180	0	60																		
	6:00	29.1734	0.3386	180	0	60																		
	6:30	29.4593	0.2859	180	0	60																		
	7:00	29.6108	0.1515	180	0	60																		
	11:54	30.2639	0.6531	180	0	60																		
	12:35	30.8473	0.5834	180	0	60																		
3/7/2010	1:00	31.0361	0.1888	180	0	60																		
	1:30	31.3418	0.3057	180	0	60																		
	2:00	31.6071	0.2653	180	0	60	2.4738 DC																	
	10:15	32.0846	0.4778	180	0	60																		
	3:13	32.0846	0.0000	180	0	60																		
	7:00	32.1288	0.0442	180	0	60	0.5217 DC																	
	10:15	32.1288	0.0000	180	0	60																		
	11:15	32.1329	0.0041	180	0	60																		
	1:15	33.2529	1.1200	180	0	60			11:15am-1:15pm	120	769.20	13.37	1.04											17.21
	3:15	34.8569	1.6040	180	0	60			1:15-2:15pm	60	815.70	14.39	1.06											19.23
3/8/2010	4:15	35.7206	0.8637	180	0	60																		
	5:15	36.1097	0.3891	180	0	60																		
	Std Day						4.0693 DC	8:49:30-4:48		478.5	569.50	8.50	0.90											15.29
	10:22	36.1981	0.0884	180	0	60																		
	1:00	37.1881	0.9900	180	0	60																		
	2:00	38.2092	1.0211	180	0	60			11am-12pm	60	896.60	17.02	1.14											13.44
	3:00	39.1770	0.9678	180	0	60			12-1pm	60	963.30	16.13	1.00											15.39
	4:00	39.9749	0.7979	180	0	60																		
	5:00	40.6094	0.6345	180	0	60																		
	7:00	41.1781	0.5687	180	0	60																		
3/9/2010	Std Day						5.0584 DC	8:49-4:48:30		479.5	692.70	10.55	0.91											14.21
	10:13	41.2565	0.0784	180	0	60																		
	1:00	41.8993	0.6428	180	0	60																		
	2:00	42.8161	0.9168	120	0	60			11am-12pm	60	809.90	15.28	1.13											13.67
	3:00	43.4608	0.6447	120	0	60			12-1pm	60	730.20	10.75	0.88											14.84
	4:00	44.0648	0.6040	120	0	60			1-2pm	60	666.80	10.07	0.91											15.84
	5:00	44.7428	0.6780	120	0	60			2-3pm	60	723.10	11.30	0.94											16.73
	6:00	45.3082	0.5654	120	0	60			3-4pm	60	570.50	9.42	0.99											16.35
	7:00	45.6255	0.3173	120	0	60																		
	Std Day						4.4044 DC, JB	8:48:30-4:49		480.5	648.40	9.17	0.85											14.01
3/10/2010	10:25	45.6609	0.0354	180	20	40																		
	1:00	46.7852	1.1243	180	20	40			8:48-11am	132	670.20	8.52	0.76	6.77	13.65	4.38	9.56	1205.85	0.171	84.30	94.89	0.55	13.32	81.57
	2:00	47.7727	0.9875	180	20	40			11am-12pm	60	781.70	16.46	1.26	4.75	20.34	4.32	10.92	1171.55	0.321	111.98	127.63	0.70	16.93	110.70
	3:00	48.7203	0.9476	120	20	40			12-1pm	60	794.70	15.79	1.19	3.52	23.81	4.26	11.66	1153.56	0.304	117.14	136.49	0.85	19.57	116.92
	4:00	49.5908	0.8705	120	20	0			1-2pm	60	730.20	14.51	1.19	2.74	25.74	4.11	12.18	1143.44	0.276	120.55	138.74	0.87	20.80	117.94
	5:00	50.3115	0.7207	120	20	0			2-3pm	60	646.30	12.01	1.12	2.61	27.36	4.03	12.82	1135.52	0.227	113.88	130.68	0.91	22.08	108.60
	6:00	50.8929	0.5814	120	20	40			3-4pm	60	515.40	9.69	1.13	3.08	27.87	4.00	13.05	1133.59	0.183	113.10	125.77	0.86	21.79	103.98
	7:00	51.3351	0.4422	120	20	40			4-5pm	60	311.81	7.37	1.42	3.68	28.19	3.99	13.21	1132.71	0.139	104.10	111.53	0.83	22.25	89.28
	Std Day						5.8045 DC, JB	8:48-4:50		482	652.70	12.04	1.11	4.31	22.23	4.19	11.54	0.228	102.50	115.93	0.72	18.10	97.83	
	10:25	51.4654	0.1303	180	20	40																		
3/11/2010	1:00	52.8550	1.1896	180	20	20			8:48-11am	132	608.70	9.01	0.89	8.61	16.12	4.82	10.19	1195.99	0.180	73.51	81.75	0.48	14.07	67.68
	2:00	53.8575	1.0025	180	20	20			11am-12pm	60	694.90	16.71	1.44	6.88	22.52	4.63	11.63	1163.39	0.324	109.54	125.69	0.81	19.03	106.66
	3:30	55.2441	1.5866	120	10	20			12-2pm	120	735.60	16.07	1.31	5.37	26.89	4.45	12.74	1140.78	0.305	118.48	136.21	0.84	22.37	113.84
	4:00	55.5854	0.3413	120	10	20			2-3pm	60	648.20	12.21	1.13	4.77	29.25	4.30	13.80	1128.90	0.230	119.22	136.28	0.92	24.13	112.15
	5:00	56.2180	0.6326	120	10	20			3-4pm	60	441.60	6.77	0.92	5.06	31.38	4.18	14.40	1118.92	0.126	111.59	122.78	0.89	24.78	96.00
	6:00	56.7243	0.4063	120	10	20			4-5pm	60	322.70	5.52	1.03	5.96	31.37	4.39	14.69	1119.92	0.103	97.02	104.56	0.82	25.44	79.12
	7:00	57.0552	0.3309	120	10	20			Std Day	483	608.90	12.37	1.22	6.39	24.72	4.51	12.45	0.222	102.29	115.30	0.75	20.52	94.78	
	10:25	57.4397	0.3845	150	10	20			3/14/2010 JB JS	8:48-4:51														
	1:00	58.2544	0.8147	150	10	20			8:48-11am	132	694.10	6.17	0.53	10.89	16.73	4.78	10.56	1195.51	0.123	70.02	77.97	0.40	14.30	63.87
	2:00	59.3116	1.0572	150	10	20			11am-12pm	60	751.40	17.62	1.41	9.30	20.79	4.98	11.47	1174.31	0.345	107.92	122.96	0.66	17.78	104.68
3/12/2010	3:00	60.4417	1.1301	150	10	20			12-1pm	60	766.20	18.84	1.48	7.66	23.89	4.78	11.91	1157.71	0.363	116.64	133.37	0.77	19.89	113.51
	4:00	61.4523	1.0106	150	10	20			1-2pm	60	741.60	16.84	1.36	6.40	24.36	4.55	12.10	1154.04	0.324	119.10	135.63	0.78	20.20	115.43
	5:00	62.3813	0.9290	150	10	20			2-3pm	60	658.20	15.48	1.41	5.61	24.08	4.38	12.16	1153.43	0.298	116.61	131.83	0.81	19.67	112.17
	6:00	63.2538	0.8725	150	10	20			3-4pm	60	520.00	11.54	1.67	5.26	24.13	4.27	12.28	1153.91	0.280	112.24	123.06	0.82	23.19	106.95
	7:00	63.7559	0.5021	150	10	20			4-5pm	60	326.90	8.37	1.54	5.34	23.79	4.11	12.10	1155.63	0.161	96.86	104.03	0.77		

90
UNCLASSIFIED

